Development of Jetting Techniques for the Delivery of Mesenchymal Stromal Cells for Therapeutic Applications

Submitted to Maynooth University for the degree of Doctor of Philosophy

Zita McCrea, B.Sc

October 2015

Supervisor

Doctor Shirley O'Dea
Department of Biology
Maynooth University
NUI Maynooth
Co. Kildare

Co-Supervisor

Professor Sally-Ann Cryan
Royal College of Surgeons
in Ireland (RCSI)
123 St. Stephens Green
Dublin 2

Head of Department

Professor Paul Moynagh
Department of Biology
Maynooth University
NUI Maynooth
Co. Kildare

Table of Contents.....**1**

Deceleration of Authorship.....**4**

Abstract.....**5**

Acknowledgements.....**7**

Publications and Presentations.....**8**

Nomenclature.....**9**

Chapter 1: Introduction.....**13**
1.1 Tissue Engineering and Regenerative Medicine.....**14**
1.2 Mesenchymal Stromal Cells.....**17**
1.2.1 MSC as a Cell Therapy.....**19**
1.2.2 MSC and Tissue Engineering applications.....**20**
1.3 The role of Jetting Methodologies in Tissue Engineering and Regenerative Medicine.....**21**
1.3.1 Electrospraying in Tissue Engineering and Regenerative Medicine.....**23**
1.3.2 Electrospinning in Tissue Engineering and Regenerative Medicine.....**28**
1.3.2.1 Electrospinning Parameters.....**32**
1.4 Biomaterial properties essential for Tissue Engineering.....**34**
1.4.1 Collagen-Glycosaminoglycan Scaffolds.....**36**
1.5 Cartilage Formation.....**38**
1.5.1 Articular-Cartilage and Lesion Formation.....**39**
1.5.2 Cartilage Regenerative Therapy.....**43**
1.6 Objectives.....**47**

Chapter 2: Materials and Methods.....**49**
2.1 Ethical Approval.....**50**
2.2 Animal Strains.....**50**
2.3 Tissue Culture.....**50**
2.3.1 Cell Lines.....**50**
2.3.2 Sub-Culture.....**51**
2.3.3 Cell Freezing.....**51**
2.3.4 Cell Thawing.....**52**
2.3.5 Cell Counting.....**52**
2.3.6 Isolation and Culture of Murine Bone Marrow-Derived MSC.....**53**
2.4 Commercial Jetting Apparatuses and Optimisation Parameters.....**54**
2.4.1 Bio-Electrospray Apparatus and Optimisation.....**54**
2.4.2 Electrospinning Apparatus and Optimisation.....**55**
2.4.3 SprayCell™ Apparatus and Optimisation.....**56**
2.5 Cell Viability from various commercial Electrospray Apparatus.....**56**
2.5.1 Viability of mBMSC post Bio-Electrospray with Spraybase®.....**56**
2.5.2 Viability of mBMSC post Bio-Electrospray with SprayCell™.....**56**
2.6 Spray Consistency and Control.....**57**
2.6.1 Measurement of Consistency of Electrospray Delivery.....**57**

2.6.2 Control of Spray from Needle tip.....**57**
2.7 Polymer Mixtures and Electrospun Polymer Fibres.....**58**
2.7.1 Fabrication of PEO/PEG/agarose fibres.....**58**
2.7.2 Fabrication of PEO/collagen/cα-MEM fibres.....**58**
2.7.3 Fabrication of PEO/agarose/cα-MEM fibres.....**59**
2.8 Characterisation of mBMSC pre and post Bio-Electrospray.....**59**
2.8.1 Surface Marker Detection on mBMSC.....**59**
2.8.2 Osteogenic Differentiation of mBMSC.....**60**
2.8.3 Adipogenic Differentiation of mBMSC.....**60**
2.8.4 Chondrogenic Differentiation of mBMSC.....**61**
2.9 T-Cell Suppression Assay.....**61**
2.10 Scratch Assay.....**62**
2.11 Bio-Electrospray of Differentiated Bone and Fat Cells.....**63**
2.12 Bio-Electrosprayed mBMSC/Chondrocytes on Collagen-Glycosaminoglycan Scaffolds using SprayCell™ Apparatus.....**64**
2.12.1 Collagen-Glycosaminoglycan (CG) Scaffold Fabrication.....**64**
2.12.2 Immunofluorescence and Confocal of mBMSC on CG-Scaffolds…….....**64**
2.12.3 Chondrogenic Differentiation of mBMSC post Bio-Electrospray onto CG-Scaffolds.....**65**
2.12.4 Bio-Electrospray of Differentiated Cartilage cells on CG-Scaffolds.....**66**
2.13 Statistical Analyses.....**67**

Chapter 3: Optimisation of commercial electrospray apparatus and the establishment of optimal bio-electrospraying parameters.....**71**
3.1 Introduction.....**72**
3.2 Design of the commercially available electrospray apparatus – Spraybase®.....**77**
3.3 Achieving a bio-electrospray of A459 cells in suspension using the single needle configuration and ring ground electrode design at low voltages.....**79**
3.4 Saline-based cells solutions were compatible with commercial electrospray to bio-electrospray A549 cells.....**82**
3.5 Bio-electrospray of mBMSC using optimised parameters.....**85**
3.6 Diverse jet-modes established at low voltages when bio-electrospraying mBMSC.....**90**
3.7 High yields of viable mBMSC were continuously distributed when bio-electrosprayed at low voltages.....**94**
3.8 Accuracy of spray from the single needle configuration maintained successful control for bio-electrosprayed mBMSC to target sites.....**98**
3.9 Discussion.....**101**

Chapter 4: Optimisation of commercial electrospinning apparatus and the establishment of optimal process and solution parameters to electrospin new polymer solutions involving PEO, Collagen and Agarose.....**108**
4.1 Introduction.....**109**
4.2 Modified electrospray apparatus capable of electrospinning fibres.....**112**
4.3 Generation of novel organic and synthetic polymer blends for electrospinning process with commercial electrospray.....**116**

4.4 Collagen versus Agarose as a primary polymer in fabrication of novel electrospun scaffolds.....**118**
4.5 Contrasting surface topography for collagen and agarose based scaffolds…….....**120**
4.5.1 Surface topography for electrospun PEO/collagen/cα-MEM scaffolds.....**120**
4.5.2 Surface topography for electrospun PEO/agarose/cα-MEM scaffolds.....**123**
4.6 Extensive pore size variation in collagen scaffolds contrasted with homogenous pore sizes for agarose scaffolds.....**126**
4.7 Electrospun PEO/collagen/cα-MEM fibre diameters varied in thickness compared to uniform PEO/agarose/cα-MEM fibres.....**129**
4.8 Discussion.....**132**

Chapter 5: Cellular and immunological analyses of bio-electrosprayed mBMSC and the development of the bio-electrospray process as a cell delivery method to target sites at low voltages.....**143**
5.1 Introduction.....**144**
5.2 Bio-electrosprayed mBMSC retained associated surface markers.....**147**
5.3 mBMSC differentiated into their multilineages following the bio-electrospraying process.....**150**
5.4 Bio-electrosprayed mBMSC suppressed T-Cell proliferation.....**152**
5.5 Bio-electrosprayed mBMSC induced wound closure for two separate cell types.....**155**
5.6 Bio-electrospray of various cell types using commercial electrospray.....**158**
5.7 Addition of catheter to electrospray apparatus developed more medically applicable device named SprayCell™.....**160**
5.8 Adherence of mBMSC onto 3D collagen-glycosaminoglycan scaffold post bio-electrospray using SprayCell™.....**163**
5.9 Bio-electrosprayed mBMSC shown to penetrate deeper in collagen-glycosaminoglycan scaffolds in comparison to pipette control.....**166**
5.10 mBMSC bio-electrosprayed using SprayCell™ apparatus differentiated into chondrocytes on collagen-glycosaminoglycan scaffolds.....**168**
5.11 SprayCell™ capable of bio-electrospraying chondrocytes directly to specific target site.....**170**
5.12 Discussion…….....……...**172**

6: Conclusions.....**181**

7: Future Directions.....**183**

8: Bibliography.....**186**

Appendix.....**212**

DECLERATION

This thesis has not been submitted in whole or part to this or any other university for any degree, and is the original work of the author except where stated.

Signed _____

Zita McCrea B.Sc

Date _____

Abstract

Mesenchymal stromal cells (MSC) are an important cell source for tissue engineering and regenerative medicine (TERM) and cell therapies. Intravenous injections (I.V.) injections and scaffold implantation are currently the predominant methods of MSC administration. However, both approaches have encountered serious problems for example with I.V. injections, cells can move through the blood stream to any site *in vivo* provoking problems such as MSC entrapment, and failure to target the injury site. For tissue engineering (TE) applications administration of MSC to a target area include the fabrication of artificial three dimensional (3D) constructs. However, the synthesised environments of these 3D constructs have been associated with numerous limitations including, poor cellular responses, lack of cell infiltration and limited access to essential nutrients and oxygen through the scaffolds. Therefore, the overall aim of the study is to address obstacles associated with MSC administration from either I.V. injections or scaffold transplantation, by using a jetting methodology called bio-electrospraying (BES) to deliver cells directly to an injured region.

A major difficulty associated with BES is reproducibility of data between different labs. This is due to the type of apparatus used as electrospray devices tend to be built "in-house", which adversely affects reproducibility of parameters, including flowrate, potential difference (PD) and voltages. To overcome these problems we used Spraybase®, a commercially available electrospray apparatus. We aimed to establish optimised "gold standard" parameters, for a commercial electrospray instrument that would allow reproducibility between experiments/labs and/or medical environments.

By modifying the shape of the ground electrode component, the commercial electrospray was transformed into a fully functional electrospinning device. 3D constructs were fabricated using our own blends of polymer mixtures involving PEO, collagen and agarose. Two distinct sets of electrospun fibres were examined in relation to surface texture, pore and fibre size.

These preliminary results may benefit future applications for TE either/or by using our polymer hybrids, electrospinning apparatus and functional parameters.

Finally, the BES technique was developed further to make it more clinically applicable. To achieve this, the jetting process was first explored to investigate its affects on mouse bone-derived mesenchymal stromal cells (mBMSC) at a cellular and immunological level. Known characterisations of MSC, i.e. expression of specific surface markers, suppression of T- cell activation, multilineage differentiation, and the pro-reparative properties were analysed for BES BMSC. It was determined that BES BMSC behaved similar to their non-BES counterparts in all biological aspects. The commercial electrospray was then modified to include a specially designed catheter with single needle configuration attached. This catheter fits all types of endoscopes suitable for keyhole surgeries. The only adjustment to the previous established BES parameters was to the flowrate. This was to accommodate the length fluid/cells had to travel through the catheter.

We assessed if the optimized parameters were effective with the catheter by BES mBMSC onto 3D collagen-Glycosaminoglycan (CG) scaffolds, and allowing them to differentiate into chondrocytes. The results from this study indicated mBMSC remained fully functional and differentiated as normal after 21days on the scaffolds. To determine if the spray from the catheter was reaching the intended target site, differentiated chondrocytes were BES to a specific area on the scaffolds. Analysis showed chondrocyte staining only at the targeted area. These results also demonstrated huge potential for cartilage regenerative therapies. BES chondrocyte cells to an injured region using arthroscopy with this catheter can eliminate issues with immune rejection caused by scaffolds, or issues with the scaffolds themselves (mentioned above).

Delivering specific number of MSC and/or other cell types directly to a specific tissue injury site, using the modified commercially available electrospray apparatus, with optimised parameters including low voltages, has revolutionised MSC delivery for therapeutic applications. This set up can potentially eliminate the complications associated with MSC entrapment, while limiting the need for artificial scaffolds in TE.

Acknowledgements

Firstly, I would like to thank my supervisor Dr. Shirley O'Dea for giving me the opportunity to undertake this PhD, it's been a privilege. I sincerely appreciate the reassurance and constant positivity over the last four years. I would also like to extend my gratitude to my co-supervisor Prof. Sally-Ann Cryan, located in RCSI, for her advice in the early days on everything Collagen-Glycosaminoglycan scaffold related.

To everyone who I've had the pleasure of working and sharing the reading room with Joanne, Louise, Deirdre, Gillian Áine, Jen, Luke, Emer and Peter, thank you guys for the laughs and motivational chats. I would like to extend a special thanks to Thérèse Lynn and Helen Kennelly, my PhD buddies. I couldn't imagine doing these last four years without you girls. Thank-you so much for everything; for all your support, thoughtfulness, encouragement and the laughs. You have been my companions on this PhD path from the start, and now, I've the pleasure to end it with you both. Thank you again – We did it girls!

To my amazing mother, without her continuous love, encouragement, and support I would never had the strength or confidence to return to university to complete an undergrad degree, let alone undertake and accomplish a postgrad degree. Thank you mam, for just being you. I would also like to thank my family and friends for their support over the last four years.

Finally, I would to thank my amazing husband. You have travelled the education road with me, from undergrad to postgrad, where you went from boyfriend, to fiancé, to husband and father. Your love, support, faith and confidence in me never wavered. So to you Gordon McCrea, and to our daughter Hannah, accomplishing this PhD is not just my achievement, it's ours as a couple and ours as a family.

I would also like to acknowledge the financial support provided for this work which was funded by the HEA under PRTLI5 and by EU FP7 Marie Cuire IAPP and is being co-funded by the Irish Government and the EU under Ireland's Structural Funds Programmes 2007-2013: Investing in your future.

Publications and Presentations

Publications

Z. McCrea[1], Y. Arnanthigo[1], Sally-Ann Cryan[2], Dr Peter Riddell[3, 4], Luke Burke[4], Michael Maguire[4] and Shirley O' Dea[1.] A novel methodology for bio-electrospraying MSC that maintains differentiation, immunomodulatory and pro-reparative functions. *Journal of Tissue Engineering and Regenerative Medicine.*
In submission.

Conferences

Z.McCrea, Y. Arnanthigo, S. Cryan, and S O' Dea (July, 2015). Using the bio-electrospray process as an alternative delivery method for MSC at low voltages (~3-5 kV).
Gordon Research Conference - Biomaterials & Tissue Engineering, Regenerative Engineering and Functional Materials Integration, Girona, Spain.

Z.McCrea, Y. Arnanthigo, S. Cryan, and S O' Dea (June, 2015). Bio-Electrospraying: an innovative delivering method for MSC.
Maynooth Biology Research Day, Kildare, Ireland.

Z.McCrea, Y. Arnanthigo, S. Cryan, and S O' Dea (Jan, 2015). Electrospraying MSC as a novel delivering method for Tissue Engineering purposes.
Bioengineering in Ireland (BINI), Kildare, Ireland

Z.McCrea, Y. Arnanthigo, S. Cryan, and S O' Dea (Dec, 2013). Electrospinning polymers for Tissue Engineering Applications.
Electrospinning, Principles, Possibilities and Practice. London, UK.

Z.McCrea, Y. Arnanthigo, S. Cryan, and S O' Dea (June, 2013). The use of Electrospraying technique as a Novel Method for Tissue Engineering.
Tissue Engineering and Regenerative Medicine International Society (TERMIS) V European Chapter, Istanbul, Turkey

Nomenclature

ac	Alternating current
ACI	Autologous-chondrocyte implantation
7 AAD	7-amino-actinomycin
ALP	Alkaline phosphatase
ANOVA	Analysis of variance
APC	Antigen presenting cell
ATCC	American type culture collection
BEAS	Bronchial epithelial airway cells
BES	Bio-Electrospray
BME	B-mercaptoethanol
bFGF	Beta fibroblast growth factor
BSA	Bovine serum albumin
CC	Cardiac cells
cα-MEM	Complete alpha MEM culture medium
cDNA	Complementary DNA
CG	Collagen-glycosaminoglycan
CFSE	Carboxyfluorescein Succinimidyl Ester
COL I	Type 1 collagen
COL II	Type 2 collagen
ConA	Concovalin A
COPD	Chronic obstructive pulmonary disease
CPM	Counts per minute
CS	Chondroitin sulphate
DAPI	4', 6- diaminido-2-phenylindole
dc	Direct current
°C	Degrees Celsius
DMEM	Dulbecco's modified eagles medium
DMSO	Dimethylsulphoxide
DNA	Deoxyribonucleic acid
EBAO	Ethidium bromide acridine orange
EC	Epithelial Cell
ECACC	European collection of cell cultures

ECM	Extracellular matrix
EDTA	Ethylenediaminetetraacetic acid
EU IEC	European Union International Electrotechnical Commission
FACS	Fluorescence Activated Cell Sorting
FBS	Foetal bovine serum
FDA	Food and Drug Administration
FITC	Fluorescein isothiocyanite
ESC	Embryonic stem cell
g	Gram
g	Relative centrifugal force
GAG	Glycosaminoglycan
GAPDH	Glyceraldehyde 3-phosphate dehydrogenase
GF	Growth factor
GvHD	Graft versus host disease
H20	water
HA	Hydroxyapatite
hADSC	Human adipose-derived stem cells
HSC	Hematopoietic stem cell
hMSC	Human mesenchymal stromal cell
h	Hour
IGF	Insulin-like growth factor
IJP	Ink-jet printing
iPSC	Inducible pluripotent stem cells
ISCT	International Society for Cell Therapy
I.V.	Intravenous injection
kV	Kilo-voltage
L-Glut	L-glutamine
LGCW	Laser guide cell writing
M	Molar
MACI	Matrix associated autologous-chondrocyte implantation
mBMSC	mouse Bone-marrow derived mesenchymal stromal cells
mg	Milligram
MHC	Major Histocompatibility Complex
min	Minute

mm	Millimetre
mM	Millimolar
MS	Multiple sclerosis
MSC	Mesenchymal stromal cells
mS/cm	milli Siemens per centimetre
nm	Nanometre
nM	Nanomolar
NSF	National Science Foundation
OA	Osteoarthritis
PBS	Phosphate buffered saline
PCR	Polymerase chain reaction
PD	Potential Distance
PDMS	Polydimethysiloxane medium
PEG	Polyethylene-glycol
Pen/Strep	Penicillin streptomycin
PEO	Polyethylene oxide
PGA	Polyglycolic acid
PLA	Polylactic acid
PCL/collagen/PES	Poly-(ϵ-carprolactone)/collagen/polyethersulfone
PET	Polyethylene terephthalate
PLCL/Col	Poly(L-lactic acid)-co-poly-(ϵ-carprolactone)/collagen
PLGA	Polylactic-co-glycolic acid
PLLA	Poly-(L-lactic) acid
ppm	Parts per million
PU	Polyurethane
PUTU	Polyurethaneurea
PVMSC	Porcine vascular smooth muscle cells
RA	Rheumatoid arthritis
RASMC	Rabbit aorta smooth muscle cells
®	Registered trade mark
RH	Relative humidity
RM	Regenerative medicine
rpm	Revolutions per minute
RT-PCR	Reverse transcriptase Polymerase chain reaction

SD	Standard deviation
SEM	Standard error of the mean
SEM	Scanning Electron Microscope
SMC	Smooth muscle cell
TE	Tissue Engineering
TGF	Transforming growth factor
TGF-β	Transforming growth factor-β
TM	Trade mark
2D	Two-dimensional
3D	Three-dimensional
μg	Micrograms
μL	Microlitre
UV	Ultraviolet
vs	Versus
v/v	Volume/volume
w/v	Weight/volume
w/w	Weight/weight

Chapter 1

Introduction

1.1 Tissue Engineering and Regenerative Medicine

The term "tissue engineering" (TE) emerged in the 1980's by the US National Science Foundation's (NSF), to identify proposals that sought to grow tissue in the laboratory. It was later expanded to the interdisciplinary approach of exploiting living cells to regenerate diseased, damaged or lost tissues inside a patient's body. This also describes the initiatives for growing structures *ex vivo* for the purpose of drug discovery or diagnostics, or alternatively, that can then be re-implanted in order to replace tissues. In 1998 the term "regenerative medicine" (RM) was coined. This refers to the approach of re-establishing the structure and function of tissues and organs as opposed to the repair of damaged tissue (Baran *et al.*, 2014).These terms are used interchangeably and occasionally together- (TERM).

Traditional methods for replacing damaged tissue include the use of autografting and allografting. Autografting involves tissue transplantation from one part of the body to another within the same individual. This is regarded as the gold standard for treatment (Giannoudis *et al.*, 2011). However, problems associated with this approach include lack of donor availability and risk of infection (Braddock *et al.*, 2001). Allografting involves the grafting of tissue obtained from a donor. However, various problems such as rejection by the patient's immune system, donor tissue shortages, risk of infection and disease transmission from donor to patient and graft-versus-host-disease, are indicative to such procedures (Younger and Chapman, 1989). The gap between tissue/organ donors and recipients is becoming more expansive, which is primarily due to increased life expectancy. It has been reported that approximately 120,000 people died in 2010 from kidney failure, and 597,000 died from heart disease, in the US alone (CDC.gov, cited 2014).

With the global market for TE estimated at $59.8 billion dollars and is expected to grow to $89.7 billion by 2016 (Research, B, cited 2014), the TE field aims to address these issues by developing new surrogates and strategies, as alternative treatments. One such substitute is the use of scaffolds on which cells can be grown. Typically three main requirements have been described for the development of a successful TE construct: (1) a biomaterial or scaffold that provides structural, morphological and biological cues, (2) growth factors or biophysical stimuli to direct cell growth and differentiation on the scaffolds and (3) cells to facilitate required tissue formation (Fig. 1.1). One particular cell type which has become synonymous with TE and cell therapy applications are Mesenchymal Stromal Cells.

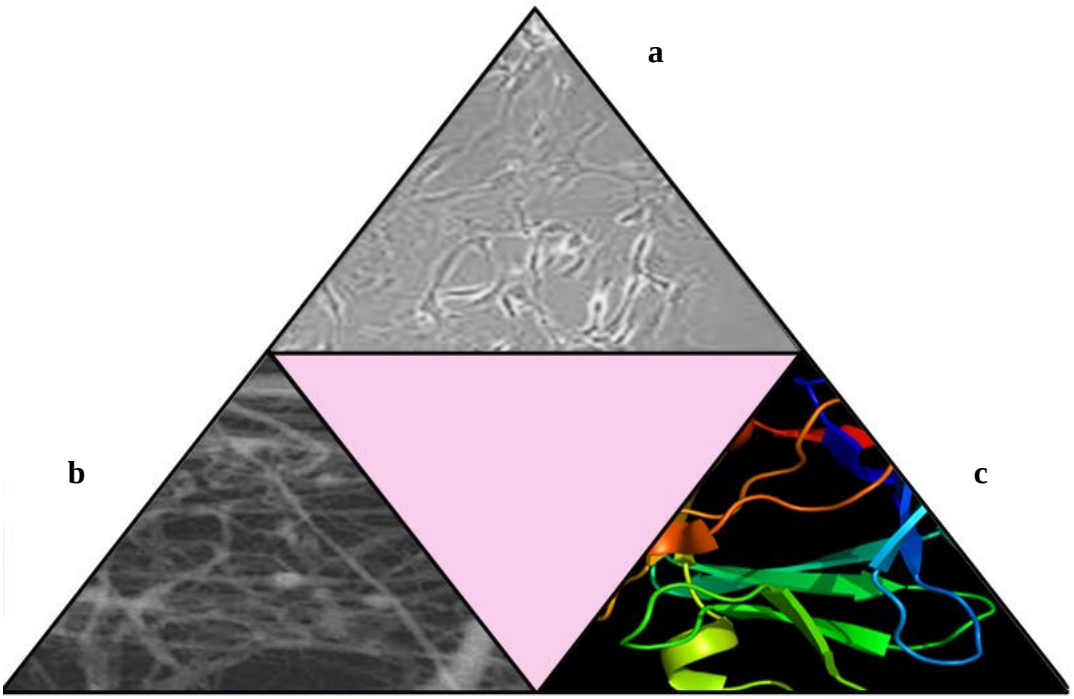

Fig. 1.1 The tissue engineering triad. The three traditional requirements of a successful TE construct consisting of (a) cells, (b) biomaterials and (c) signalling molecules, adapted from O'Brien (2011).

1.2 Mesenchymal Stromal Cells

In 1966, murine mesenchymal stromal cells (MSC) were first discovered as a population of plastic adherent bone marrow cells, with the potential to differentiate into bone (Friedenstein *et al.*, 1966). Castromalaspina *et al.* (1980) first isolated MSC from human bone marrow in 1980, with Caplan *et al.* (1991) coining the term mesenchymal stem cells over 10 years later. This was based on the cells ability to differentiate into multiple cell types indicating their potential for regenerative medicine. Pittenger *et al.* (1999) were the first to demonstrate multilineage differentiation of MSC *in vitro*. However, in the following years as MSC failed to meet previously established criteria for stemness; "a long-term self-renewing cell that is capable of differentiation into specific, multiple cell types *in vivo*"; scientists became increasingly uncomfortable with the phrase "mesenchymal stem cells". As the acronym coincided with the cells it had to be maintained, however "stem" was substituted for "stromal" to more accurately reflect the cell's phenotype (Horwitz *et al.*, 2005).

MSC have undergone rigorous characterisation analyses to prove the cells isolated from tissue are specifically non-hematopoietic MSC. The cells ability to; adhere to plastic, provide adequate expression (or absence) of thirteen specific cell surface markers described by the International Society for Cellular Therapy (ISCT), and the execution of MSC tri-lineage differentiation into osteocytes, adipocytes and chondrocytes, have been scrutinised to confirm the phenotype of the isolated MSC population (Tropel *et al.*, 2004; Dominici *et al.*, 2006).

In addition, MSC has become synonymous in suppressing T-cells proliferation *in vitro* (Di Nicola *et al.*, 2002), while studies have also indicated that the cells migrate to injury sites and promote repair through the production of trophic factors, including growth factors, cytokines, and antioxidants (Chen *et al.*, 2008; Karp and Leng 2009). Therefore thorough analyses of these abilities are also investigated for newly isolated MSC populations.

Preliminary *in vitro* work has provided insights into MSC interactions with cells of both the innate and the adaptive immune system. MSC are vital in controlling the homeostasis of hematopoietic stem cells (HSC) in bone marrow, while maintaining their undifferentiated state. (Omatsu *et al.*, 2010). With the exception of neutrophils, MSC have an inhibitory effect on immune cells, preventing activation and proliferation (Cassatella *et al.*, 2011, Raffaghello *et al.*, 2008). In the bone parenchyma, MSC facilitate in maintaining an immunosuppressive environment, suppressing autoimmune reactions by maturing lymphocytes, until naive immune cells are released to the periphery (Dazzi *et al.*, 2006). In addition, MSC demonstrate an immune privileged nature, meaning they express low levels of MHC class I and no MHC class II. This allows them to evade allogeneic reactions and NK killing (Grinnemo *et al.*, 2004).

The interaction between MSC and immune cells, coupled with easy isolation and culture *ex vivo*, makes MSC desirable candidates for cell therapy and tissue TE.

1.2.1 MSC as a Cell Therapy

The cell therapy market was valued at $2.7 billion in 2011 and estimated to be worth close to $8.8 billion by 2016 (Syed and Evans, 2013). Studies introducing MSC within a broad range of experimental animal models including, multiple sclerosis (MS) (Zappia *et al.*, 2005), type II diabetes (Lee *et al.*, 2006), myocardial infarction (Lee *et al.*, 2009) and critical limb ischemia (Lian *et al.*, 2010), have reported positive therapeutic results. Advancements in MSC cell therapy has moved from exclusively lab based experiments, towards clinical and/or industrial environments. Analyses from phase II clinical trials for graft versus host disease (GvHD), type 1 diabetes mellitus and chronic obstructive pulmonary disease (COPD), have demonstrated promising results when using MSC as a cell therapy for these diseases (Kebriaei *et al.*, 2009; Mills, 2009). There are currently 308 ongoing MSC clinical trials, while FDA approval has been granted to use MSC in the treatment of MS (ClinicalTrials.gov).

Although clinical trials have shown a number of promising results, there are challenges in using MSC. Excessive *in vitro* culture of MSC can lead to reduction in efficacy and senescence, unlike pluripotent stem cells (Katsara *et al.*, 2011). One possible solution to this is the generation of MSC from inducible pluripotent stem cells (iPSC). These are genetically reprogrammed adult stromal cells that exhibit morphology, gene expression, proliferation and differentiation capacity similar to embryonic stem cells (Takahashi *et al.*, 2007). A key advantage to using iPSC is their capability to replicate indefinitely. In addition, it has been reported that MSC differentiated from these cells keep this ability while still retaining characteristics of normal MSC (Gruenloh *et al.*, 2011).

Although safety assessments are still being implemented for this novel cell type, iPSC may have potential in regenerative medicine, allowing for autologous, patient matched cell replacement therapy.

1.2.2 MSC and Tissue Engineering applications

MSC are found in multiple tissues, including bone marrow and adipose tissue, and have the potential to self renew and differentiate into numerous cell types including osteoblasts, chondrocytes, myocytes, adipocytes and fibroblasts (Pittenger *et al.*, 1999). Significantly for TERM purposes, human MSC (hMSC) can be readily isolated from the bone marrow of patients and as such are a clinically viable cell source. Furthermore, their relative abundance and accessibility makes hMSC attractive in comparison with neural stem cells and embryonic stem cells (Granero-Molto *et al.*, 2009). Importantly, hMSC can be directly implanted back to injured regions in the same patient, significantly reducing the possibility of transplant rejection.

In their natural environment, stem cells reside within a "stem cell niche". This is a unique tissue-specific microenvironment comprising numerous ECM proteins, polysaccharides and cytokines. Biophysical and biochemical signals provided from the ECM induce complex intracellular signalling pathways that regulate gene expression and ultimately cell differentiation (Ladd *et al.*, 2011). A major challenge when using MSC for TE is sufficiently recreating the stem cell niche environment. Therefore, the fabrication of functional three-dimensional (3D) constructs has become a vital component in TE field.

Some progress has been made regarding the biochemical signals required during stem cell differentiation (Lee *et al.*, 2010; Li *et al.*, 2013).

However, the physical interactions between the cells and the ECM are also critical in directing cell fate. When developing 3D constructs, the ability to direct stem cell differentiation to the desired lineage is imperative. Failure to do so may lead to unexpected clinical consequences. The ability to combine several microenvironmental signals within a single scaffold is essential for achieving the ideal artificial stem cell niche design, that can control stem cell differentiation. In order to successfully recreate the stem cell niche and influence MSC behaviour in the desired manner, it is essential to understand the relationship between MSC and the fabricated 3D nanofibres.

1.3 The role of Jetting Methodologies in Tissue Engineering and Regenerative Medicine

Recent advances in TERM are due to the amalgamation of interdisciplinary fields, primarily biology with engineering. "Non-contact" placement of cells by jetting was originally introduced by the ink-jet (ink-jet printing: IJP) community. This technology was initially developed for the printing industry, but due to its ability to dispense controlled volumes of liquid, it was investigated as a non-contact process to direct the placement of cells onto surfaces. However, the technology itself negated several disadvantages. These included generating droplets which doubled in size once emitted from the needle. Also, increasing viscosity levels from particulate concentrations resulted in needle blockage, and finally the ink-jets had proven they

were incapable of generating fine residues with particulate based suspensions (Sanjan and Fuller, 2004).

Laser guided cell writing (LGCW) was another technology investigated to distribute cells. This technology has several unique abilities specifically, it could emit single cells for controlled proximal placement (Pirlo *et al.*, 2006). However, no viability studies examining the effect of lasers on cells were ever conducted, thus, leaving this technology much like ink-jets in a grey area.

In addition to these methods, two jet-based methods that have received increasing attention are electrospraying and electrospinning. Briefly, electrospraying involves using tiny quantities of electrical charge that are transferred to a fluid as it passes through an emitter to generate a very fine spray of the fluid. This spray is finer, more controllable and significantly faster than aerosol (Jayasinghe *et al.*, 2006). Electrospinning is a combination of electrospraying and dry spinning. Dry spinning involves dissolving a polymer in a solvent before spinning in warm air. As the solvent evaporates, the jet is elongated by a whipping process caused by electrostatic repulsion initiated at small bends in the fibre, and finally deposited on the grounded collector. The elongation and thinning of the fibres resulted in the formation of uniform fibres (Li and Xia, 2004). This technology can fabricate 3D fibrous meshes with a varied range of fibre diameters from nanometer to micron size, mimicking the structure of natural ECM components such as collagen fibrils.

1.3.1 Electrospraying in Tissue Engineering and Regenerative Medicine

Electrosprays are a physics phenomenon first observed by Gilbert in 1600's. He was reported to have observed a droplet of liquid elongate and neck between a piece of amber, placed in contact with a resting droplet. This appeared to transform by increasing the spacing between the piece of amber, and the surface on which the droplet rested (Republished: Gilbert, 1991). Approximately 200 years later, Rayleigh (1878) investigated these observations further by applying a potential difference between a conducting capillary holding the flow of a liquid in the presence of an electric field. This was done with the aid of a grounded electrode. Many others have contributed to the understanding of these electrified "jets", with recognition attributed to Zeleny (1914), Taylor (1964), Dole *et al.* (1968) and Fenn *et al.* (1998). The contributions made by these renowned physicists have led to ground breaking applications within the physical, chemical, engineering and more recently and life sciences fields. One such application was the development of electrospray ionization for mass spectrometry of large bio-molecules led by Fenn *et al.* (1998), which sees molecular characterisation for a wide range of applications within biology and the medical sciences (Fenn *et al.*, 1998; Fenn *et al.*, 2003).

Electrosprays, which are a finer and more controllable aerosol, are initiated when a voltage is applied to a liquid. The charged liquid then passes through a conducting needle which is raised to a potential difference, with respect to a grounded electrode (Hayati *et al.*, 1986). The potential difference between the electrodes provides an electric field which the charged liquid within the needle, enters.

This is subsequently subjected to a multitude of forces which draw a column of liquid towards the grounded electrode, as illustrated in Fig. 1.2. During this process, a 3D cone is seen to form at the needle tip. Stemming from the cones apex is a jet of charged droplets, which then undergoes a break-up. This cone/jet is called a Taylor cone, so named after the physicist who discovered its generation (Taylor, 1964) (Fig.1.3).

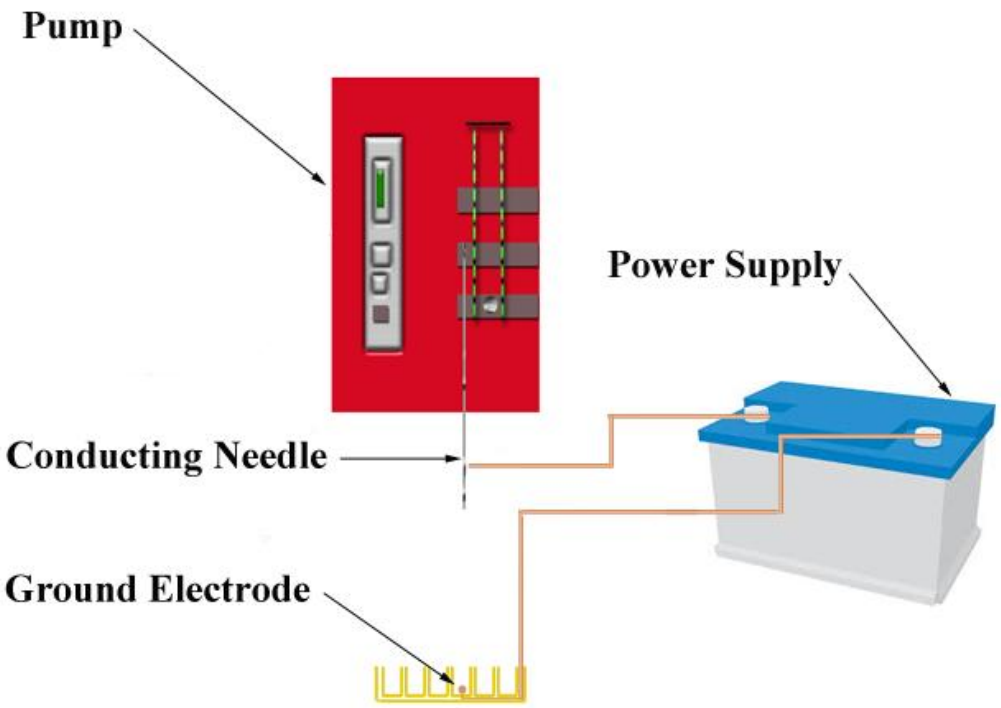

Fig. 1.2 Schematic of an electrospray apparatus. Power supply applies voltage to a liquid, which passes through conducting needle towards a grounded electrode. Potential difference between conducting needle and ground electrode provides an electric field. Pump combined with electric field applies multiply forces which draws liquid towards grounded electrode, and subsequently collecting plate.

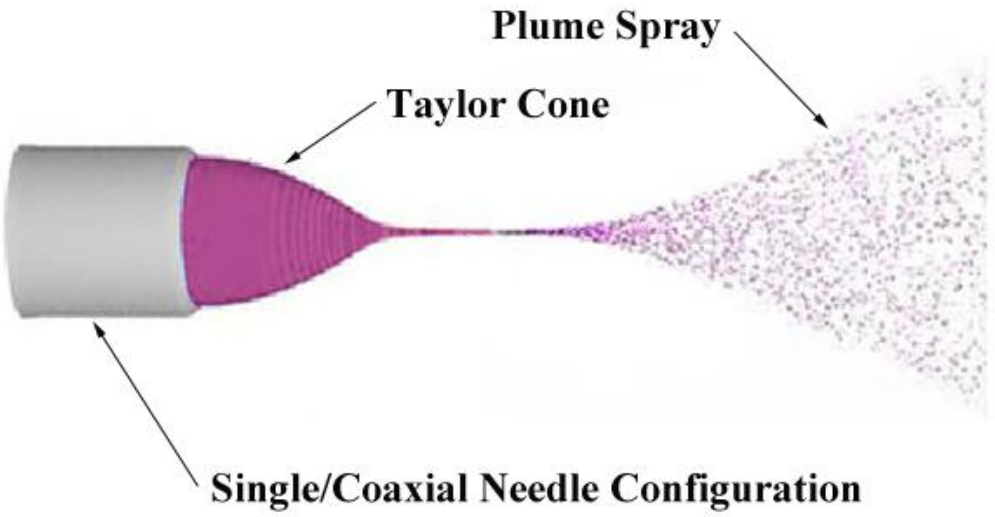

Fig. 1.3 Taylor cone. 3D cone forms at needle tip during successful electrospray. A jet of charged droplets stems from cone's apex, which then undergoes a break-up, giving plume shape to droplets.

Electrospraying conditions such as jet stability and continuity, and jet break-up point and whipping, are governed fundamentally by three specific parameters. These include; (1) the apparatus set-up (the distance between the electrodes, needle configuration and shape of ground electrode), (2) liquid properties (electrical conductivity, viscosity, surface tension, density and permittivity), and (3) external atmospheric conditions (temperature and relative humidity (RH)) (Tang and Gomez, 1996; Sullivan *et al.*, 2007; Cloupeau and Prunet-Foch (1994); Jaworek and Krupa, 1999). Various reports describe difficulties associated with all three parameters and are addressed in this project in relation to cell delivery (Chapter 3).

In 2006, the Jayasinghe group was the first to report successful electrospray of a solution containing living cells, with no apparent deleterious effect on the cells (Jayasinghe *et al.*, 2006 a, b). The term 'bio-electrospray' (BES) was coined to describe this technique. A range of cell types have been reported to have been successfully electrosprayed including primary cardiac cells (CC), mouse hematopoietic stem cells (mHSC), mouse bone marrow derived stem cells (mBMSC) and embryonic stem cells (ESC) (Abeyewickreme *et al.*, 2009; Sahoo *et al.*, 2010; Bartolovic *et al.*, 2010; Ng *et al.*, 2011; Guan *et al.*, 2009; Ye *et al.*, 2014).). Whole organisms such as nematode *Caenorhabditis elegans* were also reportedly BES with no obvious effects (Mongkoldhumrongkul *et al.*, 2010).

Electrospraying has also been used in conjunction with another methodology called electrospinning, to simultaneously electrospin polymers while electrospraying cells with the aim of improving cell penetration in 3D scaffolds (Stankus *et al.*, 2007).

1.3.2 Electrospinning in Tissue Engineering and Regenerative Medicine

Scaffolds are fabricated by various methods including solvent casting, particulate leaching, melt molding, rapid prototyping, phase separation, electrospinning and many others (Yang *et al.*, 2001). Interest in the electrospinning process for TE applications has surged in the previous two decades, as it is a relatively simple, inexpensive process for scaffold fabrication.

In constructing scaffolds for TE, it is preferable to provide cells with an environment which closely resembles their native ECM. Various scaffold fabrication techniques used in TE applications incorporate naturally derived materials such as collagen, into the scaffold. However, some methods such as melt molding require high temperatures which may denature proteins. In addition, Yang *et al.*, (2001) demonstrated that solvent casting and particulate leaching provided scaffolds with very high porosity, but potentially low interconnectivity, which also interfered with the scaffold contour (Yang *et al.*, 2001).

Electrospinning nanofibers generate scaffolds which can mimic the ECM of many tissue types structurally, chemically, and mechanically (Ladd *et al.*, 2001). In contrast to other scaffold fabrication methods, production of nanofibres by the electrospinning process provides excellent interconnectivity and control of porosity through fibre size adjustment (Pham *et al.*, 2006). Porosity or "void fraction" is a measurement of "empty space" in a material. This interconnectivity can allow for integration of cells into the scaffold if the pore size is large enough, while also allowing for dissolution of soluble factors and nutrients through the scaffold (Ju *et al.*, 2010).

Formhals published a series of patents from 1934 to 1944 describing an experimental setup for the production of polymer filaments using an electrostatic force (Formhals, 1934; Formhals, 1940; Formhals, 1943; Formhals, 1944). Since then, adaptations of this device have been created. In 1971, Baumgarten designed an electrospinning apparatus in which most current electrospinning devices are based. Acrylic fibres with diameters in the range of 0.05–1.1μm were electrospun by suspending the "spinning" from a stainless steel capillary tube. Fibre size was maintained by adjusting the feed rate of an infusion pump. A high-voltage direct current was connected to the capillary tube, whereas the fibres were collected on a grounded metal screen.

Currently most electrospinning apparatus are built in-house. However the electrospinning principals remain the same as they rely on a high voltage from a direct (dc) or alternating current (ac) source, to charge a polymer solution or melt, contained in a syringe. Typically a polymer solution is used in TE to avoid high temperatures and additional equipment. Opposite the syringe is a grounded fibre collector. The charged polymer becomes attracted to the collector, and the polymer solution is pumped out at a controlled rate. At a critical voltage, charge build-up in the solution near the tip of the syringe leads to a self-repulsive force greater than the surface tension of the liquid. This causes the solution to erupt into four distinct regions as described below, which form a polymer current, terminating on the grounded collector. Polymer current releases its charge and forms solid polymer fibres (Reneker and Chun (1996).

The first region is the base where the polymer jet emerges from solution and tapers away to form the Taylor cone. This points in the direction of the grounded collector (Greiner & Wendorff, 2007). Following this, the jet negotiates the distance between the syringe and the collector and in which the polymer strand stretches, the solvent largely evaporates, causing the fibre diameter to decrease and solidify. The third region, often called the "splay" consist of a single rapidly whipping strand of polymer, which forms an opening spiral pattern as it approaches the collector. Finally the fourth region is the grounded collector where the polymer releases its charge and any remaining solvent evaporates, leaving only thin polymer fibres (Ladd *et al.*, 2011) (Fig. 1.4).

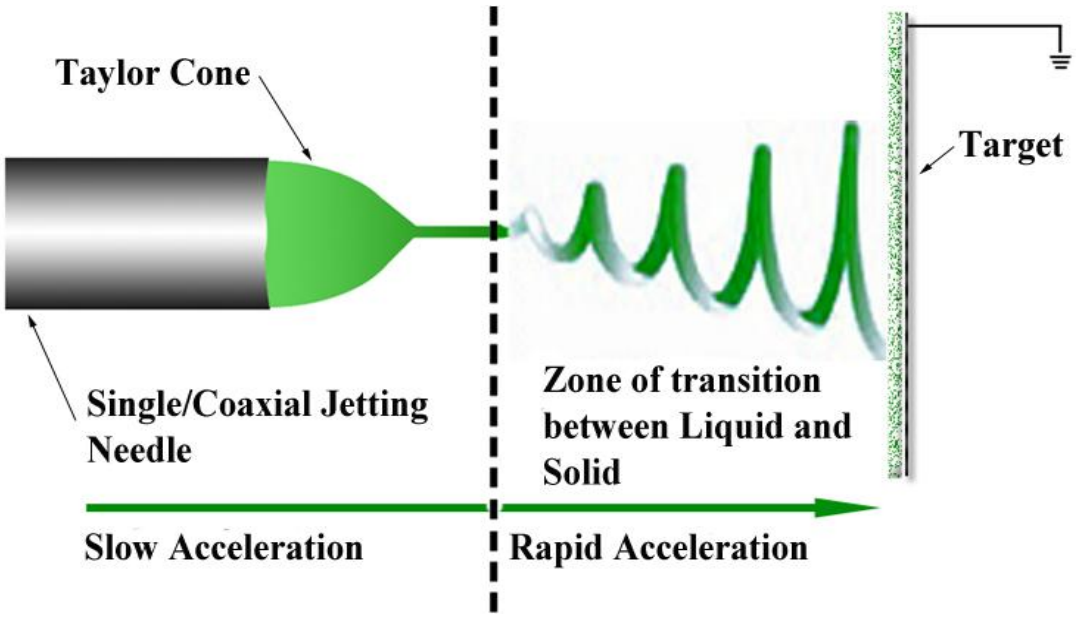

Fig. 1.4 Schematic illustrating the electrospinning process. High voltage from a dc or ac source, charges a polymer solution or melt, contained in a syringe. Opposite the syringe is a grounded fibre collector in which the charged polymer becomes attracted. The polymer solution is pumped out at a controlled rate, and at a critical voltage, charge build-up in the solution near the tip of the syringe leads to a self-repulsive force greater than the surface tension of the liquid. Solution then erupts into the four distinct regions. The first region is the base where the polymer jet emerges from solution and tapers away to form the Taylor cone. The second involves the jet negotiating the distance between the syringe and the collector and in which the polymer strand stretches. The solvent largely evaporates causing the fibre diameter to decrease and solidify. The third region, often called the "splay" consist of a single rapidly whipping strand of polymer, which forms an opening spiral pattern as it approaches the collector. Finally the fourth region is the grounded collector where the polymer releases its charge and any remaining solvent evaporates, leaving only thin polymer fibres on the grounded collector.

1.3.2.1 Electrospinning Parameters

Electrospinning provides a wide range of controllable parameters making it beneficial when fabricating fibres. These parameters can be divided into three categories: processing parameters, solution parameters and ambient parameters.

(1) Processing parameters include applied voltage, distance from the syringe to the collector (PD), needle gauge and shape, collector shape, flow rate, movement, and construction. Variation in these parameters is mostly due to the electrospinning apparatus being manufactured in-house. This has created major problems with reproducing results. Studies have shown that adjustments to increase or decrease the voltage, flow rate and/or potential difference, all resulted in unwanted beading developing on the fibres (Deitzel *et al.* 2001; Megelski *et al.* 2002; Doshi & Reneker, 1995). Thus, optimal conditions for electrospinning may vary between different polymer/solvent systems (Sill & von Recum, 2008).

Scaffold geometry is essential in TE. This can be manipulated by altering the shape of the collector, in combination with rotational and translational movement. Flat electrospun mats are fabricated by spinning onto a flat collector, while tubular shaped constructs can be formed by spinning onto a cylindrically shaped collector undergoing rotational, and optionally translational, movement (Ladd *et al.*, 2001). Fibres can also be electrospun in an aligned format which potentially can be useful, depending on the application (Theron *et al.*, 2001; Xu *et al.*, 2004).

(2) Solution parameters include polymer concentration, polymer molecular weight, solution conductivity, solution volatility, and solution surface tension. Polymer concentration is fundamental to the electrospinning process as it affects both fibre morphology, and other parameters such as surface tension (Sill & von Recum, 2008). A sufficient amount of polymer must be dissolved in the solvent in order for fibre formation to occur. It is essential for polymer strands to have sufficient chain overlap in order to physically link and form fibres. In general, increasing polymer concentration typically increases fibre diameter (Gupta *et al.*, 2005).

(3) Ambient parameters include temperature and relative humidity (RH). It has been observed that temperature may influence fibre diameter by changing the viscosity of the polymer jet (Pham *et al.*, 2006). Humidity may potentially affect fibre morphology. In polymers which dissolve in aqueous solution, excessive humidity may prevent solvent evaporation (Ladd *et al.*, 2011). Controlling these parameters in many common lab setting may prove difficult, leading to interference in producing consistent results.

1.4 Biomaterial properties essential for Tissue Engineering

As aforementioned, electrospinning fibres is the predominant method used to fabricate 3D fibres. However, although the electrospinning process has shown potential and has existed over several decades, there is still a very limited understanding of this nanotechnology. One possible reason may be due to the wide variation in biomaterials used. To date, it is believed that nearly one hundred different polymer types have been successfully electrospun into nano or microfibers.

Essential properties required when selecting a biomaterial for 3D scaffold fabrication include; providing sites for cell attachment, have the capability to develop porous and interconnected pore network for interaction with the host, while supporting cell migration, nutrient and waste movement, have strong mechanical stability, and initiates vascularisation by both seeded cells and the host tissue (Langer and Vacanti, 1993). In addition, the ideal scaffold must possess a number of macro and microstructural properties to facilitate adequate tissue formation (Hutmacher, 2000). These properties are known to affect cell signalling, growth, survival, propagation, and differentiation. Cells must be able to adhere to and proliferate throughout the biomaterial before depositing a new matrix.

In addition, fabrication of scaffold architecture and pore sizes are vital properties especially in bone and articular - cartilage repair. It is generally agreed that a highly porous, interconnected structure and a large surface area are conducive to cell infiltration as well as the diffusion of nutrients, oxygen and waste (Yannas, 2001). The ability to generate several pore sizes is essential due to cell size variation for the different cell types used in TERM applications.

A smaller mean pore size leads to a higher surface area of the material allowing more cells to bind. However, large pores sizes are required to allow cell penetration and migration through the material (Yannas *et al.*, 1989; O' Brien *et al.*, 2005; Murphy *et al.*, 2010).

The mechanical strength of the scaffold is another essential component which must be considered, especially in relation to repair of load-bearing defects. It is vital that scaffolds are capable of withstanding the hydrostatic pressures *in vivo*, especially with load-bearing tissue such as bone and articular cartilage. In addition, the rate of biodegradation should coincide with the rate of tissue formation *in vivo.* Scaffolds should function for a sufficient time frame pending on the length for the in-growing tissue to support itself, whilst replacing the degrading scaffold (O' Brien, 2011).

In vivo, scaffolds must induce minimum immune reaction so as not to impair healing or be rejected by the body. Biomaterials used in bone and cartilage TE fall into three primary categories including, synthetic bioceramics and, natural and synthetic polymers. These are designed into a variety of structures, including porous scaffolds for tissue repair. One such scaffold is based on the natural polymers collagen and glycosaminoglycans (GAG) named collagen-glycosaminoglycan (CG) scaffolds (Yannas *et al.*, 1989).

1.4.1 Collagen-Glycosaminoglycan Scaffolds

The addition of linear polysaccharides in the structure of GAGs has been reported to improve collagen function and regenerative abilities. GAGs are found within the natural ECM on cell surfaces, and are involved in cell-matrix interactions and wound healing. The most predominant GAG, chondroitin sulphate, is generally used in combination with a collagen, to fabricate scaffolds which can provide cells with an environment similar to the natural ECM. Therefore, cells tend to attach, migrate, infiltrate and differentiate on these scaffolds (Tierney *et al.*, 2009). The concept of using crosslinked CG scaffolds (Fig. 1.5) was first introduced by Prof. Ioannis Yannas, to regenerate skin tissue (Yannas *et al.*, 1989). This composite scaffold was later used for a number of other applications including nerve (Chamberlain *et al.*, 1989), bone (Farrell *et al.*, 2006) and cartilage regeneration (Lee *et al.*, 2003). Early studies have shown that CG copolymers degraded over extended periods of time when compared to GAG-free collagen polymers, which degraded rapidly. Therefore tissue formation and CG scaffold degradation coincided with that of the innate healing process (Yannas *et al.*, 1975; Yannas and Burke, 1980). Crosslinking chondroitin sulphate with collaged fabricate scaffolds also enhanced mechanical properties, indicating these CG scaffolds are more advantageous than collagen alone scaffolds.

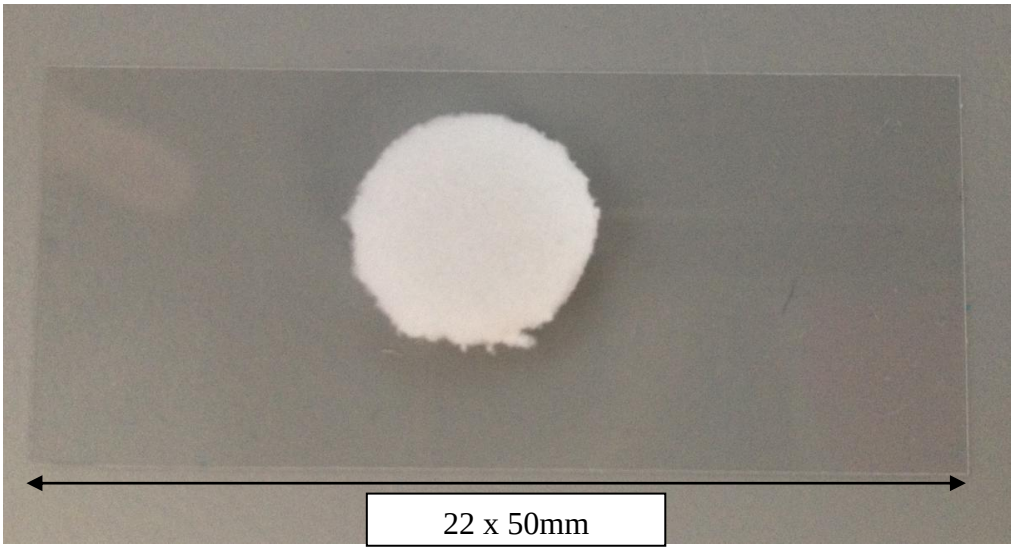

Fig. 1.5 3D Collagen-Glycosaminoglycan (CG) Scaffold with 325µm mean pore size. These spongy type scaffolds used as 3D *in vitro* model due to their fabrication from collagen and glycosaminoglycans. These are vital components of the natural ECM and crucial to wound healing in bone and articular-cartilage. Scale of CG scaffolds indicated by microscope slide measuring 22x50mm.

1.5 Cartilage Formation

Cartilage is a strong, flexible and semi-rigid supporting tissue found in the joints between bones, rib cage, ears, nose, bronchial tubes and the intervertebral discs. It forms the articulating surfaces of bones, and is a template for the growth and development of long bones, and fetal skeletons, which are eventually replaced by bone. In addition, cartilage can withstand compression forces, whilst maintaining the ability to bend. Cartilage is divided into three classifications: hyaline, fibrocartilage and elastic. The most common, hyaline, produces a glassy appearance to fibres. Fibrocartilage provides reinforcement with parallel bundles of collagen fibres, while elastic cartilage has elastic fibres as well as collagen fibres which are flexible and resilient (Messner and Gillquist, 1996).

During chondrogenesis, cartilage is generated from immature chondroblast cells which mature into chondrocytes and secretes molecules that form the cartilage ECM matrix. The collagenous ECM secreted by chondroblasts is composed primarily of approx 10% aggrecan, 75% water, and a mix of collagen and GAG fibres and a host of macromolecules. Collagen Type II fibers are responsible for giving the future cartilage matrix its very high tensile strength (Asanbaeva *et al.*, 2008; Pearle *et al.*, 2005). Proteoglycans generate the swelling pressure responsible for shielding the matrix from stress of compression loading. These attach themselves to up to 100 molecules of chondroitin sulphate and up to 50 keratan sulfate glycoaminoglycan chains, which bind to one molecule of hyaluronic acid (HA) (Asanbaeva *et al.*, 2008).

As the chondroblasts secrete matrix and fibres, they become entrapped and embed themselves in the cartilage matrix, maturing into chondrocytes (Van Osch *et al.*, 2009). Chondrocytes are the only cells found in healthy cartilage.

1.5.1 Articular-Cartilage and Lesion formation

The thin ends of mammalian synovial joints are lined with a layer of articular cartilage, which allows two opposing skeletal rudiments to facilitate the transfer of forces between them and their practically frictionless movement. In addition it acts as a weight absorber during sustained static loading (Hunzike, 1992). Synovial joint are considered an organ due to their various mechanisms, with the articular-cartilage layer as one functional component. Articular-cartilage is a highly sophisticated tissue. The structural and physiological properties of this layer affiliates with the synovial fluid, the synovial membrane, the subchondral bone-plate and the subchondral bone-marrow, as well as with the trabecular bone and its vascular system (Fig 1.6). Both positive and negative influences such as cell recruitment from synovial membrane and cartilage erosion respectively, on articular-cartilage repair are generally related to this highly-vascularized tissue-compartments (Hunziker and Rosenberg, 1996 and Bromley and Woolley, 1984). From the beginning of the 20th century it was suggested that if articular-cartilage lesions penetrate the layer of subchondral bone and the bone-marrow spaces a “spontaneous repair” reaction will occur. This involves filling these spaces with blood consisting of diverse chondroprogenitor cells and fibrin, which then acts as a supportive, blood clotting scaffold, with limited healing responses (Shapiro *et al.*, 1993; Altman *et al.*, 1992). However, this repaired tissue is only functional for a few months (Jackson *et al.*, 2001; Dell’accio and Vincent, 2010).

In addition, even if the repaired tissue persists for longer periods of time, the tissue function remaining ineffective (Metsaranta *et al.*, 1996; Schmitt *et al.*, 2014). Despite these poor results, current surgical treatments still use this spontaneous repair reaction, in clinical use today. These are classified as "bone-marrow-stimulation" approaches (Buckwalter and Brown, 2004).

Articular-cartilage lesions are defects that rarely heal, or in some instances, partially heal under certain biological conditions. Symptoms such as joint pain, joint-locking phenomena and reduced or disturbed joint function are indicative of these lesions. It has been reported that the size of the articular-cartilage lesion does not impact on the seriousness of the symptoms such as joint pain (Jones, 2013; Haviv *et al.*, 2013). Moreover, the lesion progression is generally believed to lead to the onset of osteoarthritis (OA). In western countries, OA is one of the most common diseases suffered by elderly people. Primary OA is a disabling joint disorder where origins in individual cases, although multifactorial, are usually unknown. However, OA can also be triggered by physical injury such as sports or occupational accidents and is known as secondary OA (Buckwalter and Mankin, 1997; Gilbert, 1998; Madry *et al.*, 2011).

The underlining mechanisms of OA are still relatively unknown, however, age and obesity are primary risk factors associated with this disease. Life-expectancy and youth obesity are both steadily increasing, resulting in a more prevalent disease (Chaganti and Lane, 2011). Characteristics associated with early stages of this disease include structural defects such as fibrillation of the cartilaginous layer and loss of proteoglycans.

These are confined to the articular-cartilage layer and do not penetrate the subchondral-bone plate. Such lesions do not heal spontaneously and broaden and lengthen over time. Therefore, what is initially an isolated condition progresses into a crippling disease, with larger joints such as the knee, hip and shoulder being most frequently affected (Grenier *et al.*, 2013; Aigner and Soder, 2008; Hunziker and Rosenberg, 1996; Kim *et al.*, 1991). Once the process is initiated, lesion growth is progressive and no prophylactic or medical interventions can prevent it. Similarly, there are no effective biologically-based treatments available to induce healing of the structural defects (Lefkoe *et al.*, 1993; Gratz *et al.*, 2008; Hunziker and Stahli, 2008; Simon and Aberman, 2009). This is due to the tissues structure and physiology such as the fact that the cartilage in avascular, aneural and is lightly populated with chondrocytes (Hunziker *et al.*, 2002; Quinn *et al.*, 2013). Chondrocytes are reported to slowly respond to internal and external stimuli under pathological conditions, when lesions develop *in vivo*. They demonstrate limited proliferation abilities, with reduced potential for the de-novo synthesis of an ECM (Hunziker and Rosenberg, 1997; Shapiro *et al.*, 1993; Hunziker, 2002).

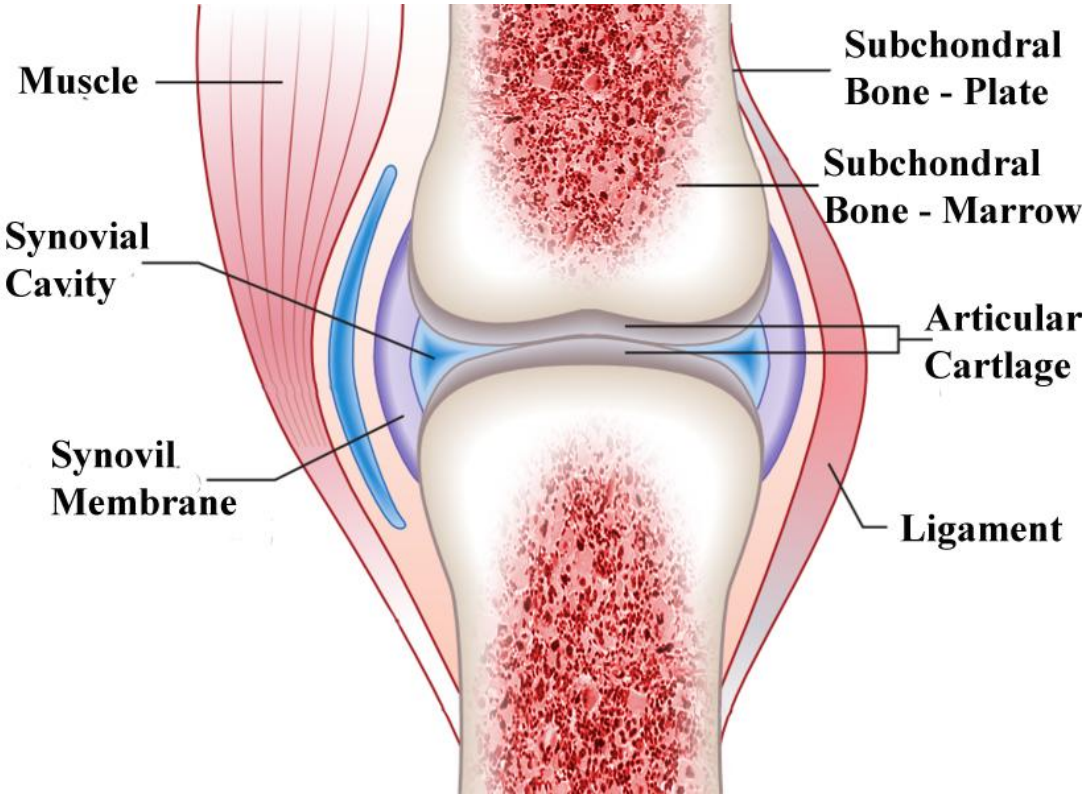

Fig. 1.6. Schematic drawing of a normal synovial joint. The structural properties of a synovial joint with articular-cartilage layer connected with the synovial cavity, the synovial membrane, subchondral bone-plate and subchondral bone-marrow. Reproduced from Hunziker *et al.*, (2014).

1.5.2 Cartilage Regenerative Therapy

In 1959, a technique by Pridie introduced the drilling of holes through injured articular-cartilage layer into the subchondral bone-marrow spaces. This is surgical treatment which exploits the spontaneous repair response by a "stimulation of the bone marrow" which is based upon surgically-induced bleeding from the subchondral-bone spaces, and subsequent blood-clot formation (Insall, 1974; Muller and Kohn, 1999, Insall, 1967). Various other surgical approaches including abrasion chondroplasty and microdrilling use similar methods (Kim *et al.*, 1991; Altman *et al.*, 1992; Hoemann *et al.*, 2007; Chen *et al.*, 2009). However, analyses from these surgical techniques indicate that these methods are highly inconsistent with non-reproducible results. In addition, the tissue that is formed is a fragile fibre, with a limited functional time-scale (Chen *et al.*, 2009). Therefore the necessity for new and improved cartilage therapies was apparent.

In 1989, Grande *et al* developed a new technique named autologous-chondrocyte implantation (ACI) in a preclinical study with rabbits. However, it wasn't until 1994 that Brittberg *et al.* introduced this technique into to the clinical orthopaedic field. ACI involves arthroscopically harvesting a biopsy of healthy articular cartilage from a low- or a non-load-bearing location of the diseased joint. The cartilaginous tissue is then enzymatically digested to release chondrocytes and are subsequently expanded in culture. A suspension of the cultured autologous chondrocytes is introduced directly into the defect, beneath a surgically-sutured periosteal flap, which is usually removed from the medial tibia (Fig. 1.7). Systems involving the application of freely-suspended cells are technically more complex than those in which matrix-embedded cells are grafted.

This is due to the careful placement and suturing of periosteal flaps, required to retain the cells and provide optimal integration with the surrounding articular-cartilage. However, it has been reported that these flaps can become dislodged during the postoperative recovery period if joint movement is not restricted. Therefore, consequences of flap displacement are the loss of the implanted cells (Driesang and Hunziker, 2000). More recently, a matrix associated variant of the ACI method (MACI), was introduced (Jones *et al.*, 2008). This involves embedding the autologous chondrocytes within a matrix such as collagen or hyaluronan, instead of suspending them in a fluid. This potentially eliminates issues with periosteal bioincompatibility, inflammation and degradation. However, an appropriate carrier has not yet been developed thus far, and remains the focus of this type of research.

One disadvantage to the ACI method is that it involves a minimum of two surgeries resulting in costly process, with long-term patient planning. In addition, extra lesions are created within the joint during the harvesting of healthy cartilage which may contribute to the development of OA (Lee *et al.*, 2000; Hjelle *et al.*, 2002). It has been suggested that the chondrocytes may be removed from osteoarthritic rather than healthy articular cartilage, or even from other tissue sources (Dehne *et al.*, 2009; Giannini *et al.*, 2005). For cartilage therapies, ACI is the predominant technique, although its superiority to other methods including microdrilling has not been proven. Moreover, a study by Knutsen *et al.* (2007) indicated that there was no advantage in using ACI method compared to microdrilling, in patients with cartilaginous lesions in the femoral condyle.

This was a 5-year trial clinical trial and although it is suggested that the repaired tissue for ACI is structurally superior to that laid down after microdrilling, 1 year after treatment the clinical outcome was the same for both methods (Saris *et al.*, 2008). One possible explanation is that the biological and biomechanistic properties for both treatments are basically the same. During the ACI application the defected floor and walls of are usually "neatened" by shaving, which induces local bleeding and a spontaneous repair response from the bone-marrow spaces.

Both microdrilling and ACI have proven clinically ineffective in patients over 50 years of age. This is possibly due to the microdrilling method which involves the use of hBMSC, and the transplanted autologous chondrocytes suffering age-related losses in their potential to proliferate and differentiate (Zheng *et al.*, 2007). This demonstrates the lack of effective cell-based repair strategies especially for elderly persons, who are particularly prone to osteoarthritic lesions of the articular-cartilage layer.

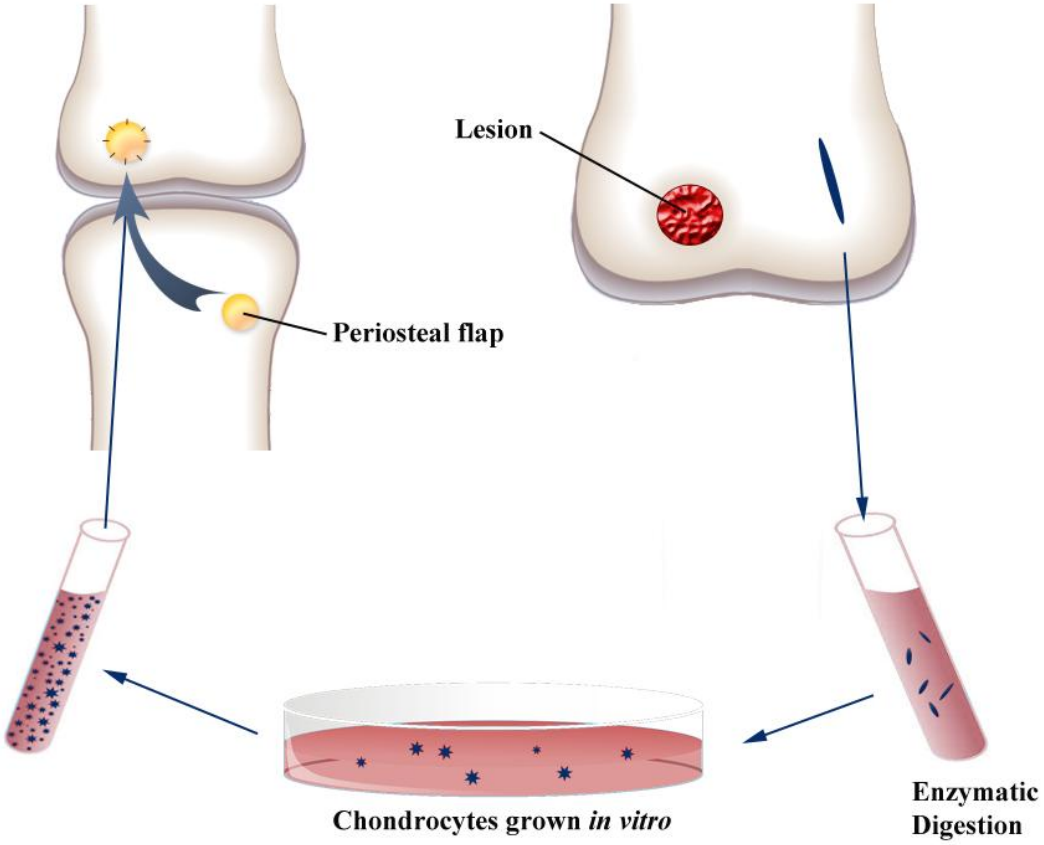

Fig 1.7.Schematic representation of the ACI technique. A fragment of articular cartilage is removed from the periphery of the joint that bears the lesion. This fragment of tissue is digested to release the chondrocytes, which are grown *in vitro* for up to 21 days. A periosteal flap is then removed from the medial tibia and sutured over the lesion. A suspension of the expanded chondrocytes is injected beneath the flap into the lesion. Reproduced from Hunziker *et al.*, (2014).

1.6 Objectives

The overall goal for this research was to develop an alternative cell delivery strategy for TERM and cell therapy purposes. Specifically, this study aimed to investigate whether the jetting methodology BES, can be improved upon to deliver various cell types at low voltages. Issues with reproducing data between experiments were addressed by the introduction of a commercial bench-top electrospray apparatus and gold standard parameters. In addition, studies into the effects BES had on cellular and immunological characteristics of mBMSC following electrospraying at low voltages were also examined. Furthermore, investigations focused on whether BES mBMSC and BES chondrocytes were viable and functional following electrospray, using a specially designed medical catheter and gold standard parameters on CG scaffolds. Results suggested a 3D representation of possible *in vivo* applications and indicated if BES process of cells can be promoted from "bench to beside".

Fundamentally, the objective for this research was to refine the BES jetting methodology to electrospray MSC and/or various cell types, in order to provide an alternative strategy for cell delivery.

The specific aims of this thesis were:

1) To establish reproducible gold standard parameters and cell solutions compatible with the design of a commercial electrospray apparatus, to BES mBMSC at low voltages, as a cell delivery method (Chapter 3)

2) To generate new polymer mixtures and establish gold standard parameters compatible with same commercial electrospray apparatus for the fabrication of unique 3D scaffolds, for future cell delivery method (Chapter 4)

3) To investigate the full effects the BES process had on the cellular and immunological characteristics of mBMSC, at low voltages (Chapter 5).

4) To investigate BES mBMSC and BES chondrocyte on CG-scaffolds using gold standard parameters and specially designed commercial catheter to (1) demonstrate viability and function of the cells post BES (2) to demonstrate spray emitted from catheter needle is controlled and cells directly reach a targeted site (3) to give more comprehensive results to challenge current therapies either for MSC or cartilage specific therapies, with the addition of CG scaffolds (4) to demonstrate advancement in the BES process towards an alternative cell delivery system with the addition of catheter, as it fits all types of endoscopes for application through key hole surgery (Chapter 5)

Chapter 2

Materials and Methods

2. Methods

2.1 Ethical Approval

All procedures involving animals were carried out by licensed personnel. Ethical approval for all work was received from the ethics committee of Maynooth University (Ref: BSRESC-2012-015)

2.2Animal Strains

The following mouse strains were used: BALB/c and C57/BL6 (Charles River Lab Manston Rd, Margate, UK). All mice were housed in accordance with EU Directive 2010/63/EU, regulated by the Health Products Regulatory Authority and used with ethical approval. Sample sizes for animal experiments were determined by statistical power calculations.

2.3 Tissue Culture

2.3.1 Cell Lines

The human adenocarcinoma cell line, A549, was obtained from the European collection of cell cultures (ECACC). The human bronchial SV-40 transformed cell line, BEAS-2B, was obtained from the American Type Culture Collection (ATCC). Cells were routinely cultured in culture medium consisting of a 1:1 mixture of DMEM: Hams-F12 medium supplemented with 5 % fetal bovine serum (FBS) and 2 mM Lglutamine (L-glut) (all components for medium from Gibco, Paisley, UK). Cells were maintained at 37 ºC in a humidified atmosphere of 5 % carbon dioxide (CO^2). Experiments were carried out within eight passages.

2.3.2. Sub-culture

Cell lines were sub-cultured upon reaching 80 %-100 % confluency. Culture medium was removed from the flask and cells were washed with 5 ml PBS. 0.5 % trypsin-EDTA (Gibco) solution was added to the flask and incubated at 37 ºC until the cells had detached (not exceeding 20 min). At this point, an equal volume of serum-containing medium was added to the flask and the entire contents were transferred to a 30 ml sterilin and centrifuged at 259 x g for 5 min in a bench-top centrifuge. The supernatant was discarded and the pellet was re-suspended in fresh culture medium. Cells were used to either re-seed the tissue culture flask or for experimental set up.

2.3.3. Cell Freezing

Cells were periodically frozen and stored in liquid nitrogen to maintain cell stocks. Cells at 50-70 % confluency were ideal for freezing (i.e. they were in the log phase of growth and actively dividing). Freezing medium consisting of a 9:1 ratio of FBS: DMSO (Sigma-Aldrich, Wicklow, Ireland) was first prepared and protected from light. Cells were trypsinised as described above and the resulting pellet was re-suspended in 500 µl FBS. Dropwise 500 µl freezing medium was added to the cell suspension using a Pasteur pipette and the entire volume (1 ml) was then transferred to a cryovial and stored on ice. Cryovials were initially placed at -70 ºC for no longer then two weeks before being transferred to liquid nitrogen for long term storage.

2.3.4. Cell Thawing

DMSO can enter living cells and quickly freezes thus preventing crystal formation within the cell at reducing temperatures. However, at room temperature this chemical is toxic to cells. Culture medium (1:1 DMEM/F12, 5 % FBS, 2 mM L-glut) was prepared initially and 10 ml was added to a sterilin prior to thawing of cells. The cryovial was removed from liquid nitrogen and kept on ice. Cells were thawed by placing cryovial in a 37 ºC water bath. On thawing cells were quickly transferred to the sterilin containing 10 ml culture medium (1:1 DMEM/F12, 5 % FBS, 2 mM L-glut) and spun at 259 x g for 5 min. Pellet was re-suspended in culture media and entire volume was transferred to a tissue culture flask and placed in a 37 °C incubator humidified with 5 % CO2. Culture medium was changed 8 – 17 hrs later to remove any excess DMSO and dead cells.

2.3.5. Cell Counting

Cells were trypsinised, spun at 259 x g and re-suspended in an appropriate volume of culture medium. A haemocytometer (Sigma-Aldrich) was used onto which a glass coverslip was fixed. Approximately 10 µl of the cell suspension was allowed flow between the haemocytometer and the coverslip by capillary action to fill the upper chamber. Cells contained within each of the four 16 corner squares were counted and an average obtained. This count was representative of the total number of cells x 10^4 /ml of the original cell suspension. In order to determine cell viability, cells were stained with Ethidium Bromide Acridine Orange (EBAO) (0.025 mM Ethidium Bromide, 0.027 Acridine Orange) (Sigma-Aldrich) at a 1:1 ratio of cell suspension to EBAO solution. The EBAO stained cell suspension was counted by similar means as described above using a UV microscope.

Viable cells were labelled with the cell permeable Acridine orange and fluoresced green under UV light. Non viable cells were labelled with Ethidium bromide and so emitted an orange fluorescence.

2.3.6 Isolation and Culture of Murine Bone Marrow-Derived MSC

Six - eight week old female BALB/c or C57BL/6 mice were sacrificed by cervical dislocation. Femurs and tibias were dissected and the surrounding muscle removed. Murine BMSC (mBMSC) were isolated and expanded using modifications of methods previously described (Peister *et al.*, 2004; English *et al.*, 2007). Modifications included flushing out bone marrow using specialised mesenchymal stem cell medium 'Mesenchymstem' (GE Healthcare Life Sciences, Buckinghamshire,UK). Isolated cells ($6.0\text{-}6.5\times10^7$) were suspended in mesenchymstem containing 10µg/mL penicillin/streptomycin (pen/strep) (Gibco) in T75 flasks and incubated in hypoxic conditions (5% O_2). Non-adherent cells were removed after 3 hours. The flasks were washed with sterile PBS after 24 and 48 hr and incubated for 3 weeks until colonies of fibroblast-like cells appeared. Cells were passaged by trypsinisation with 0.2mM trypsin / 1 mM EDTA (Invitrogen-Gibco) for 2 minutes at 37°C. Cells were centrifuged (400 x g, 5 min) and re-seeded at 5-6 × 10^6 cells in T75 (passage 1). Passage 2 cells were cultured in mesenchymstem media, 10µg/mL pen/strep and 1ng/mL murine basic fibroblast growth factor (bFGF) (Peprotech, Rocky Hill, NJ,US). Passage 3 cells were cultured in expansion medium (cα-MEM medium) consisting of Minimum Essential Medium Alpha medium (Gibco) supplemented with 10% (v/v) heat inactivated FBS (Gibco), 10% (v/v) equine serum (Hyclone laboratories, Logan, UT), 10µg/mL pen/strep, 10µg/mL L-glut (Gibco) and 1ng/mL murine bFGF in T-175 flasks.

Cells were maintained in either hypoxic (5% O_2) (passage 1-3) or normoxic (21% O_2) (passage 4-10) conditions. Surface marker expression, multilineage differentiation and T-cell suppression assay was carried out as described below to ensure that MSC were not contaminated with hematopoietic or other cell contaminants, and that cells retained differentiation capacity as previously described (English *et al.*, 2007). Cells were used between passages 3–10.

2.4 Commercial Jetting Apparatuses and Optimisation Parameters

2.4.1 Bio-Electrospray Apparatus and Optimisation

The 'Generation 1' BES instrument was purchased from AVECTAS (Dublin, Ireland) and consisted of a voltage supply, double syringe pump, a single extrusion needle (30 gauage) configuration, lab jack, camera, laser and ring-shaped ground electrode. Working in a dark, non-sterile environment, A549 cells ranging from 1 x 10^6 and 6 x 10^6 cells/ml, suspended in either PBS or PBS+0.5M EDTA (Sigma-Aldrich) (Table 1) liquid solutions, were delivered using the syringe pump via a 1ml syringe to the extrusion needle. The conductivity of the PBS and PBS+0.5M EDTA saline solutions was measured at 13.5 and 15.5 (mS/cm) respectively using a conductivity metre (Mettler Toledo, Ireland). An electric field was applied to the needle to draw the cells into jets and deposit them in droplets into 6-well or 24-well sterile tissue culture plates. Sprays were illuminated with the laser and photographs were taken with the camera 1 frame per second over 5 seconds in order to determine when a continuous, stable Taylor cone was achieved. Voltages of 1, 2, 3, 4, 5 and 6kV were tested and distances and flowrates were varied.

It was established the optimum conditions for electrospraying A549 cells with this device used voltages between 3-6kV, which varied depending on the relative humidity (RH), flow rate at 5μL/min and potential difference (PD) of 22mm. Exact same parameters were applied when BES mBMSC in cα-MEM culture medium. Conductivity level recorded for this cell solution was at 22.18mS/cm using the conductivity meter. 24-well plates were used to collect cells for studies examining BES mBMSC viability and pro-reparative properties. BES mBMSC were collected in 6-well plates for differentiation studies, while mBMSC electrosprayed into 96-well plates were examined for immunodulatory studies.

2.4.2 Electrospinning Apparatus and Optimisation

The 'Generation 1' BES instrument (AVECTAS) consisting of a voltage supply, double syringe pump, a single extrusion needle configuration, lab jack, camera, laser and ground electrode, was used to electrospin polymer fibres. Modifications to the apparatus included changes in needle gauge and ground electrode shape. The needle gauge changed from 30 to 23 gauge and ground electrode was modified from a ring-shape to rectangular-shape approx 300mm in length. Working in a non-sterile environment, voltages varied between 7-9kV, depending on RH, and charged the polymer solutions contained in a 5mL syringe. The rectangular-shaped ground electrode was placed opposite the single conducting needle at an optimum PD of 24mm, where an electric field drew the charged polymer solutions towards the grounded electrode. The polymer solution was pumped out at an optimal controlled rate of 3μL/min and at a critical voltage (~7-9kV). Once the charge from the polymer was released, forms of solid polymer fibres were observed for various polymer blends.

As with BES optimisation various, flowrates, PD, and voltages were tested to establish the optimal parameters mentioned.

2.4.3 SprayCell™ Apparatus and Optimisation

The SprayCell™ BES catheter device containing a 30 gauge single needle was obtained from AVECTAS, Dublin, Ireland. The catheter was attached to the electrospray apparatus described above and used to BES mBMSC. Parameters remained the same as the electrospray apparatus described above except for the flowrate which was 10μL/min. Voltage remained at 6kV irrespective of RH. Final optimal parameters for this apparatus were, flowrate at 10μL/min, voltage applied at 6kV, PD of 22mm using 30 gauge single needle.

2.5 Cell Viability from various commercial Electrospray Apparatus

2.5.1 Viability of mBMSC post Bio-Electrospray with Spraybase®

1 x10^6 electrosprayed mBMSC were re-suspended in 5mL PBS supplemented with 1% (v/v) FBS (FACS buffer). 5 μL of 7-amino-actinomycin D (7-AAD) Staining Solution (e-Bioscience, San Diego, CA, US) was added, the cells were incubated for 15 minutes at 4°C and then analysed by flow cytometry (FACS Accuri, California, USA) using CFlowPlus software (BD Biosciences, Oxford, UK).

2.5.2 Viability of mBMSC post Bio-Electrospray with SprayCell™

1 x 10^6 BES mBMSC were re-suspended in FACS buffer, stained with 7-AAD staining solution, incubated for 15 minutes at 4°C, and analysed using flow cytometry, as described above.

2.6 Spray Consistency and Control

2.6.1 Measurement of Consistency of Electrospray Delivery

3.5 x 10^6 mBMSC were suspended in 300µL cα-MEM medium and BES at a flow rate of 5 µL/min. Three 100 µL fractions were collected sequentially in 3 separate wells of a 24 well plate. These cells were immediately harvested and counted using a haemcytometer and Olympus CK40 Light Microscope (Olympus, Germany).

2.6.2 Control of Spray from Needle tip

1x10^6 mBMSC/mL were BES onto commercially bought polyethylene Alvetex®Scaffold disc (AMS Biotechnology Ltd., Abingdon, UK). Cells were stained with 500 µL Methylene Blue solution (Sigma-Aldrich) and 500 µL Neutral Red stain (Sigma-Aldrich), and incubated at room temperature for 5 minutes. Scaffolds were washed x3 times with PBS (2 ml/well) for cells stained with neutral red, and a further x2 times for cells stained with Methylene Blue. After the last PBS wash, scaffolds were placed onto a 22 x 50mm microscope glass slide where either a circular shape of electrosprayed mBMSC (Methylene Blue) or semi-circle shape of BES mBMSC (Neutral Red) were observed. mBMSC BES onto scaffold disc and stained with Neutral red were also observed using brightfield imaging under Olympus CK40 Light Microscope (Olympus) at x4 magnification.

2.7 Polymer Mixtures and Electrospun Polymer Fibres

2.7.1 Fabrication of PEO/PEG/agarose fibres

4mL PEO, 2mL PEG and 2mL agarose, all dissolved in dH_2O (all Sigma-Aldrich) were blended together using a magnet stir bar and a hot-plate magnetic-stirrer device (Nordic Scientific, Sweden), in a 10mL sterlin for 15 minutes. PEO/PEG/agarose fibres were electrospun from this polymer mixture using optimised parameters, flowrate at 3µL/min, applied voltage ~7-9kV and a PD of 24mm. Similar results were seen for polymer blends of 30%w/v PEO, 50%w/v PEG and 100%w/v agarose dissolved in dH_20 (Sigma-Aldrich) at ratios 1: 0.4 :0.6 and 1: 0.5 :0.5.

2.7.2 Fabrication of PEO/collagen/cα-MEM fibres

Modifications to manufactures protocol for commercial 3D Culture Matrix™ Rat Collagen I were made (AMS Biotechnology Ltd). Specifically, 98mL of cα-MEM culture medium was added to 2mL of 3D Culture Matrix RGF BME, to give a final concentration of 2%, in 100mL duran bottle. This was lightly swirled to mix and incubated at 37°C for 30 minutes. 6mL of PEO dissolved in dH_2O, was blended with 1mL of 2% collagen I, and 1mL of cα-MEM, using magnetic stir bar and magnetic stirrer device (Nordic Scientific) for 15 minutes. Polymer mixture had appropriate viscous consistency to successfully electrospin PEO/collagen/cα-MEM fibres at optimal parameters (Flowrate - 3µL/min, Voltage - ~ 7-9KV, PD – 24mm).

2.7.3 Fabrication of PEO/agarose/cα-MEM fibres

6mL of PEO dissolved in dH_2O, was blended with 1mL of agarose dissolved in dH2O, and 1mL of cα-MEM, using magnetic stir bar and magnetic stirrer device (Nordic Scientific) for 15 minutes. PEO/agarose/cα-MEM fibres were then electrospun using optimal parameters of flowrate at 3μL/min, applied voltages of ~ 7-9KV and PD at 24mm, in combination with suitable viscosity levels from polymer mixture.

2.8 Characterisation of mMSC pre- and post- Bio-Electrospray

2.8.1 Surface Marker Detection on mBMSC

BES mBMSC were harvested, washed in sterile PBS and re-suspended in FACS buffer to yield approximately 1 x 10^5 cells/4 ml polypropylene FACS tubes (Falcon, BD Biosciences). Fluorochrome conjugated antibodies (Table 2) or isotype controls were incubated with cells for 15 min at 4 °C. Cells were then washed in 2 ml FACS buffer, vortexed and centrifuged (300 x g, 5 min). The supernatant was removed and cells were re-suspended in 200 mL FACS buffer. Cells were then analysed by flow cytometry.

2.8.2 Osteogenic Differentiation of mBMSC

1 x10^6 mBMSC/mL were BES, harvested, and seeded at a density 5 x 10^4 cells/mL into a 6-well plate and incubated at 37 °C, 5% CO_2. Once confluent, typically after 3-4 days, cells were incubated for 21 days in osteogenic differentiation medium containing α-MEM, 1mM dexamethasone (Sigma-Aldrich, Dublin, Ireland), 20mM β-glycerolphosphate (Sigma-Aldrich), 50μM L-ascorbic acid-2-phosphate (Sigma-Aldrich), 50ng/ml L-thyroxine sodium pentahydrate (Sigma-Aldrich). The medium was then removed and cells were fixed in 10 % (v/v) neutral buffered formalin for 20 min at room temperature. After several washes in PBS, cells were incubated for 20 min in 1 ml of 1% (w/v) Alizarin Red S Stain. Cells were then washed with dH_2O. For visualisation, 1 ml of dH_2O was added to each well and cells were examined under the microscope.

2.8.3 Adipogenic Differentiation of mBMSC

1 x10^6 mBMSC/mL were BES, harvested, and seeded at a density 5 x 10^4 cells/mL into a 6-well plate. Once confluent, cells were incubated for 21 days in adipogenic differentiation medium consisting of α-MEM, 5.0μg/ml insulin in 0.1N acetic acid (Sigma-Aldrich), 50μM indomethacin (Sigma-Aldrich), 1μM dexamethasone (Sigma-Aldrich), 0.5μM 3-isobutyl-1-methylxanthine (IBMx) in methanol (Sigma-Aldrich). Cells were fixed in 10 % neutral buffered formalin for 20 min at room temperature, washed in PBS, stained with 1 ml of 0.5% (w/v) Oil Red O Isopropanol fat differentiation stain and examined using a microscope.

2.8.4 Chondrogenic Differentiation of mBMSC

1 x10^6 mBMSC/mL were BES into a 24-well plate, immediately harvested and 2 x 10^5 BES mBMSC were centrifuged (300 × g, 5 min) in a 15 ml polypropylene tube. The pellet was cultured in 500 µl chondrogenic medium and incubated in normoxic incubator. The chondrogenic medium consisted of α-MEM, 100nM dexamethasone, 50µg/ml ascorbic-acid-2-phosphate (Sigma, Dublin,Ireland), 40µg/ml proline (Gibco), 1mM sodium pyruvate (1:99) ITS + supplement (Gibco), 10ng/ml TGF-β3(Peprotech). Fresh medium was added every 3-4 days for 21 days, after which the pellet was washed with Dulbecco's PBS. Total RNA from cells growing in a 15ml tube was isolated using TRIZOL Reagent (Invitrogen-Life Technologies). RNA was DNase treated (Invitrogen-Life Technologies) and reverse transcribed using Superscript® III Reverse Transcriptase (Invitrogen-Life Technologies). PCR products were separated by agarose gel electrophoresis and visualised using GelRed Nucleic Acid Stain (Biotium, Cambridge, UK) using Quantity One software version 4.4.1 (Biorad, Hemel Hempstead, Hertfordshire, UK). Target transcripts were amplified using primers for Collagen 2a and Aggrecan (Sigma) and GAPDH (Eurofins) (Table 3).

2.9 T-Cell Suppression Assay

BES mBMSC were seeded at 1.5x10^4/mL in a 96-well plate in 100µl of cα-MEM and incubated overnight. The next day, splenocytes were isolated from the spleens of two MHC mismatched mice (BALB/c and C57/BL6). The re-suspended pellets were stained with carboxyfluorescein diacetate succinimidyl ester (CFSE) Proliferation Kit (CellTrace™, Life Technologies, Dublin, Ireland) using a previously described method (Quah and Parish, 2012).

Briefly, splenocyte pellets re-suspended in 1mL RPMI 1640 (Invitrogen-Gibco) supplemented with 5% FBS were placed in 15mL polypropylene tubes and laid horizontally. 110µL of PBS was placed at the top of the 15mL tube, ensuring the PBS and the pellet did not mix. 1.1µL of 5mM CFSE (CellTrace™) was added to the PBS. The solutions were then quickly inverted and vortexed to mix the cells and CFSE together. The tube was covered with foil and incubated for 5 minutes at room temp. 10mL 20°C PBS containing 5% FBS was added and centrifuged (300 × g, 5 min). The pellets were then re-suspended in 1mL RPMI 1640 supplemented with 10% (v/v) FBS, 10µg/mL pen/strep, 10µg/mL L-Glut. Splenocytes were seeded at 2 x 10^5/well and incubated for 72 hr. On Day 5, splenocytes were transferred to 96 well V-bottom plates (Corning Inc., NY, USA), centrifuged (950 × g, 5 min) and supernatant was discarded. Cells were washed with 100 µL FACS buffer, centrifuged (950 × g, 5 min) and supernatant was discarded. 0.3 µL CD3-APC (e-Bioscience), 0.3µL 7-AAD and 2.4 µL FACS buffer were added to each well and plates were incubated at 4°C for 15min. Cells were washed again with 200µL FACS buffer, centrifuged (950 × g, 5 min) and supernatant was removed. 100µL FACS buffer was added to each well and splenocytes were analysed by flow cytometry.

2.10 Scratch Assay

A549 or BEAS-2B cells were seeded at 5 x10^4 cells/well in culture medium (Dubeco's Modified Eagles Basal Medium (DMEM-F12) (Gibco, Paisley, UK), 5% FBS, 2 mM L-Glutamine) into the lower chambers of a 24-transwell plate. After 24 hr, a P200 pipette tip was used to scratch a line through the confluent monolayer of A549 or BEAS-2B cells in each well to make a wound. Either pipette mBMSC, BES mBMSC or control media was added to the transwell inserts.

After 24 hr, the A549 or BEAS-2B cells were fixed with 500µL of 10% formalin at room temp for 20 min and then stained with 1% crystal violet dye (Sigma, Dublin, Ireland) at room temp for 20 min. Plates were washed five times with PBS and cells were examined using a microscope. The width of the wound was measured at the top, middle and bottom of each well and an average width was determined for each well.

2.11 Bio-Electrospray of Differentiated Bone and Fat cells

mBMSC were seeded at 2 x 10^5/well in 6-well culture plates, and differentiated into osteogenic and adipogenic lineages as described in section 2.8.2 and 2.8.3 respectively. At day 21, cells were typsinised, suspended in 1mL cαMEM and BES into 6-well plates. Voltage and flowrate remained at ~3-6 kV depending on RH and at 5µL/min respectively. PD changed from 22mm to 25mm. 2mL cαMEM was added to each well and incubated for 24hr. The BES cells were stained with either Alizarin Red S Stain (bone differentiation stain) or Oil Red O Isopropanol (fat differentiation stain), and examined under the microscope for red deposits (osteogenesis) or orange/red fat globules (adipogenesis).

2.12 Bio-Electrosprayed mBMSC/Chondrocyte on Collagen-Glycosaminoglycan Scaffolds using SprayCell™ Apparatus

2.12.1 Collagen-Glycosaminoglycan (CG) Scaffold Fabrication

CG scaffolds were fabricated as described by O' Brien *et al.* (2004) using a freeze-drying process. Briefly, a Ultra Turrax T18 Overhead blender (IKA Works Inc., Wilmington, NC) was used to blend a suspension of 0.5% microfibrillar bovine tendon collagen and 0.044% shark-derived chondroitin-6-sulfate in 0.05M acetic acid. This was done at 15,000 rpm at 4°C for 3hr, "degassed" under a vacuum of 50mTorr for 1hr, to remove all the air bubbles created from the mixing process. The resultant, known as slurry, was frozen to a temperature of -10°C, at a constant cooling rate. The scaffolds were then crosslinked and sterilised using a dehydrothermal process at 105°C for 24hrs in a vacuum oven at 50mTorr (VacuCell 22, MMM, Germany) post freeze-drying, to make a CG co-polymer graft.

2.12.2 Immunofluorescence and Confocal of mBMSC on CG-Scaffolds

CG-scaffolds containing BES mBMSC were placed into inserts of 12 well transwell plates. Inserts were covered with 650 µL cα-MEM medium with 1200µL medium added to lower chamber. After 24hr cells were methanol fixed to scaffolds. The medium was removed and scaffolds were rinsed x3 with PBS. Ice cold methanol was added to wells and scaffolds were placed at -20 ºC for 5 min. The methanol was removed and cells were allowed air dry for approximately 15-20 min. Following air dry, cells were used immediately. BES mBMSC were stained with 10µL DAPI nuclear stain (300 nM in PBS) and 10µL MitoTracker Red mitochondrial stain (500 nM in methanol).

Scaffolds were mounted in DPX mounting medium (BDH) onto 22x50 mm microscope slides and covered with a coverslip. Fluorescently tagged stains were examined using an Olympus IX81 fluorescent microscope (Mason Technologies, Dublin, Ireland) where camera and microscope settings (exposure time, brightness and light intensity) were kept constant for examining both DAPI and MitoTracker Red stained BES mBMSC.

Similarly, BES mBMSC were methanol fixed to CG-scaffolds, with scaffolds then mounted to microscope slides as described above. Following this, confocal microscopy was used to analyse cell distribution through the scaffold with Olympus FluoView™ (Olympus, Germany) after 24hr incubation.

2.12.3 Chondrogenic Differentiation of mBMSC post Bio-Electrospray on CG-Scaffolds

2 x 10^5 mBMSC were BES onto CG-scaffolds and placed into inserts of 12 well transwell plates. Inserts were covered with 650 µL chondrogenic medium and 1200µL of medium was added to lower chamber followed by incubation for 21 days. Cells were then fixed with 10% formalin for 24hrs and scaffolds were processed for Toluidine Blue O (Sigma) staining. This was done using an automated processor (Shandon Pathcentre, Runcorn, UK) which immerses the scaffolds in fixatives and sequential dehydration solutions, including ethanol (70%, 80%, 95% x 2, 100% x 3) and xylene (x 2) (BDH AnalaR® Laboratory Supplies Poole, UK).

Scaffolds were then embedded in paraffin wax using the Shandon Histocenter 2 (Shandon) and left to set overnight at 4 °C. 5μm sections were cut using a microtome (Shandon Finesse 325, Thermo-Shandon, Waltham, MA, USA), placed on microscope slides and incubated at 56 °C for a minimum of 1 h. Slide sections were immersed in two changes of xylene for 10 min each, following by re-hydration in three decreasing concentrations of ethanol (100% x 2, 95% and 80% v/v) for 5 min each, then placed in two changes of water to rinse off excess xylene. Sections were stained with Toluidine Blue O for 2 min and washed with dH_20. Finally, slides were subjected to a series of dehydration steps in ethanol (80%, 95% and 100%) for 5 min each, mounted with DPX mountant (BDH) and examined under a light microscope.

2.12.4 Bio-Electrospray of Differentiated Cartilage cells on CG-Scaffolds

mBMSC were seeded at 2 x 10^5 into in a 15 ml polypropylene tube and differentiated into chondrocytes as described in section 2.8.4. At Day 21, the pellet was broken up using a pestle and mortar, re-suspended in 1mL cαMEM and electrosprayed onto CG-scaffolds at voltages 6kV. Cells were incubated in undifferentiated medium for 24hr, fixed and processed for Toluidine Blue O staining as described in section 2.12.3.

2.13 Statistical Analyses

Statistical analysis was performed using GraphPad Prism software (GraphPad, San Diego,CA). Paired t-test was used when statistical analysis was required between two experimental groups. One way ANOVA was used to test for statistical significance of differences when multiple experimental groups were compared with post hoc tukey. Data are presented as the ± standard error of the mean (SEM). P-values of $p<0.05$ (*), $p<0.01$ (**) or $p<0.001$ (***) were considered statistically significant.

Table 1: A549 Saline Cell solutions

Buffer	**Components**	**Concentration**	**Supplier**
PBS	Sodium chloride	0.137 mol	Oxoid (Ireland)
	Potassium chloride	0.003 mol	Oxoid (Ireland)
	Disodium hydrogen phosphate	0.008 mol	Oxoid (Ireland)
	Potassium dihydrogen phosphate	0.0015 mol	Oxoid (Ireland)
PBS+EDTA	Sodium chloride	0.137 mol	Oxoid (Ireland)
	Potassium chloride	0.003 mol	Oxoid (Ireland)
	Disodium hydrogen phosphate	0.008 mol	Oxoid (Ireland)
	Potassium dihydrogen phosphate	0.0015 mol	Oxoid (Ireland)
	EDTA	0.5 mol	Qiagen (Ireland)

Table 2: Antibodies used for flow cytometry analysis

Antibody	**Fluorochrome**	**Isotype**	**Supplier**
CD 11b	FITC	Rat IgG2b	eBioscience
CD 34	FITC	Rat IgG2a	eBioscience
CD 44	PE	Rat IgG2b	eBioscience
CD 45	PE	Rat IgG2b	eBioscience
CD 73	PE	Rat IgG1	eBioscience
CD 86	PE	Rat IgG2a	eBioscience
CD 90.2	FITC	Rat IgG2b	eBioscience
CD 105	PE	Rat IgG2a	eBioscience
CD 106	FITC	Rat IgG2a	eBioscience
CD 117	FITC	Rat IgG2b	eBioscience
Sca-1	PE	Rat IgG2b	eBioscience
MHC Class l	FITC	Mouse IgG2a	eBioscience
MHC Class ll	PE	Rat IgG2b	eBioscience

Table 3: RT-PCR Chondrocyte primers

Primer	Forward 5'-3'	Reverse 3'-5'	Size (bp)	Anneal Temp (C°)
Collagen IIa	GCGATGACATTATCTGTGAAG	TATCTCTGATATCTCCAGGTTC	150	58
Aggrecan	CTACCTTGGAGATCCAGAAC	TGGAACACAATACCTTTCAC	121	58
GAPDH	GCACAGTCAAGGCCGAGAAT	GCCTTCTCCATGGTGGTGAA	151	58

Chapter 3

Optimisation of commercial electrospray apparatus and the establishment of optimal bio-electrospraying parameters

3.1 Introduction

In 2006, Jayasingh *et al.* integrated physics, engineering and biology to develop a technique named “bio-electrospraying”. This involves applying a voltage to a liquid solution of living cells and dispersing them through a controllable spray. This is an innovative cell delivery method for TERM purposes. However, although a number of cells including various stem cells were reported to have been successfully electrosprayed, a number of key issues have not been addressed. These issues include the lack of a non-universal electrospray apparatus resulting in a wide variation in parameters applied to electrospray cells, which adversely affects the ability to reproduce data between experiments. The apparatus design, specifically the needle and electrode configuration significantly influences both establishment of a Taylor cone and the various parameters used. This study addresses these issues by employing a commercial bench-top electrospray apparatus to establish a set of “gold standard” parameters to accompany the apparatus. Therefore, applying these parameters in conjunction with the commercial electrospray will establish a method to reproduce data between experiments.

To date, previous studies described building in-house electrospray apparatuses, modifying the systems to accommodate their experimental design. All electrospray devices include a power supply, pump, needle, ground electrode and collecting plate (Fig. 1.2). The key differences reported in several apparatuses were the type of needle configuration and ground electrode construct used. Needle configuration can either include a single or coaxial needle, whereas electrode geometry refers to ring, plate or point-shaped electrodes. These components directly influence the establishment of a stable, continuous Taylor cone.

Jayasingh *et al.* (2006 a&b) and Odenwalder *et a.l* (2007) were unsuccessful when they attempted to BES cells in suspension using a single needle configuration. In their studies jurkat cell line in a saline solution, and primary rabbit aorta smooth muscle cells (RASMC) or porcine vascular smooth muscle cells (PVSMC) in a polydimethysiloxane (PDMS) medium, were electrosprayed through a single needle respectively. Both studies reported similar results such that, an unstable and volatile spray of cell suspension intermittently emitted from the needle tip. Cell viability analyses recorded high percentages in cell death for these studies. As a result both groups opted to use a coaxial needle for the remainder of their investigations.

A coaxial needle consists of incorporating one needle within another, accommodating cells in the inner needle, and a gas or medium in the outer needle. Sheath gas is predominantly used in BES studies. This is a gas that is discharged through a tube that is coaxial with the electrospray emitter to pneumatically assist the formation of the sprayed droplets. Pneumatic systems are commonly powered by compressed air or compressed inert gases (Murray *et al.*, 2013). This introduces extra parameters to this type of electrospray system including gas flowrate and compressed pressure measurements, which also requires optimisation for each in-house electrospray apparatus. Therefore, the introduction of more variables significantly increases problems associated with reproducing data between experiments. Hence, optimising a single needle configuration, where cells in solutions emit from one needle, eliminates issues with extra parameters which adversely affect replicating data. This is also more cost effective, due to less equipment required for the electrospray apparatus.

In addition, coaxial needles have separate needles for cells and gas/medium, therefore the formation of spray emitted remains the same. However, since both cells and solution are BES through one needle diameter when using a single needle, variations in cell numbers can effect spray formation, generating various types of sprays and/or jets (as shown in this chapter, Fig 3.6). Adjusting spray formation may prove beneficial to future electrospraying applications either *in vivo* or *in vitro*.

Ground electrodes have varied in geometry between different labs, as its shape is designed for the sole purpose of in-house experiments. This inevitably impacted on the optimum parameters used to BES cells, between the different labs. Jaysingh *et al.* (2006) used a copper collecting plate with a large circumference, resulting in using voltages ~ 10kV and flowrates of 10^{-7} to 10^{-12} m^3 s^{-1} to electrospray their cell suspensions. Whereas Odenwalder *et al.* (2007) choose a ring-shaped ground electrode placed in a culture well and BES their cell solution at 7kV. Where in flowrates for the study was between 10^{-7} to 10^{-12} m^3 s^{-1}. Neither study stated exact figures for flowrates, giving only approximates, indicating flowrate may have fluctuated within experiments. In addition, Odenwalder *et al.* (2007) reported using PD of 15mm for their investigations, whereas Jayasinghe *et al.* (2006 a,b) described varying PD between 18 – 22mm depending on the study. Both the ring and plate configurations encourage the development of a diverging droplet spray, resulting in a similar electrospray (Jayasinghe *et al.,* 2003). However, the parameters used to achieve the Taylor cone with the different apparatus varied between each study.

Applied voltage, PD, flowrate needle gauge, viscosity and electrical conductivity of cell solutions are vital in BES living cells. Differences in these parameters suggest there is no universal set of optimal parameters for electrospraying. Sahoo *et al.* (2010) BES mBMSC between 7.5 -15kV, where as Ye *et al.* (2014) applied voltages of 10kV when electrospraying human adipose-derived stem cells (hADSC). For both studies difficulties with low viscosity were overcome by adding high numbers of cells to the suspensions, 1 x 10^6 cells/mL. However, it is known that living cells have high ion concentrations which inadvertently lead to the generation of high conductivity levels. Although a coaxial needle was used in these studies, it was never fully explained by either Sahoo *et al.* (2010) or Ye *et al.* (2014) how the groups overcame this problem, using their in-house electrospray apparatus. Odenwalder *et al.* (2007) in contrast demonstrated how they overcame problems associated with high ion conductivity and low viscosity, using the coaxial needle configuration. The inner needle contained PVSMC or RASMC cells, and the outer needle was filled with unique medical grade silicone PDMS oil. This medium has a very low electrical conductivity, with high viscosity levels eliminating the issues connected with these parameters.

As each in-house constructed electrospray apparatus has its own specific parameters applied, this leads to a significant problem with reproducing results between experiments. The primary aim of this study was to overcome issues with reproducing data by using a commercially available electrospray device, Spraybase® procured from AVECTAS, to develop a set of "gold standard"

parameters. Possessing a commercial apparatus with universal parameters will permit replication of data between experiments.

Secondly, this chapter focused on BES cells at low voltages, and generating cell suspensions compatible with Spraybase® electrospray. High external electric fields have been proven to be detrimental to cells. They induce pore formation within cell membranes and/or internal heat damage to cells, resulting in cell death and function (Gass and Chernomordik, 1990; Ho and Mittal, 1996; Chen *et al.*, 1998). Hence, BES cells at the lowest possible voltage was a vital overall aim of this study. Spraybase® is designed with a ring-shaped electrode in conjunction with single needle configuration. Therefore, designing new cell solutions compatible with the electrospray of cells in a suspension through a single needle was imperative. Determining viscosity and conductivity properties of these new solutions was critical, so not to interfere with the establishment of a stable Taylor cone, for the BES of cells. The A549 cell line was used for optimization purposes for both parameters, and cell suspensions. These optimal parameters were proven reproducible with this commercial device, when they were applied to electrospray mBMSC primary cells. This study concluded with investigations demonstrating the accuracy of the cell spray to a target area for this apparatus, where in cells can be directed and/or aligned depending on the study, without spray settling at unintentional areas. Furthermore, Chapter 5 demonstrates the importance of spray control in promoting our overall aim, employing BES method as alternative strategy for MSC delivery in TERM.

3.2 Design of the commercially available electrospray apparatus - Spraybase®

A typical electrospray apparatus was assembled incorporating a power supply, a pump, conductive single extrusion needle, ground electrode and collecting plate. Spraybase® is a commercial electrospray equipped with a 30 gauge single needle configuration, ring-shaped ground electrode, camera and laser. The inclusion of laser and camera allowed for accurate results to demonstrate when a continuous, stable Taylor cone was achieved. Unlike conventional in-house built electrospray devices, Spraybase® is a purpose built power supply is certified to EU IEC safety standards. This makes it safe to operate in any environment, lab or medical (Fig. 3.1).

A

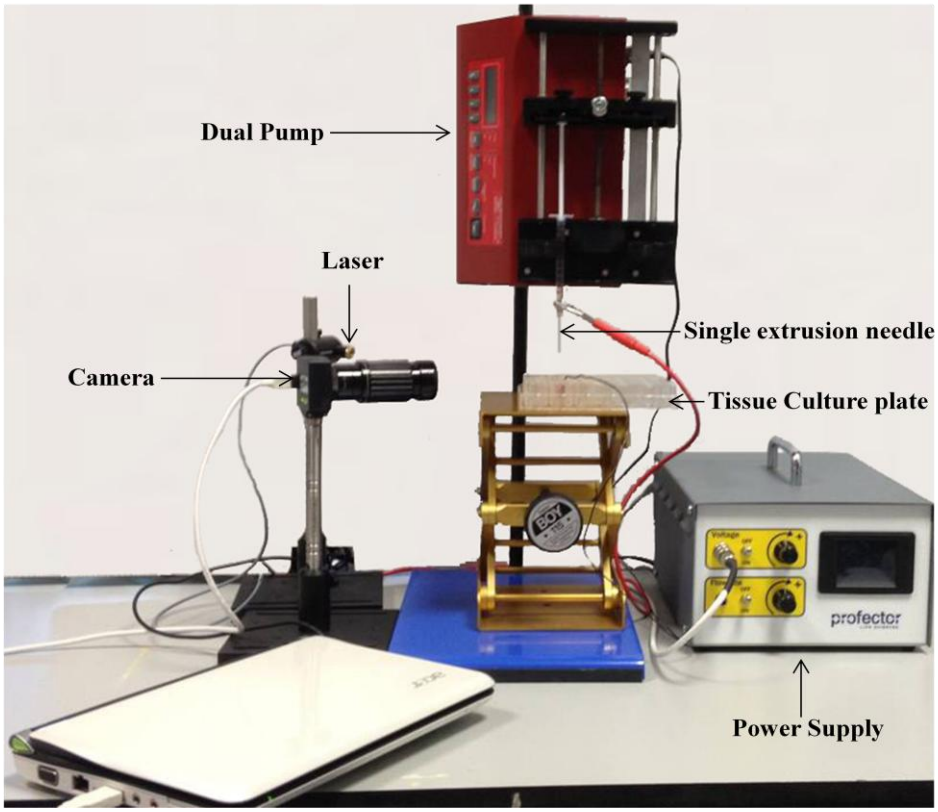

B

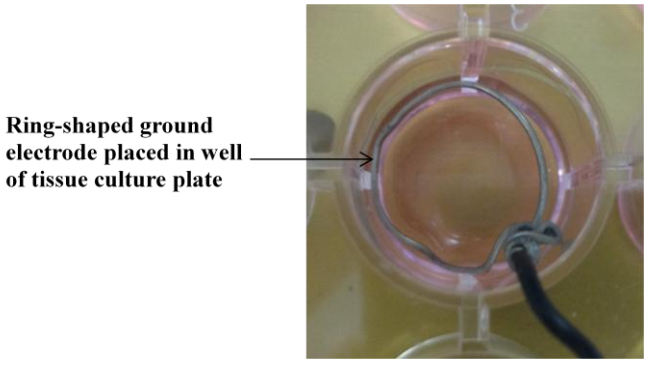

Fig. 3.1 Configuration of electrospray set-up. (A) 'Generation 1' BES instrument supplied by AVECTAS. The instrument comprised a syringe pump, which delivered cell suspensions to a single extrusion needle, charged by IEC standard approved power supply unit, with laser and camera. (B) Ring-shaped ground electrode in well of a 24-well tissue culture plate.

3.3 Achieving a bio-electrospray of A549 cells in suspension using the single needle configuration and ring ground electrode design at low voltages

Given the single needle/ring-shape electrode arrangement for the Spraybase® apparatus, initial studies involved determining if it was possible to generate a stable electrospray of cells in solution, using this system. A549 cells suspended in different saline solutions were used to examine several needle gauges, at various potential differences, flowrates, voltages, temperature and RH. Table 4 demonstrates the conditions favourable with a successful electrospray of cells in suspension and are highlighted in red. Those shown in black indicate the parameters examined but cannot produce a stable, continuous Taylor cone of cells. It was found that temperatures above 30°C and RH over 50% significantly influenced BES occurring. Therefore, those highlighted in red where further analysed to determine optimal parameters to BES A549 cells in saline solutions.

Using the laser and camera combination for visualization, the optimised parameters for a stable Taylor cone and spray of A549 cells were recorded at; flowrate 5μL/min, 30 gauge single needle and PD of 22mm, once temperature and RH remained below 30°C and 50% respectively. It was also determined high RH resulted in an automatic higher voltage range i.e. 43% RH determined voltage started between 4.5 – 5kV The most significant result from this study demonstrated cells were BES at voltages measuring between ~ 3-6kV, depending on temp and RH. This signifies the lowest voltages recorded to date for the BES of cells using an electrospray device, regardless whether it's single or coaxial needle configurations (Fig. 3.2).

Table 4: Summary of parameters wherein an electrospray of A549 cells occurred (red) and the parameters examined but unsuccessful in BES A549 cells (black) in saline solutions using single needle configuration and ring-shape electrode.

Flowrate (µL/min)	**Voltage (kV)**	**Single Needle (Gauge)**	**Potential Difference (mm)**	**Temperature (°C)**	**Relative Humidity (%)**
3	2.69	23	17	15.6	29.6
5	3.32	27	19	17.5	36.5
10	3.48	30	20	18.5	41.6
15	4.25	32	22	19.4	43.6
20	4.69		23	20.0	45.9
	4.78		24	20.1	48.2
	4.98		25	20.6	50.2
	5.36			22.5	53.3
	5.49			23.8	55.2
	5.87			25.3	56.2
	6.00			28.0	60.7
	6.25			29.5	
				30.8	
				32.1	

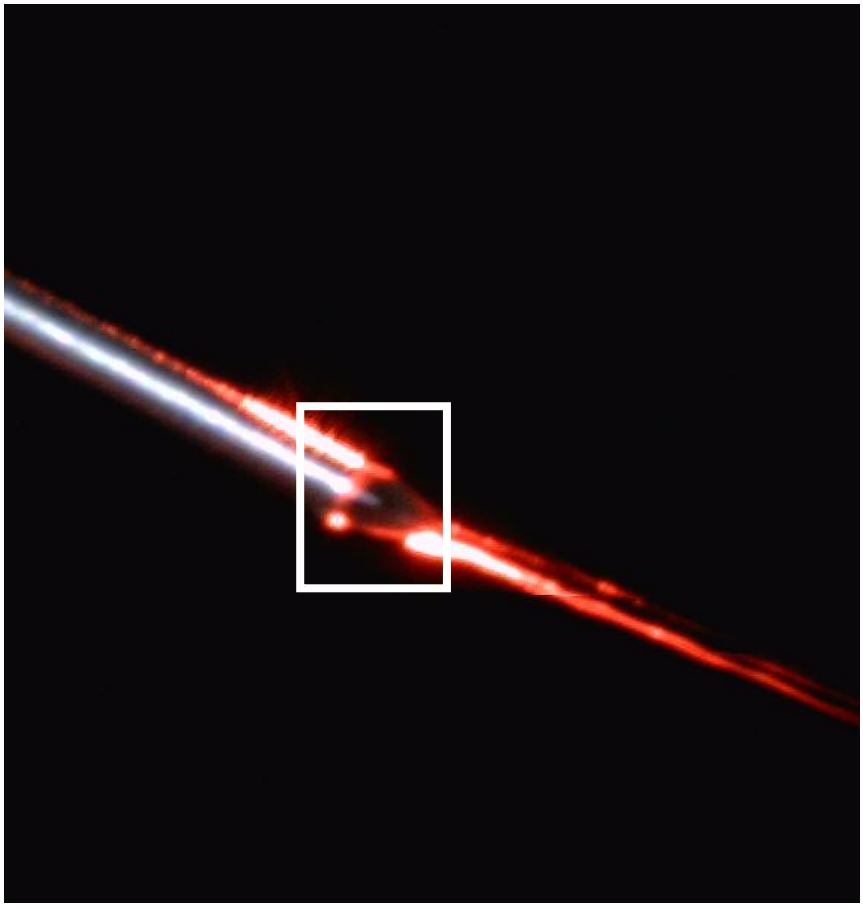

Fig. 3.2 Taylor Cone achieved using single needle configuration and ring-shape electrode. BES A549 cells in saline solution established and maintained stable Taylor cone (white box), when using the single needle configuration and ring electrode components of Spraybase®. Red hue from the laser, in combination with the camera gives visual confirmation of the electrosprayed cells in solution. Optimal parameters included flowrate at 5μL/min, voltages between ~ 3-6kV (depending RH), 30 gauge single needle at potential difference of 22mm.

3.4 Saline-based cell solutions were compatible with commercial electrospray to bio-electrospray A549 cells

In addition to determining optimal parameters to BES A549 cells, establishing cell suspensions compatible with the single needle/ring electrode configuration were simultaneously investigated. Viscosity and electrical conductivity are influenced by the chemical and physical properties of solutions, and have been shown to interfere with Taylor cone stability when using single needle configurations. As the commercial electrospray includes a single needle, solutions were developed for compatibility with the device, cell survival and counteracting problems associated with viscosity and conductivity.

Saline solutions such as PBS and PBS supplemented with 0.5M EDTA have low conductivity and are none toxic to cells. For these reasons, 1x 10^6 A549 cells/mL were added to PBS and PBS+0.5M EDTA, and investigated as possible cell suspensions for BES with the commercial apparatus, at optimized parameters. The addition of such high cell numbers was to overcome problems associated with low viscosity.

BES A549 cells in solutions of PBS and PBS+0.5M EDTA, allowed formation of a stable Taylor cone, using the single needle/ring electrode arrangement. After 24hrs, brightfield imaging demonstrated that A459 cells which were in the two solutions adhered to the plastic culture wells following electrospray. Cell proliferation was evident for both cell suspensions due to the presence of daughter cells observed in the culture wells. Cell morphology for each suspension of electrosprayed cells resembled that of the pipette control (Fig. 3.3).

In addition, it appeared that there was a higher cell number present in culture wells containing BES A549 cells in PBS+0.5M EDTA solution, compared to BES A549 cells in PBS. This is possible due to the chelating agent EDTA which prevents clumping of cells, permitting fewer blockages within the needle, and allowing for a more improved electrospray.

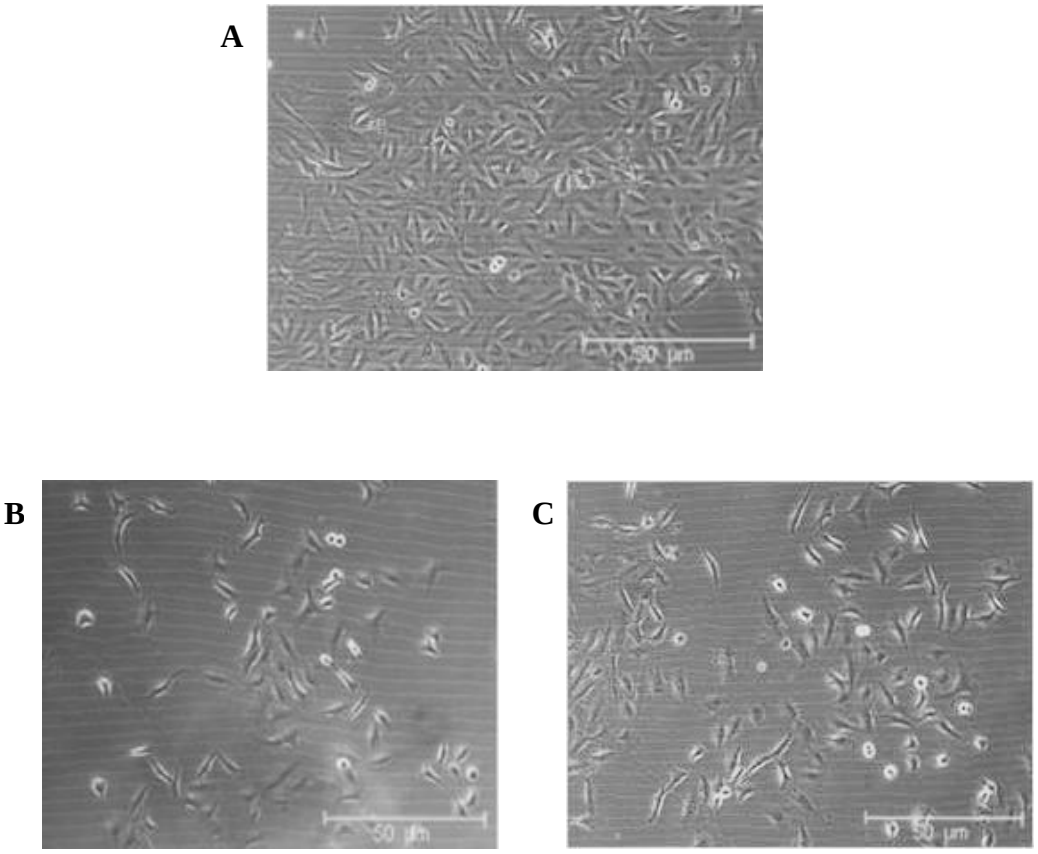

Fig. 3.3 Brightfield images of BES A549 cells in PBS and PBS+0.5M EDTA solutions. (A) Pipette A549 cells growing in culture (control). (B) 1 x 10^6 BES A549 cells/mL suspended in PBS after 24hr. (C) 1x10^6 BES A549 cells/mL suspended in PBS+0.5M EDTA after 24hrs. Both electrosprayed A549 cell suspensions adhered to the plastic culture wells and demonstrated similar morphology to control. BES cells also demonstrated cell division was evident as daughter cells were observed. Cell numbers appeared higher in culture well containing BES A549 cells in PBS & 0.5M EDTA. Parameters for both included flowrate 5μL/min, voltages of ~ 3-6kV (depending RH), using 30 gauge single needle at PD of 22mm.

3.5 Bio-electrospray of mBMSC using optimised parameters

The previous studies established optimal parameters to BES A549 cells in saline solutions, which are compatible with single needle/ring electrode configuration of Spraybase® electrospray apparatus. Subsequently, the following studies addressed the significant problem with reproducing results by employing the optimised parameters to BES mBMSC, in saline solutions, using the commercial electrospray.

mBMSC were isolated and cultured as described previously (Chapter 2- Section 2.3.6). These cells were then BES using established optimal parameters including flowrate at 5μL/min between voltages of ~3-6 kV (depending RH), using 30 gauge single needle at PD of 22mm. Similarly, 1x 10^6 mBMSC cells/mL were BES to negate low viscosity issues for both PBS and PBS+0.5M EDTA saline solutions.

mBMSC were successfully BES using optimal parameters. Brightfield imaging demonstrated the BES mBMSC adhered to the plastic culture well after 24hr, for both solutions. This vital characteristic associated with MSC indicated the electric field from the voltage did not affect the cells in these suspensions, post electrospray. mBMSC morphology for the electrosprayed cells resembled that of pipette control cells. However, the number of mBMSC present in the well after 24hr for both PBS and PBS+0.5M EDTA appeared low (Fig. 3.4).

mBMSC are substantially larger cells than A549 cells, and it was hypothesised that the cells were too big to emit from the small needle gauge. Therefore the effect of needle size was examined. However, the results remained the same for various needle gauges such as 23, 27, 30 and 32 gauge.

Adjusting flowrates and/or increasing the cell numbers in suspension ($6x10^6$ cells/mL) also resulted in similar findings, and the number of BES mBMSC observed in the wells remained considerably low.

Therefore, having eliminated the possibility that the optimised parameters influenced the quantity of mBMSC sprayed, the effect of cell solution on BES mBMSC numbers was carried out. Using the original parameters, 5μL/min, 30 gauge needle, 22mm PD and voltages of ~3-6kV (depending on RH), mBMSC in cα-MEM culture medium were bio-electrosprayed. Brightfield images revealed a significant increase in BES mBMSC present in the wells after 24 hr. These cells adhered to the wells and demonstrated mBMSC morphology similar to their pipette control (Fig. 3.5). Further analysis demonstrated on three separate days, approximately 80 x 10^4 ± 1.7%, 82 x 10^4 ± 1.9% and 80 x 10^4 ± 0.7% of original 1 x 10^6 mBMSC/mL in solution, BES into the wells suggesting a high yield of mBMSC were electrospraying using this apparatus at optimal parameters (n-3) (Fig. 3.5 C).

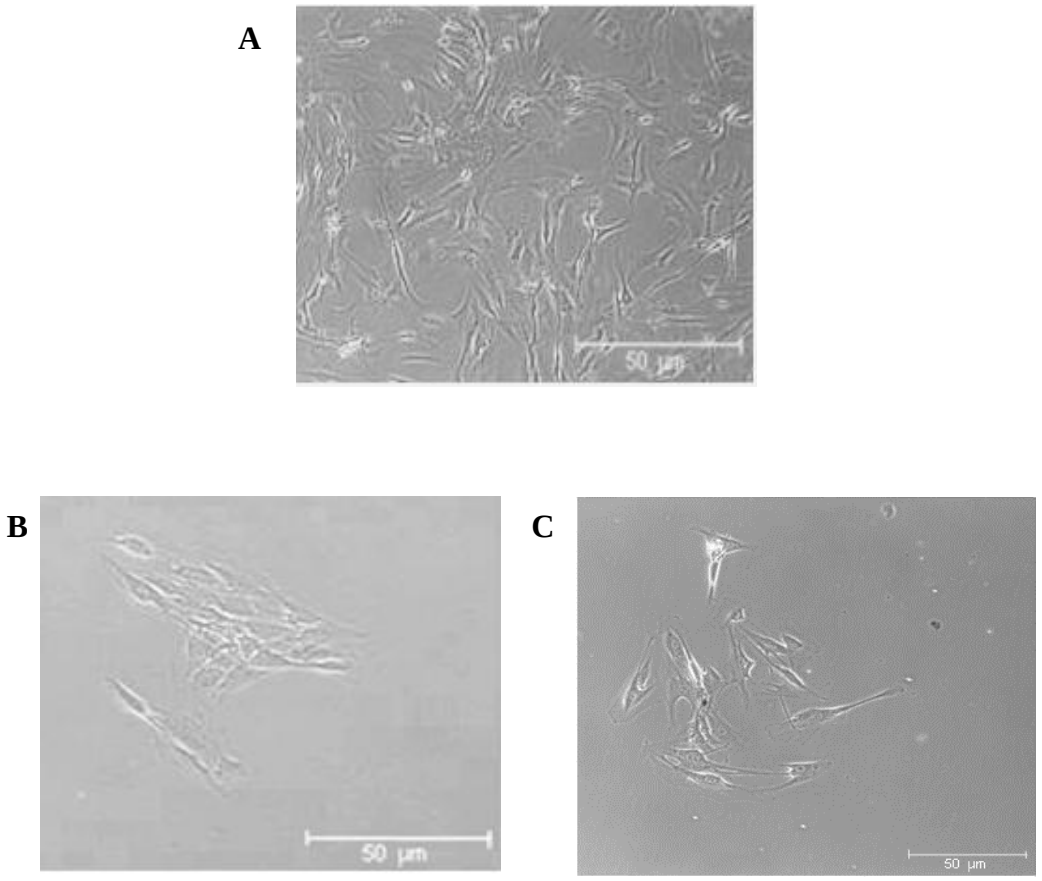

Fig. 3.4 Brightfield images of BES mBMSC cells in PBS and PBS+0.5M EDTA solutions. (A) Pipette mBMSC cells growing in culture (control). (B) BES mBMSC suspended in PBS after 24hr. (C) BES mBMSC suspended in PBS & 0.5M EDTA after 24hr. BES mBMSC adhered to the plastic culture wells for both cell suspensions after 24hr, indicating vital cellular characteristics was unaffected by voltage. BES mBMSC maintained similar morphology to pipette control. Cell numbers appeared low for BES mBMSC in both wells. Parameters for both included flowrate 5µL/min, voltages of ~ 3-6kV (depending RH), using 30 gauge single needle at PD of 22mm.

A

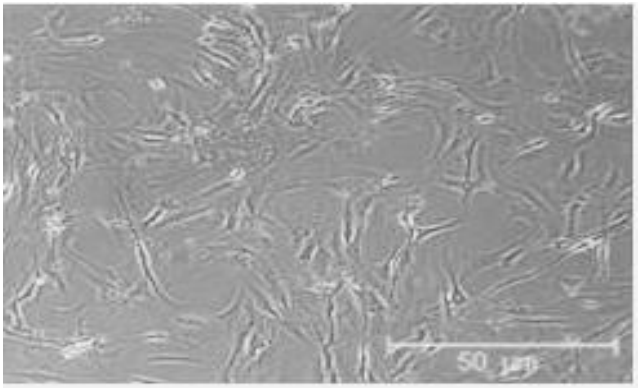

B

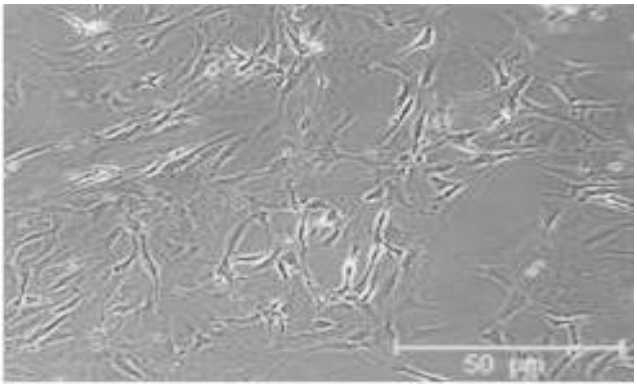

Fig. 3.5 Brightfield images of BES mBMSC cells in cα-MEM medium. (A) Pipette mBMSC cells growing in culture (control). (B) BES mBMSC suspended in cα-MEM culture medium. Increased quantity of mBMSC appeared to have electrosprayed when submerged in cα-MEM culture medium. mBMSC morphology for both BES and pipette cells appear similar. In addition, cell adhesion, a vital characteristic associated with MSC, remained unaffected by the applied voltage, as cells adhered to the plastic culture wells, after 24hr. It was suggested the nutrients in the cell solution which increased cell survival while suspended in solution between experiments. Parameters included flowrate 5μL/min, voltages of ~ 3-6kV (depending RH), using 30 gauge single needle at PD of 22mm.

.

C

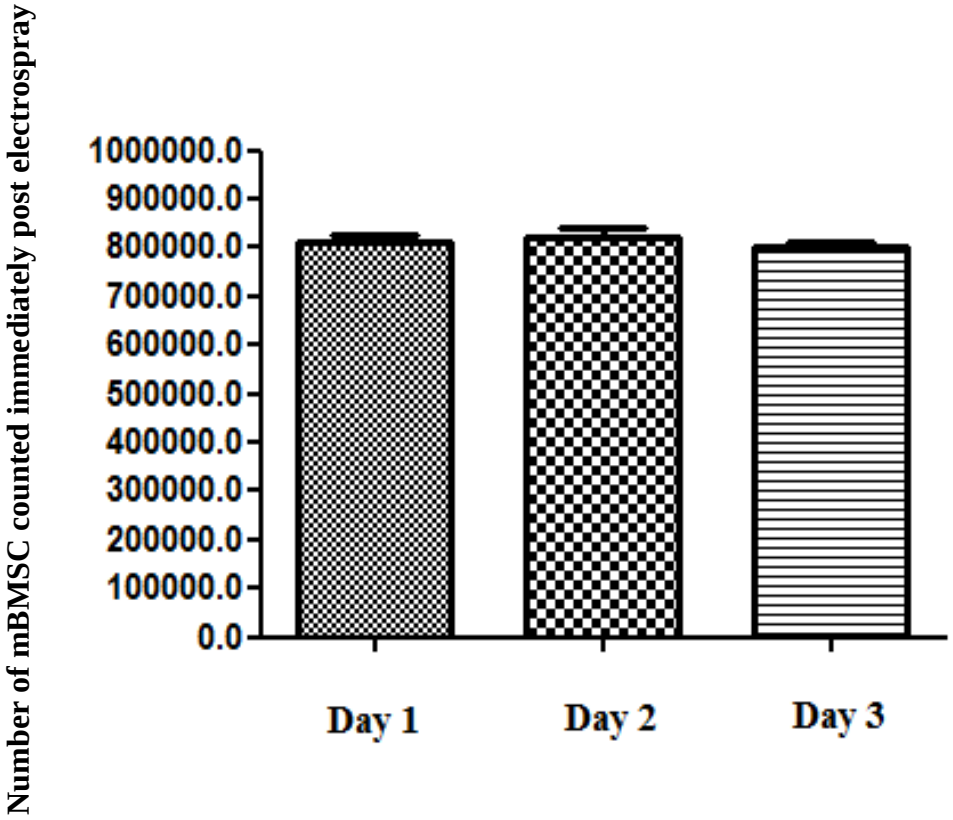

Fig. 3.5 mBMSC count immediately post electrospray. (C) 1 x 10^6 mBMSC/mL were BES into three wells of 24-well plate using flowrate of 5µL/min, 30 gauge single needle, 22mm PD and voltages ~3-6kV on three separate days. The cells were immediately harvested from the wells and counted using a haemocytometer. Approximately 80 x10^4 ± 1.7%, 82 x10^4 ± 1.9% and 80 x10^4 ± 0.7% mBMSC were counted post BES. This indicated a high volume of mBMSC were electrospraying into the wells (n-3).

3.6 Diverse jet-modes established at low voltages when bio-electrospraying mBMSC

Jet-based technologies involve charging liquid solutions to several thousand volts, passing through a large-bore needle to divide into droplets (Eagles *et al.*, 2006). By definition an electrosprayed liquid solution or polymer is only achieved when a continuous, stable Taylor cone is generated.

Two distinctive types of electrospray, plume spray and cone-jet mode, were generated when mBMSC suspended in cα-MEM culture medium were BES using Spraybase® apparatus (Fig. 3.6 A & B). While both sprays maintained continuous, stable Taylor cones, the spray formation changed with different cell numbers. 1 x 10^6 mBMSC /mL in cα-MEM culture medium electrosprayed into a "plume" shape, covering a large area of the culture wells. Whereas, 3 x 10^6 mBMSC/mL in cα-MEM culture medium, electrosprayed a cone-jet configuration generating a central ligament of cells. Due to the high cell numbers, mBMSC were forced together in the jet mode, which directed all cells to a smaller, more specific area of the well. Significantly, voltages were maintained between ~3-6kV regardless of spray mode.

mBMSC electrosprayed at ~10kV using Spraybase® generated volatile, unstable sprays and occasional sparking was observed under these conditions. The cell suspension was ejected intermittently from the needle and dispersed to various parts of the well (Fig. 3.6 C). Viability assays proved difficult to carry out due to the limited numbers of cells present in the well after 24 hours. Several BES mBMSC were found floating in the wells indicating their adherence capabilities had been seriously affected by the high voltage.

In addition, brightfield images demonstrated mBMSC morphology was circular in shape instead of long, spindle- fibroblasts after 24hr (Fig 3.7 A). Cell debris was also found scattered throughout the culture wells indicating cell membranes had burst resulting in cell death, presumably from the high voltage applied during the spray (Fig 3.7 B).

A Jet mode - 3 x 10^6 mBMSC/mL BES with central ligament of cells at ~3-6kV

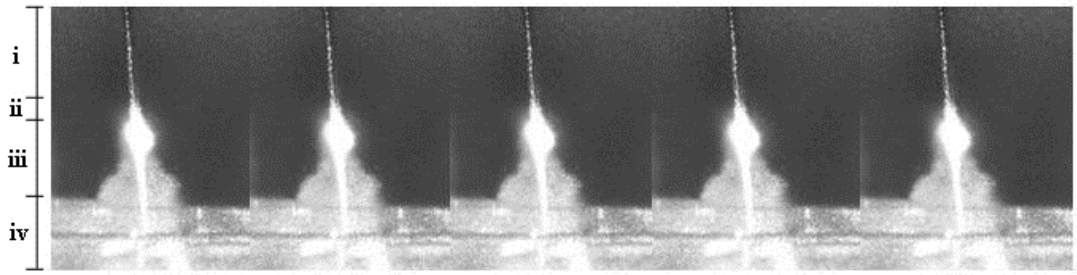

B Plume spray – 1 x 10^6 mBMSC/mL BES at ~3-6kV

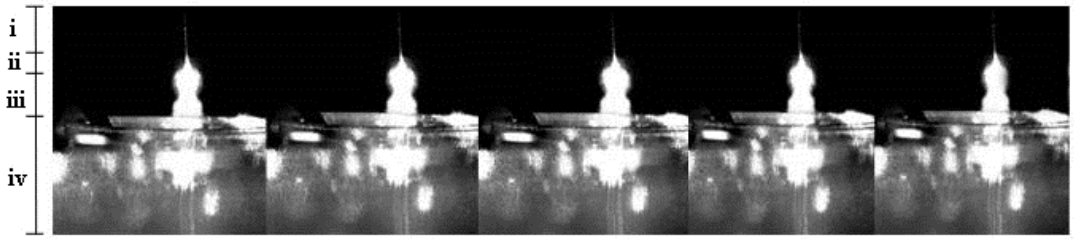

C Unstable jet/spray intermittently emitting 1x 10^6 mBMSC/mL at 10kV

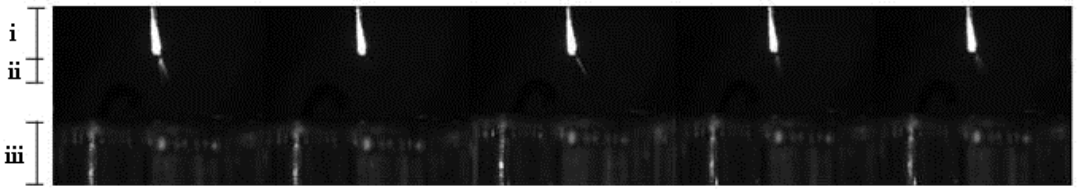

Fig. 3.6 Spray modes achieved with electrospray set-up. mBMSC suspended in cα-MEM culture medium were BES at different voltages to achieve desired jet/spray. (A) Jet mode involving 3 x 10^6 mBMSC/mL with central ligament of cells visible. (B) plume spray of 1 x10^6 mBMSC/mL. Both jet and spray achieved at 3-6kV (depending on RH), flowrate of 5µL/min, PD of 22 mm, internal diameter of syringe 1.457mm and 30 gauge single needle. (C) Unstable jet/spray of 1 x 10^6 mBMSC/mL at 10kV intermittingly emitted cell suspension from the needle. All photographs were taken 1 frame/second for 5 frames.

Key: (i) Needle for (A) (B) (C) **(ii)** Taylor cone for (A) & (B) and intermittent emitted cells for (C) **(iii)** (A) jet mode with central ligament of cells (B) plume spray (C) 24-well plate **(iv)** 24 - well plate for (A) & (B).

A

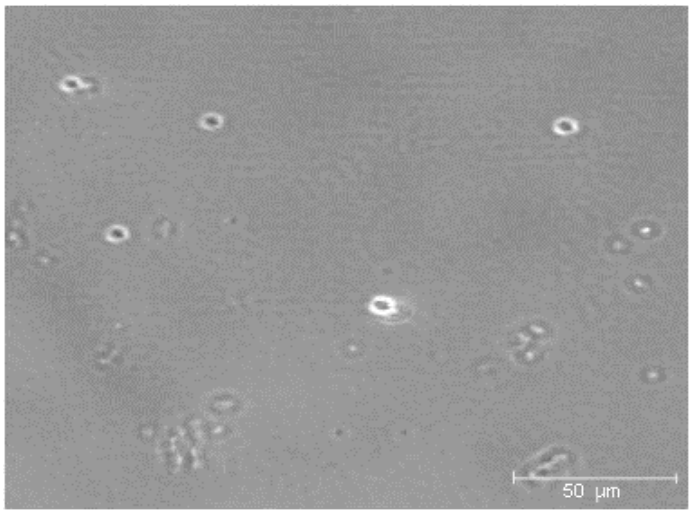

B

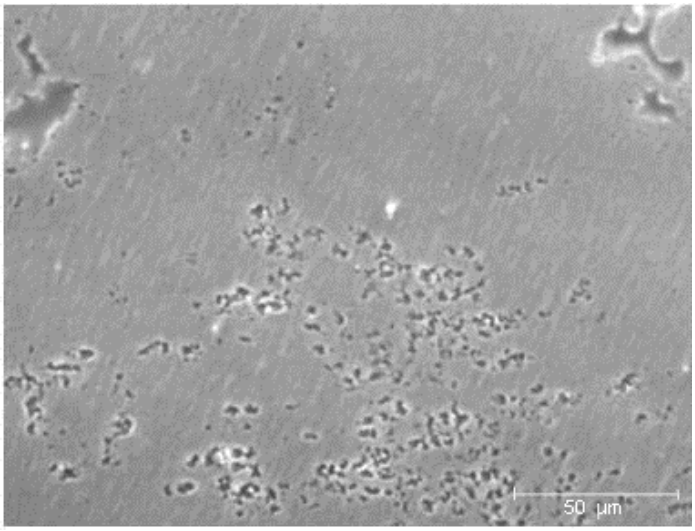

Fig 3.7 Brightfield images of BES mBMSC at 10kV. 1 x 10^6 mBMSC/mL were BES at 10kV, flowrate of 5µL/min, PD of 22 mm, resulting in (A) circular morphology and (B) cell debris scattered throughout culture well. This indicated the cell membranes burst during electrospray process at 10kV, resulting in non-viable BES mBMSC.

3.7 High yields of viable mBMSC were continuously distributed when bio-electrosprayed at low voltages

Analyses using viability exclusion assay determined if BES mBMSC were affected by the low voltages used in these studies. mBMSC viability for both pipette, and electrosprayed cells, were determined using 7-AAD staining assay and flow cytometry. Analysis at day 1, 7, and 14 shown that approximately 90 ± 0.9% , 89 ± 2.9%, 90 ± 0.4% cells remained viable for pipette and 80 ± 3.9%, 80 ± 2.6%, 79 ± 1.2% cells remained viable following BES (n-3) (Fig. 3.8 A and B). It was also shown that there was no significance between electrosprayed cells 80 ± 1.3% and non-BES mBMSC 90 ± 1.5 (Fig. 3.8 C). In addition, determining if cells were delivered in continuous distribution of even numbers during a spray period was also investigated. To demonstrate that mBMSC were not accumulating near the front or the back of the flow and BES at even rates into the collecting plate, we collected sequential fractions of cells as they emerged from the emitter. A suspension of mBMSC at 1 x10^6cell/mL in cα-MEM medium was sprayed at a flow rate of 5ul/min and 100µL, at ~3-6kV. Three sequential fractions were collected in individual wells of a 24 well plate. Theoretically, if the flow of cells was continuous, 1.166 x 10^6 cells should be present in each fraction. It was found that over three separate experiments, fractions 1, 2 and 3 contained 90 ±0.04% , 87 ±0.1% and 90 ± 0.02% of the theoretical value (Fig. 3.9). This indicates that the cells were being delivered in even numbers during the spray period.

A

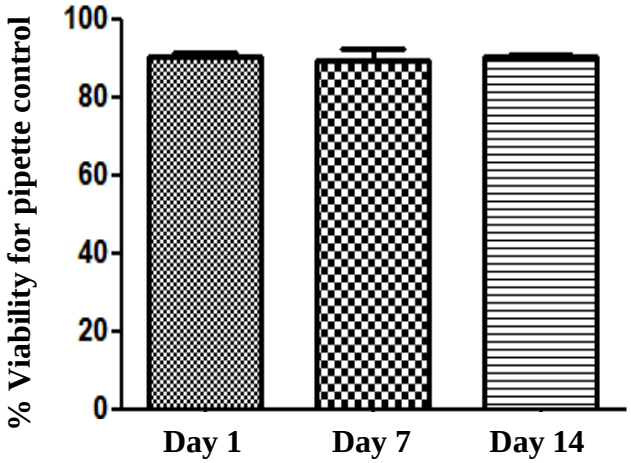
% Viability for pipette control
100
80
60
40
20
0
Day 1
Day 7
Day 14

B

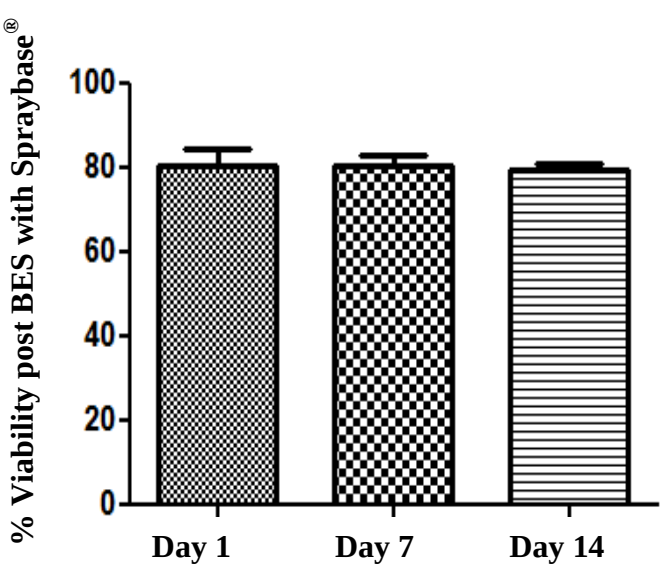
% Viability post BES with Spraybase®
100
80
60
40
20
0
Day 1
Day 7
Day 14

C

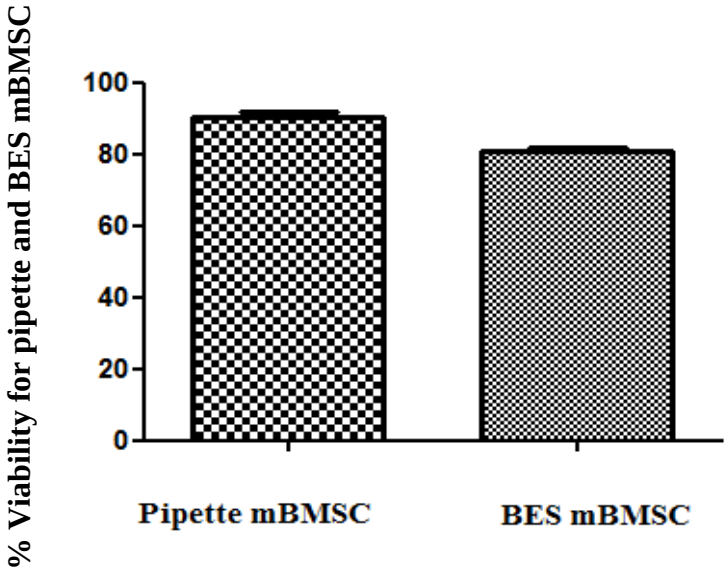

Fig 3.8 Viability of BES mBMSC. 1 x 10^6 mBMSC/mL in cα-MEM were either pipette or BES into three wells of 24-well plate using flowrate of 5μL/min, 30 gauge single needle, 22mm PD and voltages ~3-6kV on three separate days (day 1, 7, 14). Viability of mBMSC for both pipette (A), and electrosprayed cells (B) were determined using 7-AAD staining assay and flow cytometry. It was shown that approximately 90 ± 0.9% , 89 ± 2.9%, 90 ± 0.4% cells remained viable for pipette and 80 ± 3.9%, 80 ± 2.6%, 79 ± 1.2% cells remained viable following BES. (C) Demonstrates an average viability for both pipette and electrosprayed cells while also indicating there were no significant difference between the non-BES cells 90 ± 1.5% compare to the BES mBMSC 80 ± 1.3% (n=3).

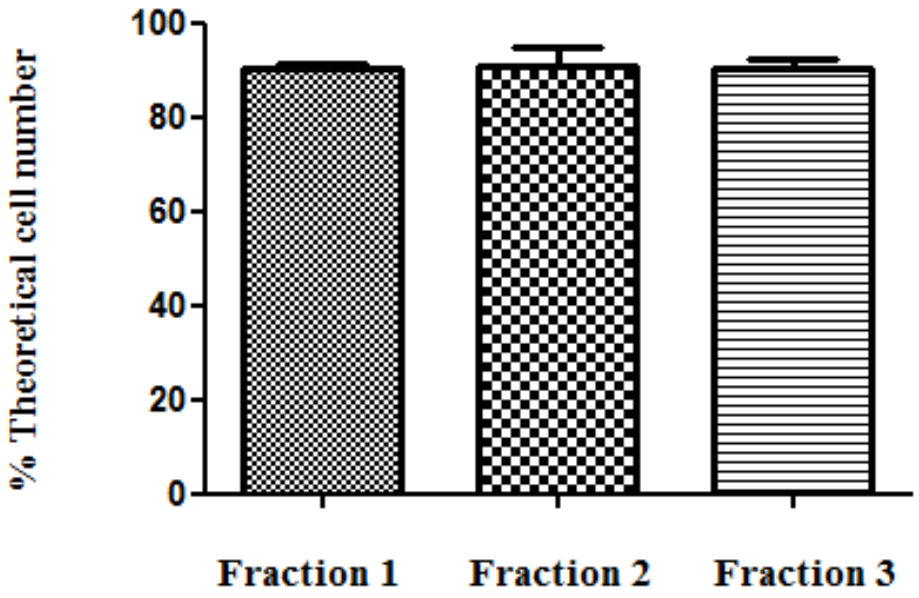

Fig 3.9 Distribution of BES mBMSC. A suspension of mBMSC at 1 x10^6cell/mL in cα-MEM medium was sprayed at a flow rate of 5ul/min and 100µL, at ~3-6kV. Three sequential fractions were collected in individual wells of a 24 well plate. Theoretically, if the flow of cells was continuous, 1.166 x 10^6 cells should be present in each fraction. It was found that over three separate experiments, fractions 1, 2 and 3 contained 90 ±0.04%, 87 ±0.1% and 90 ± 0.02% of the theoretical value. Analysis of sequential fractions demonstrated that cells were evenly distributed within the spray over the course of a 60 min spray (n=3).

3.8 Precision of spray emitted from the single needle configuration controlled the bio-electrospray mBMSC to target sites

Controlling the BES of mBMSC is essential in TERM studies primarily to ensure cells reach their intended sites of interest. mBMSC were BES onto commercially available polyethylene fabricated scaffolds in a circular shape, to determine the accuracy of the spray emitted from the single needle configuration. The scaffolds were immediately stained with Methylene blue, wherein a blue/purple circle on the scaffolds demonstrated the presence of cells, and the lack of Methylene blue elsewhere on the scaffolds indicated the spray exclusively emitted towards its targeted site (Fig. 3.10 B).

A similar study was carried out where mBMSC were BES to an intended area on the scaffold semi circular in shape. The scaffolds containing mBMSC were cultured in cα-MEM medium and Neutral Red stain. Although this is a vitality stain, it was used for observation purposes only in this study. A bright red semi-circle of BES mBMSC, in addition to a cluster of electrosprayed cells were observed on the scaffolds after 24hr (Fig. 3.11 B). In addition, brightfield images demonstrated similar results, while also showing no red staining in the surrounding areas at x4. This indicated that the spray emitting from the single needle configuration maintained a precision aim and BES mBMSC towards the target area (Fig. 3.11 D). Controls for both studies included mBMSC pipette onto scaffolds (Fig. 3.10 A and Fig. 3.11 A & C).

A

B

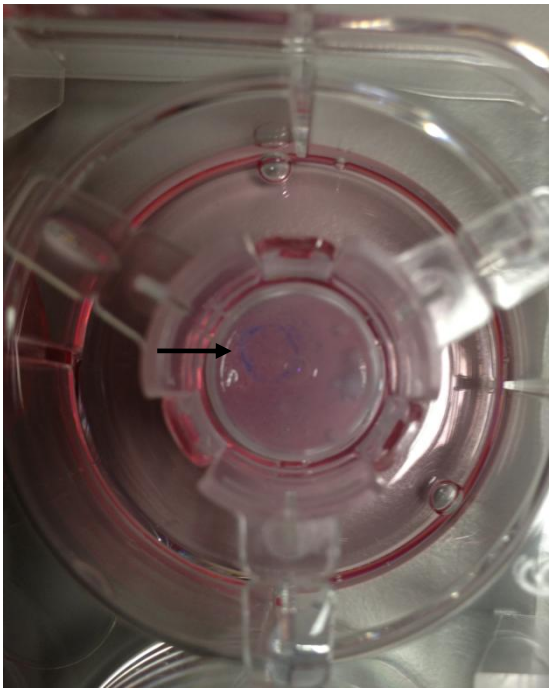

Fig 3.10 Accuracy of electrospray. Scaffolds were placed in transwell of 12-well plate and (A) Pipette mBMSC were dropped onto scaffold surface. (B) BES mBMSC were directed in a circular shape at ~3-6kV (depending on RH), flowrate of 5µL/min, PD of 22mm and 30 gauge needle. Scaffolds were immediately stained with Methylene blue following electrospraying revealing blue/purple circle of cells. This demonstrated a precision spray emitted from the single needle configuration of Spraybase®.

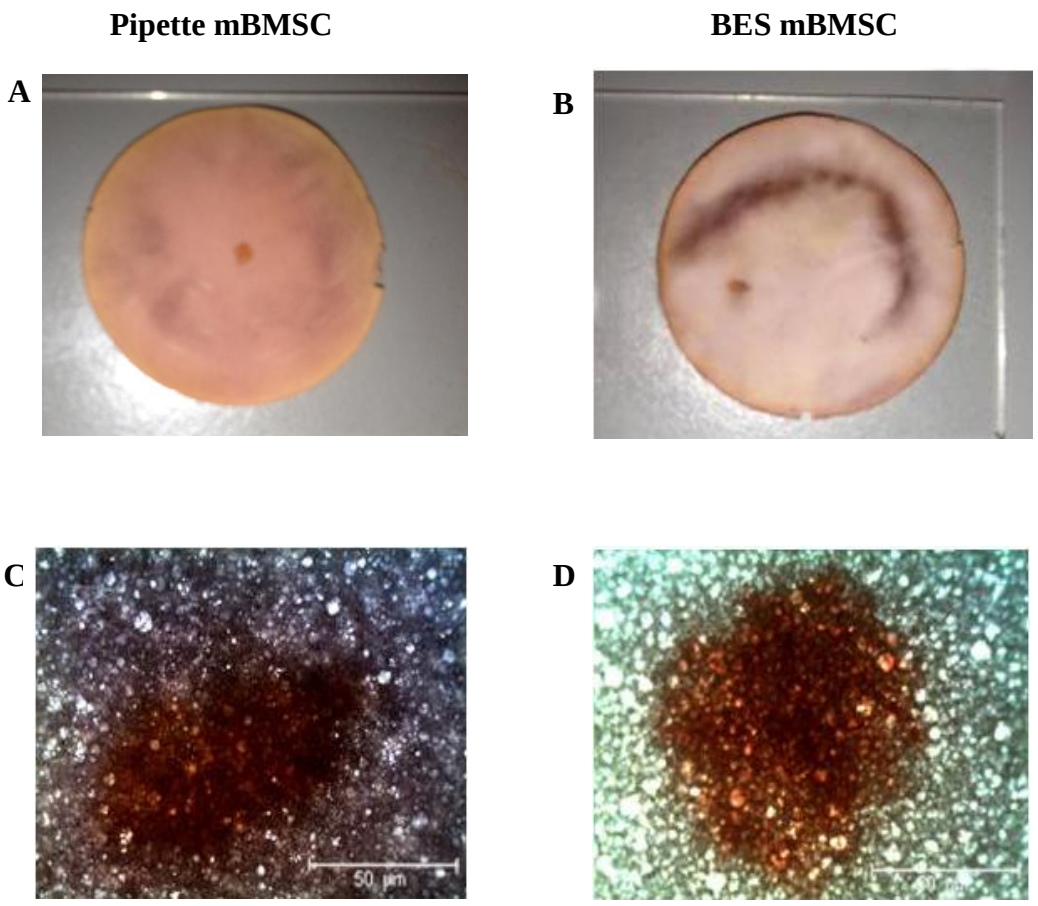

Fig 3.11 In-depth study for electrospray accuracy. (A) Pipette mBMSC and (B) BES mBMSC directed in a semi-circle in addition to cells electrosprayed to specific site on commercially available scaffolds. Brightfield images for (C) pipette mBMSC and (D) BES mBMSC on scaffold at x4 magnification. All scaffolds were stained with Neutral Red. Accuracy of BES mBMSC to intended sites on scaffolds demonstrated the precise control of spray from the single needle configuration of the commercial electrospray apparatus. The lack of staining in the surrounding areas as shown by brightfield imaging confirms this result. Parameters included ~3-6kV (depending on RH), flowrate of 5µL/min, PD of 22mm and 30 gauge needle.

3.9 Discussion

Vital electrospraying conditions such as jet stability and continuity are fundamentally affected by the apparatus set-up, liquid properties and external atmospheric conditions. Variations in in-house electrospray apparatuses and liquid solutions properties in different labs, directly impact on the parameters applied to achieve a stable, continuous Taylor cone. For the BES process, these parameters, in particular voltage, are critical to cell survival. Therefore, possessing a universal electrospray apparatus with a set of gold standard parameters has become a necessity for this cell delivery method. Furthermore, due to ambiguity in electrospray experiments, reproducing data between labs have proven near impossible. Hence, this study addresses these problems by using a commercially available electrospray apparatus, Spraybase®, to create a set of universal parameters, while developing non-toxic cell solutions with efficient properties for bio-electrospraying to occur.

In establishing reproducible parameters, selecting compatible liquid solutions to BES cells which coincide with the single needle/ring-shape electrode configuration of Spraybase®, was a critical component. As previously discussed, it's been widely reported that BES cells using a single needle causes an unstable Taylor cone with volatile sprays of cell solutions (Jayasingh *et al.*, 2006 a&b; Odenwalder *et al.*, 2007; Mongkoldhumrongkul *et al.*, 2009). This is primarily due to issues with solution properties such as viscosity and electrical conductivity. Previous reports by Sahoo *et al.* (2010) and Ye *et al.* (2014) have described how high cell number with a minimum of $1x10^6$ cells/mL counteracted low viscosity levels, making it possible to BES cells. These studies also described using saline solutions such as PBS to negate difficulties with electrical conductivity.

However, a key component to the success of these studies included the use of a coaxial needle when BES the cells. Using Spraybase® single needle configuration a stable, continuous Taylor cone was achieved, when high numbers of A549 cells were BES in common saline solutions, suggesting that the design of the commercial electrospray instrument supported this. In addition to Spraybase® single needle configuration, its ring-shape electrode also contributed to a successful electrospray of viable A549 cells in PBS and PBS+0.5M EDTA (Fig. 3.3). To date, this is the first study reported to successfully BES cells in solution using a single needle, at low voltages, thus making it a break-through in electrospraying cells.

Following this success, the next study was to prove that the parameters established herein regarding BES A549 were reproducible using a different cell type. Substituting the immortalised cell line A549 cells with primary mBMSC, cells were BES using identical parameters. Preliminary studies demonstrated that mBMSC electrosprayed at the exact same parameters. This indicated the commercial electrospray was capable of BES any cell type using the optimal parameters, suggesting reproducing data is achievable between experiments. However, further analyses demonstrated that mBMSC numbers had reduced significantly in comparison to initial studies with A549 cells following BES (Fig. 3.4). One possible explanation for this was due to the cell size. A549 cells are significantly smaller than mBMSC and it was hypothesised that mBMSC were too large to emit from the 30 gauge single needle. However, having preformed similar studies described in Fig. 3.2 and Table 4, it was quickly discovered that in addition to cell size, the number of cells involved and flowrate velocity, did not influence the quantity of viable mBMSC electrosprayed using this system.

Further studies revealed it was the saline solutions in which the cells were suspended, that proved detrimental to the BES high yields of viable mBMSCs. The cell solutions consisting of either PBS or PBS & 0.5M EDTA contained little to no nutrients for cell survival. The immortalised A549 cells are far more robust when surviving in unfavourable conditions compared to primary mBMSC cells. It was suggested that the lack of nutrients within the cell solutions may have account for limited cell viability, while cells were suspended in solution between experiments. Therefore, when mBMSC suspended in their own media (cα-MEM) were BES, a significant increase of sprayed cells was observed in the culture wells, after 24hrs (Fig. 3.5). These cells also retained vital MSC characteristics such as adhesion to plastic post electrospray, suggesting the low voltages were not having any immediate effect on the cells. This was confirmed by viability assays which determined that approximately 80% of mBMSC that were BES remained viable (Fig. 3.8).

High ion charges from primary cells in addition with the culture medium, resulted in a highly conductive cell suspension (22.18mS/cm). Applying voltages to the highly electrically charged cell solution should have resulted in sparking and cell death. Interestingly however, it emerged to have a counter effect with positive results in relation to lowering amount of voltage applied for our experiments. It is suggested that the design of the Spraybase® single needle/ring electrode configuration, in combination with mBMSC culture medium, which provided a balanced environment compatible with BES viable mBMSC, using reproducible parameters, at low voltages (~3-6kV).

As previously discussed achieving and maintaining a stable, continuous Taylor cone is essential to any electrospray experiment. Mongkoldhumrongkul *et al.* (2009) reported that they wanted to be the first to BES hTERT immortalized MSC at low voltages. However, they stated that jet stability and continuity was not a primary focus. Although they attempted to electrospray the cells at ~10kV using a coaxial needle, they eluded to the fact that jetting took place in an "unstable mode". This prompted the group to investigate other jetting methodologies such as aerodynamically assisted bio-jets (AABJ) for cell delivery.

Our studies demonstrated that the commercial electrospray apparatus at optimal parameters can generate two types of stable electrospray modes. This was depended on cell number within culture medium. mBMSC numbers were increased from $1x10^6$ - $6x10^6$ cells/mL to initially determine if a specific cell number was relevant to establishing optimal parameters for the commercial electrospray. Spraybase® visualization system demonstrated that the amount of cells did not affect the parameters applied, however, cell number significantly influenced the mode of electrospray generated. Sprays alternated between a plume and a jet mode when cells increased from $1x10^6$ cells/mL to $3x10^6$ cells/mL (Fig. 3.6 A & B). Unlike a coaxial needle where cells and liquid solutions are separate, the internal diameter of a single needle is required to accommodate both. By increasing the amount of cells in the solution possibly forced the cells into a central ligament, resulting in a jet mode emitting from the needle. Conversely, lower cell numbers in suspension indicated the solution was more liquid, allowing freedom for the spray to follow the shape of ring electrode. This type of spray covered more surface area of the well of collecting plate, which was also recorded by Odenwalder *et al.* (2009).

A continuity study indicated that BES mBMSC were evenly distributed into different culture wells, with high numbers spraying in solution for either mode (Fig. 3.9).

Establishing the different types of spray modes was carried out between voltages of ~3-6kV depending on the RH. In addition to cell numbers, determining if voltage contributed to spray mode variation was investigated when mBMSC were BES at 10kV. Studies by Mongkoldhumrongkul *et al.* (2009), Sahoo *et al.* (2010) and Ye *et al.* (2014) all successfully BES stem cells at 10kV. However, once 10kV was applied to the solution of cells, the spray immediately became erratic and volatile, intermittently emitting the cell solution from the needle tip (Fig. 3.6 C). Sparking was observed on several occasions, immediately ending the experiment due to the danger to the user. The low numbers of mBMSC which successfully electrosprayed at this voltage, did not retain MSC morphology. In addition, cell debris was scattered throughout the culture well (Fig. 3.7). These results suggested that the high voltage induced cell death. Lowering the voltages to 7kV demonstrated similar results to studies carried out between ~3-6kV. When cell numbers were increased a BES of cells in jet mode was established. Similarly when cell numbers were decreased, a plume spray of BES mBMSC was observed, regardless of the voltage applied.

Our final optimization study in the creation of a set of gold standard parameters to use with a commercial electrospray, for the sole purpose of reproducing data involved verifying accuracy of spray emitting from the needle. Directing an electrospray of cells towards an intended target site is crucial to delivery of cells when using jetting methodologies.

In addition, Choi *et al.* (2008) and Ghasemi-Mobarakeh *et al.* (2008) described aligning stem cells onto scaffolds to grow in the direction of aligned fibres. This enhanced cell adhesion and proliferation for both skeletal muscle cell and nerve cells respectively. mBMSC were BES in circular shapes onto commercially bought scaffolds and stained with two different staining materials. The results demonstrated that the cells reached the intended target site indicating a precision electrospray was emitting from the single needle. In addition, the cell solution was controllable as the cells BES into circular shapes, as directed by the user. This demonstrated that this type of control and precision may prove advantageous in alignment studies, as cells can BES in even distribution along a contour. This assembly of cells is far more precise and intricate in comparison to seeding cells with a pipette in alignment along scaffold fibres (Fig. 3.10 and Fig. 3.11). The lack of staining elsewhere on the scaffolds further indicated that the BES mBMSC settled only at their intended areas.

In summary, this study demonstrated that the commercially available electrospray apparatus can BES various cell types using specific parameters, generating a system for reproducing data between labs. Significantly this study demonstrated that a stable Taylor cone can be achieved using the single needle configuration at low voltages, a result thus far, which has not yet been reported. In addition, the BES of cells from the needle includes a continuous electrospray of high yields of viable cells, with mBMSC still maintaining vital MSC characteristics. These results indicated that the low voltages are not affecting the cells. The BES has displayed great precision in cells reaching intended target site while also demonstrating meticulous control over spray.

Furthermore, BES mBMSC in different circular shapes indicates that this system could be beneficial to new method in TE whereby cells maybe aligned along fibres which may prove beneficial to skeletal and nerve studies.

Chapter 4

Optimisation of a commercial electrospinning apparatus and the establishment of optimal process and solution parameters to electrospin new polymer solutions involving: PEO, Collagen and Agarose

4.1 Introduction

Electrospinning is a well documented technique that can generate fibrous structures of nano – to micrometre diameter. These fabricated constructs should mimic the structure and functions of natural ECM components (Chen *et al.* 2007; Chen *et al.* 1998). Advances in electrospinning technologies for tissue engineering have been described previously in several reviews which discuss the importance of various criteria such as the electrospinning apparatus, voltage parameters, polymers, surface areas, fibre and pore sizes, scaffold morphology, cell types and growth factors, when electrospinning fibres (Rim *et al.* (2013); Tamayol *et al.* (2013); Shin *et al.* (2012); (Agarwal *et al.* (2008); (Huang *et al.* (2003)).

As previously discussed (chapter 1), modern electrospinning instruments are manufactured based on a design by Baumgarten (1971). The fundamental principles include using a power supply to induce high voltage in order to charge a polymer solution, contained in a syringe. Since this is an inexpensive method for scaffold fabrication, most systems are in-house set-ups. Consequently, optimal conditions for electrospinning vary between the different polymer/solvent systems, wherein each system parameters must be optimised through a time consuming process. Furthermore, this adversely affects the ability to reproduce results between experiments, as there are no set of standardised parameters for electrospinning fibres.

In addition to the apparatus, particular consideration must be given to the types of polymers used when electrospinning fibres. Physical and chemical properties of polymers directly influence whether electrospinning can be achieved.

These properties determine the outcome of scaffold surface topography and fibre morphology, in addition to fibre and pore size.

Both organic and synthetic polymers have been used in the development of artificial 3D constructs. Although hydrophilic organic polymers such as chitosan, collagen, gelatin and fibrin provide cell adhesion and vital cellular signals, they have poor mechanical properties and are relatively weak. In contrast, hydrophobic synthetic polymers, such as polylactic acid (PLA), polyglycolic acid (PGA), and their copolymers including FDA-approved poly(lactic-co-glycolic acid) (PLGA), provide easy control of microstructure, strength and degradation rate. However, these polymers lack growth factors and other signals to direct cell growth, proliferation and differentiation. There is no universal solvent for both hydrophilic natural polymer and hydrophobic synthetic polymers so the polymers cannot simply be blended together. Therefore, a range of new techniques are being developed for the generation of hybrid scaffolds.

The primary aim of this study was to address the problems associated with (1) the time consuming process of establishing parameters for in-house built electrospinning apparatuses, (2) electrospinning hybrid polymers and (3) issues associated with experimental replication. These obstacles were addressed by modifying the commercial electrospray apparatus to electrospin common polymers such as poly(ethylene oxide) (PEO) and polyethylene glycol (PEG), generating a set of standardised parameters for these polymers and system. PEO and PEG were blended either together, and/or with organic polymers to create novel hybrid polymer blends.

The resultant electrospun fibres were examined in relation to scaffold surface texture, fibre morphology, and fibre and pore sizes.

4.2 Modified electrospray apparatus capable of electrospinning fibres

Several studies have accredited the success of their functioning, 3D fabricated constructs, to the design of their in-house built electrospinning systems. Li *et al.* (2013) developed a novel method whereby they combined micropatterning using a femtosecond laser, with electrospinning. This technique allowed for the fabrication of porous structures with microchannels that can direct hMSC cellular responses. Whereas Wang *et al.* (2009) developed a technique for rapid fabrication (<3 h) of scaffolds by simultaneously electrospinning elastase-sensitive polyurethaneurea (PUTU) nanofibres while electrospraying and encapsulating growth factor IGF-1 into poly (lactide-co-glycolide) (PLGA) microspheres. During the electrospinning/electrospraying process, these nanofibres were assembled into scaffolds. Although these studies have shown some success in addressing issues associated with artificial constructs, their systems are highly complex. For other groups to attempt and replicate these systems may prove near impossible. We propose that the commercially available Spraybase® instrument could be used to standardise instrumentation between experiments. We therefore examined if and how Spraybase® could be used to electrospin fibres.

Ground electrode shape was modified from ring-shape into a rectangular-shape. Electrode lengths measuring from 100mm – 500mm were investigated to electrospin fibre meshes. It was found that the ground electrode approx 300mm provided the adequate length to encourage fibres to attach to the sides of the electrode (Fig. 4.1 A). This allowed for a build up of thin layers, ultimately resulting in a fibrous mesh (Fig 4.1 B).

Several process parameters were adjusted including voltage, needle gauge, flowrate and PD to electrospin PEO/PEG/agarose, PEO/collagen/cα-MEM culture medium and PEO/agarose/cα-MEM culture medium, fibres using this device. Table 5 demonstrated the conditions favourable with successful electrospinning of fibres and are highlighted in red. Those shown in black indicate the parameters examined but cannot fabricate fibres using this device. It was found that temperatures above 32°C and RH over 50% significantly influenced electrospinning from occurring. Therefore, those highlighted in red where further analysed to determine optimal parameters to electrospin fibres with either/or PEO and PEG included in the polymer blends. Optimal electrospinning parameters for this instrument include, 3μL flowrate, with voltages varying between ~7-9kV, using single needle configuration with 23 gauge conducting needle at a potential difference of 24mm.

A

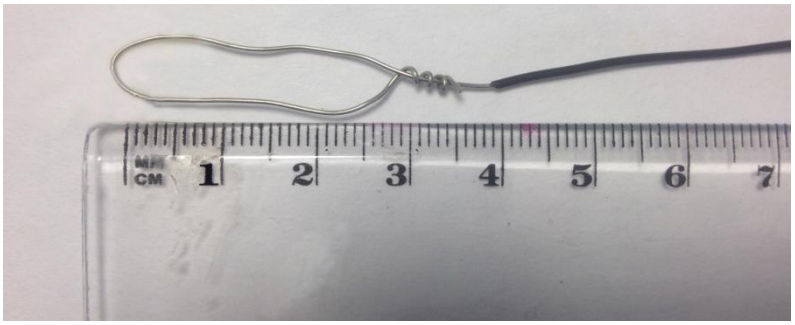

B

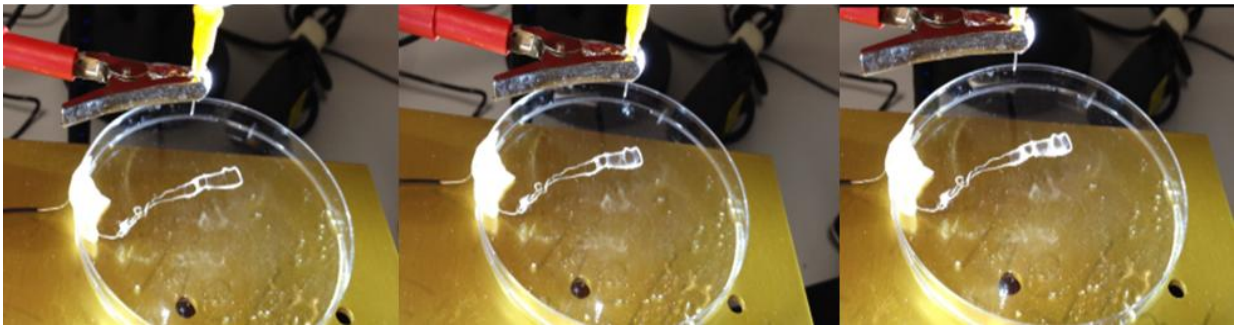

Fig. 4.1 Configuration of electrospinning set-up. (A) Rectangular-shape ground electrode measuring approx 300mm to support mesh fabrication. (B) Optimal parameters for electrospinning fibres using 'Generation 1' BES instrument supplied by AVECTAS. Flowrate 3µL, voltage ~7-9 kV, 23 gauge conducting needle, with potential difference of 24mm. Photographs taken at various stages of the electrospinning process.

Table 5: Summary of parameters wherein polymer blends involving PEO and/or PEG electrospun fibres (red) and parameters examined but unsuccessful in electrospinning fibres (black) using single needle configuration and ring-shape electrode.

Flow Rate (µL/min)	**Voltage (kV)**	**Single Needle (Gauge)**	**Potential Difference (mm)**	**Temperature (°C)**	**Relative Humidity (%)**
1	3.50	23	17	15.6	29.4
2	3.55	27	19	17.5	30.5
3	4.00	30	20	18.5	36.7
4	4.55	32	22	19.4	39.2
5	5.55		23	20.0	41.3
6	6.00		24	20.1	45.2
	6.55		25	20.6	46.3
	7.50		26	22.5	46.9
	7.55		27	23.8	48.0
	7.90			25.3	51.4
	8.50			28.0	55.6
	8.80			29.5	56.6
	9.3			30.0	58.0
				31.3	60.3
				31.5	
				32.6	

4.3 Generation of novel organic and synthetic polymer blends for electrospinning process with commercial electrospray

Initial electrospinning studies involved using both PEO and PEG. Although these polymers have critical features required for electrospinning purposes such as high viscosity levels and strong elasticity capabilities, it is widely reported that these solutions will dissolve easily at room temperature. Having attempted and failed to electrospin numerous concentrations of these two polymers, agarose, a polysaccharide polymer generally extracted from seaweed, was introduced to the polymer blend. Bonino *et al.* (2011) had previously described using alginate which is also a natural polysaccharide extracted from seaweed, to successfully electrospin alginate-based nanofibres in combination with PEO. Agarose has similar properties to alginate thus the reason for its selection to this polymer blend. In addition to providing increased viscosity to polymer mix for electrospinning to occur, agarose also acted as a strengthening agent for the scaffolds.

PEO/PEG/agarose scaffolds were electrospun using Spraybase® and optimal processing parameters, at varying agarose concentrations (Table 6). Ambient parameters particularly RH, significantly influenced agarose polymer concentrations present in the mixture, while also impacting on whether electrospinning of these scaffolds transpired. Increasing RH from 30 – 40% resulted in increased agarose polymer concentrations (w/v), while electrospinning ceased functioning completely, when RH rose above 40%. Some success was achieved with this polymer combination, but the resulting mesh proved extremely fragile. No analyses were performed on this fibrous construct as it dissolved at room temperature almost immediately post spinning.

Table 6: Summary of PEO/PEG/Agarose solutions electrospun at various concentrations using optimal parameters of flowrate 3µL/min, voltage ~7-9kV. 23 gauge single needle and PD 24mm.

PEO/PEG/Agarose **30%w/v/50%w/v/25%w/v**		**PEO/PEG/Agarose** **30%w/v/50%w/v/50%w/v**		**PEO/PEG/Agarose** **30%w/v/50%w/v/100%w/v**	
Ratio: PEO/PEG/Agarose	**Spun Fibre Y/N**	**Ratio: PEO/PEG/Agarose**	**Spun Fibre Y/N**	**Ratio: PEO/PEG/Agarose**	**Spun Fibre Y/N**
1: 0.1 :0.9	N	1: 0.1 :0.9	N	1: 0.1 :0.9	N
1: 0.2 :0.8	N	1: 0.2 :0.8	N	1: 0.2 :0.8	N
1: 0.3 :0.7	N	1: 0.3 :0.7	N	1: 0.3 :0.7	N
1: 0.4 :0.6	N	1: 0.4 :0.6	N	1: 0.4 :0.6	Y
1: 0.5 :0.5	N	1: 0.5 :0.5	Y	1: 0.5 :0.5	Y

4.4 Collagen versus Agarose as a primary polymer in fabrication of novel electrospun scaffolds

The fundamental objective when fabricating fibres is to mimic the natural ECM, ultimately encouraging cell adhesion and survival *in vivo*. Collagen is a major insoluble fibrous protein in natural ECM and connective tissue, making it a preferred material when fabricating artificial 3D constructs as seen in studies by Prabhakaran *et al.* (2009), Chan *et al.* (2009) and Kazemnejad *et al.* (2009). Therefore, commercially sourced 3D collagen I Rat Tail was combined with PEO and MSC cα-MEM culture medium, to create a novel polymer mix. PEO was selected due to its superior viscosity properties, compared to PEG, while the presence of cα-MEM culture medium was to provide nutrients to cells. Additionally, results from electrospinning PEO/PEG/agarose fibres although week, proved promising, prompting further investigations into the use of agarose in electrospinning. Thus, a second polymer mix was created, combining agarose with PEO and cα-MEM culture medium.

Numerous concentrations of PEO, collagen, cα-MEM culture medium and agarose were examined in order to electrospin PEO/collagen/cα-MEM, and PEO/agarose/cα-MEM fibres, using Spraybase® commercial electrospray. Final optimal concentrations for commercially bought 3-D collagen and PEO were 2% and 30% w/v respectively. However increasing agarose polymer to a final concentration of 150% w/v, provided the best viscosity levels essential for fabrication of PEO/agarose/cα-MEM scaffolds. It was also recorded that by increasing the ratio of PEO to collagen or agarose, and culture medium x6 (6:1:1), both polymer blends electrospun fibres at flowrate 3μL/min and PD of 24mm.

Voltage was inconsistent for collagen based scaffolds and fluctuated constantly between ~6-9 kV, within the same experiment. In contrast, agarose based scaffolds electrospun repetitively between 6-7 kV regardless of the experiment.

Environmental parameters such as temperature and RH impacted on scaffold fabrication for both polymer mixtures. It was near impossible to electrospin fibres above 32°C or with RH of 50%. However, once parameters reached optimal conditions, solid PEO/collagen/cα-MEM and PEO/agarose/cα-MEM scaffolds were fabricated, and their surface texture, pore and fibre sizes investigated.

4.5 Contrasting surface topography for collagen and agarose based scaffolds

Surface topography refers to the surface texture of a scaffold. It is generally characterised by a predominant surface pattern and its surface roughness. This "roughness" is a measure of the finely spaced surface irregularities (Degarmo *et al.*, 2003). Functional 3D scaffolds can electrospin fibres in various patterns including "random pattern" or "aligned patterns". These contribute in providing the scaffolds with strong, smooth, flat surface textures, in order to accommodate cell viability and cellular responses such as adherence, proliferation and differentiation.

4.5.1 Surface topography for electrospun PEO/collagen/cα-MEM scaffold

The surface texture for electrospun PEO/collagen/cα-MEM scaffolds was initially examined visually, by eye. The surface was found to be a rough mesh, with apertures sporadically located within the scaffold (Fig. 4.2 A). Brightfield microscopy confirmed these observations with perforations visible throughout the scaffold (Fig. 4.2 B). It was also apparent that several layers of fibres electrospun at some areas on the rectangular-ground electrode, while minimum layering was formed at others (Fig. 4.2 C). Further investigations using scanning electron microscope (SEM) revealed the extent of irregularities in the surface texture for these scaffolds. Although fibres were electrospun in a random pattern, the amount of inconsistencies in the fibrous layers covering the electrode demonstrated the random pattern was not intentional, but more accidental as to wherever the fibres settled (Fig. 4.3 A & B). Furthermore, SEM demonstrated inconsistencies in fibre morphology. In addition to fibre thickness, random bead shape globules were also present (Fig. 4.3 C). Gaps and tears were observed throughout the construct indicating fabrication of a week scaffold.

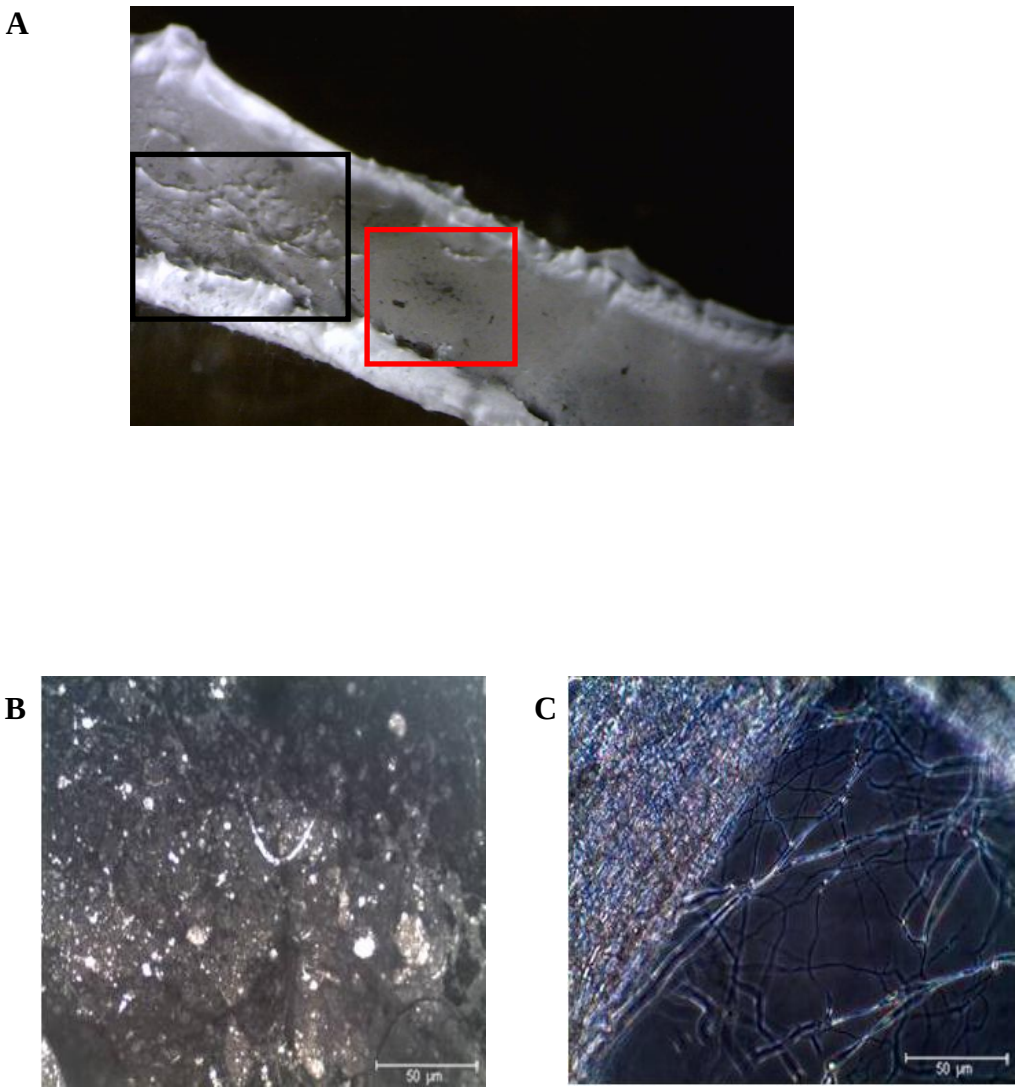

Fig 4.2 Surface texture for PEO/collagen/cα-MEM scaffold at ratio 6:1:1. (A) Photograph exposing rough surface texture (black box) with perforations (red box) throughout scaffold. (B) Brightfield image of holes within scaffold at x4. (C) Brightfield imaging of fibrous mesh layers electrospun at one position, while disregarding other areas at x4. Optimal parameters used involved flowrate 3µL/min, voltage ~7-9kV. 23 gauge single needle and PD 24mm.

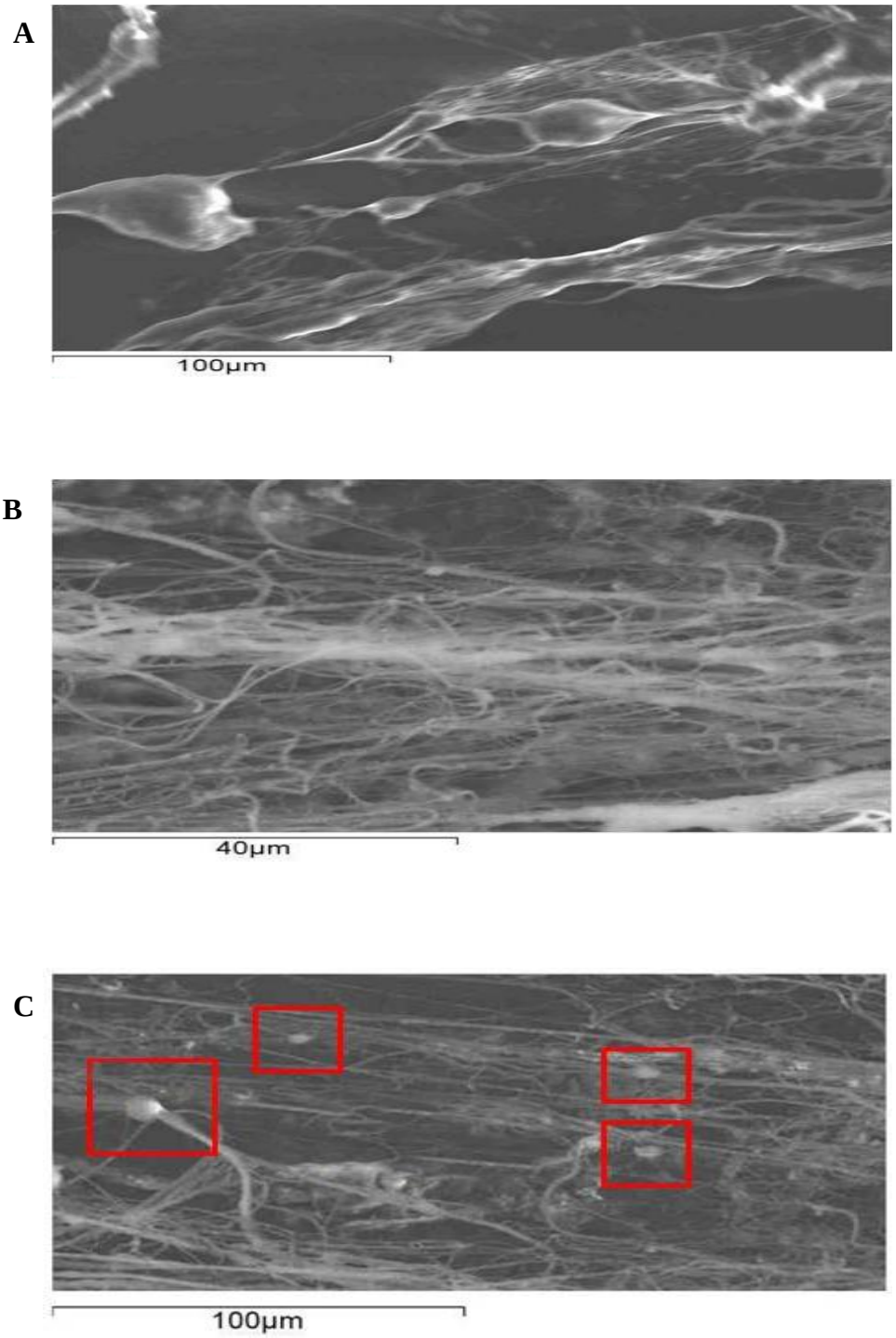

Fig 4.3 SEM of surface texture for PEO/collagen/cα-MEM scaffolds at ratio of 6:1:1. (A) Limited electrospun fibrous layer with inconsistent fibre morphologies. (B) Abundant fibrous layers in random pattern settled at a specific scaffold location on ground electrode. (C) Bead formation on scaffold. Optimal parameters used involved flowrate 3µL/min, voltage ~7-9kV. 23 gauge single needle and PD 24mm.

4.5.2 Surface topography for electrospun PEO/agarose/cα-MEM scaffold

In contrast to the collagen based scaffold, surface texture for PEO/agarose/cα-MEM scaffold revealed a smooth, even surface, with no obvious perforations (Fig. 4.4 A). Brightfield microscopy confirmed these findings with images showing flat, uniform scaffold surface featuring consistent layers of PEO/agarose/cα-MEM fibres at x10 (Fig.4.4 B). When compared to a commercially available pre-fabricated polyethylene scaffold using brightfield imaging, results demonstrated that both scaffolds appear to have the similar surface textures. This indicated that the agarose scaffolds were more cohesive than the collagen-based scaffolds, suggesting that the former agarose electrospun fibres have similarities with apparent conventional fibre properties, when using the commercial apparatus (Fig. 4.4 B & C).

SEM imaging further demonstrated random pattern fibres were electrospun, creating a stable mesh, covering all areas of the construct. Fibre morphology appeared homogeneous with little to no bead formation (Fig 4.5).

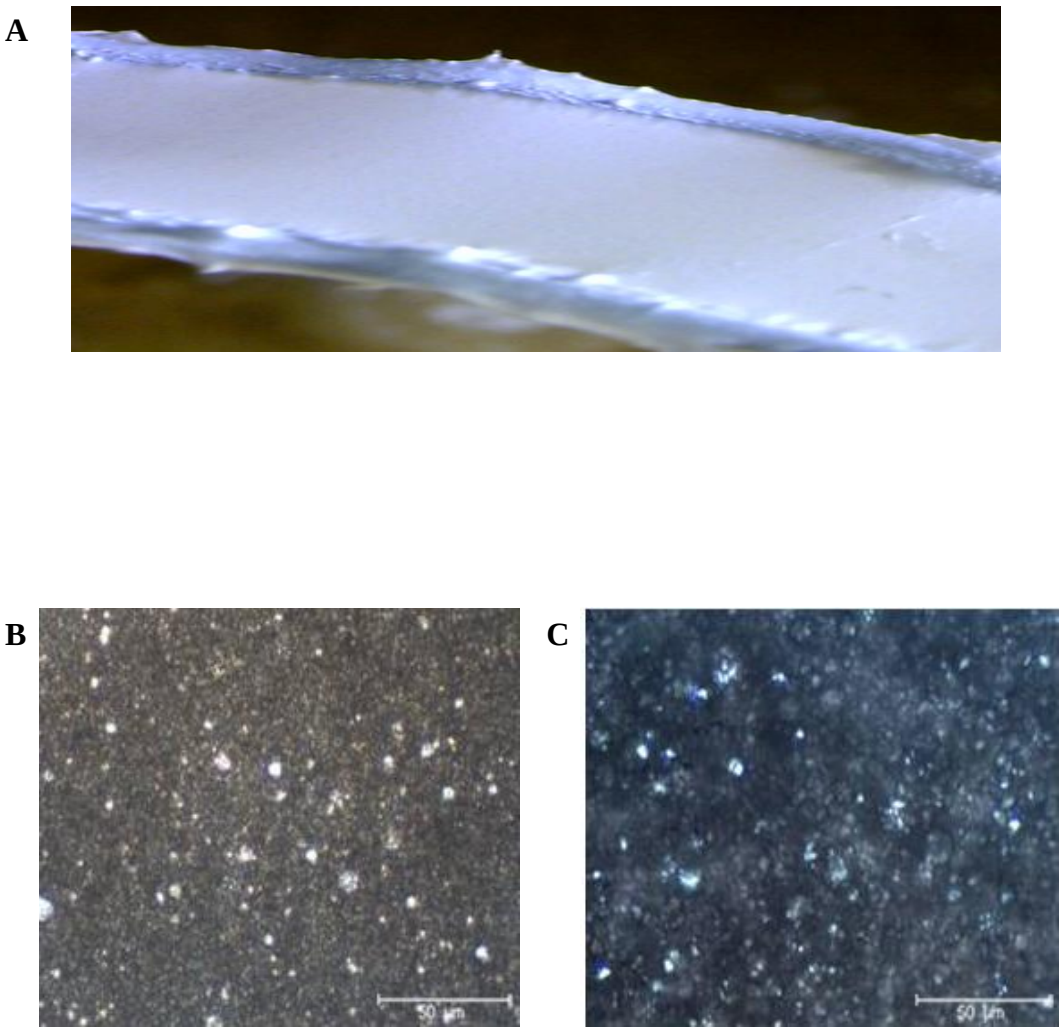

Fig 4.4 Surface texture for PEO/agarose/cα-MEM scaffolds at ratio 6:1:1. (A) Photograph of smooth, even surface texture with no obvious perforations. (B) Brightfield image of PEO/agarose/cα-MEM scaffold surface texture including pores at x10. (C) Commercially available pre-fabricated polyethylene scaffolds at magnification x10. PEO/agarose/cα-MEM scaffold demonstrate similar surface texture to commercially bought polyethylene scaffolds. Optimal parameters used for electrospinning fibres involved flowrate 3µL/min, voltage ~7-9kV. 23 gauge single needle and PD 24mm.

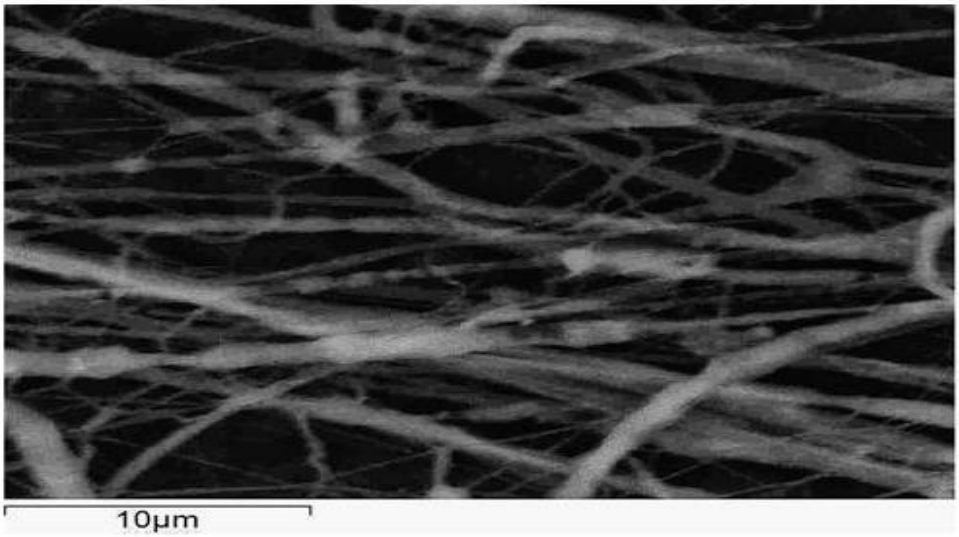

Fig 4.5 SEM of surface texture for PEO/agarose/cα-MEM scaffolds at ratio 6:1:1. Fibres electrospun in a random pattern. Fibres are uniform and appear to assemble in consistent layers. This is seen for all PEO/agarose/cα-MEM scaffolds. Fibres electrospun using optimal parameters of flowrate 3µL/min, voltage ~7-9kV. 23 gauge single needle and PD 24mm.

4.6 Extensive pore size variation in collagen scaffolds contrasted with homogenous pore sizes for agarose scaffolds

An inherent limitation to using electrospun scaffolds in TE applications is small pore size. This has proven to be a major problem as mammalian cells varies in size making infiltration for large cells, such as MSC, through scaffolds almost impossible. Migration of cells through a biodegradable scaffold is crucial for successful transplant and healing of a synthetic graft onto a defect. Additionally, small pore sizes restrict nutrient delivery and the removal of biomaterial waste.

SEM analyses indicated that electrospun PEO/collagen/cα-MEM scaffolds comprised of various pore sizes throughout the scaffold. Smallest pore size recorded was 10.1μm, with the largest pore size measuring at 75.1μm (Fig.4.6). In comparison, electrospun PEO/agarose/cα-MEM demonstrated uniform pore sizes ranging from 5.97μm – 6.38μm (Fig. 4.7). These results were consistent for several electrospun collagen and agarose scaffold.

A

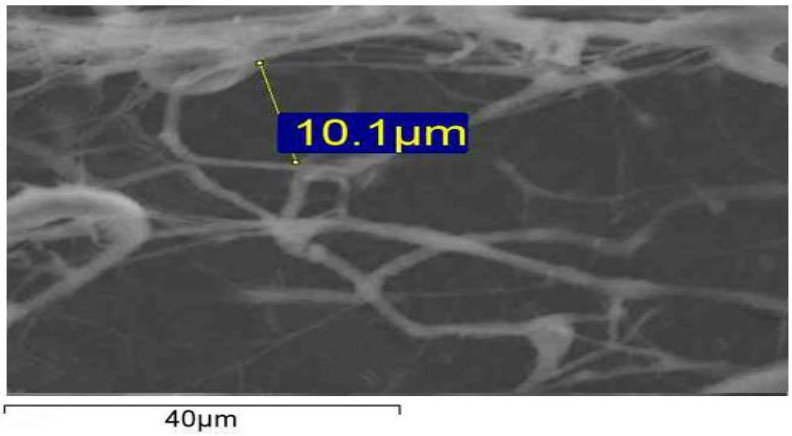

B

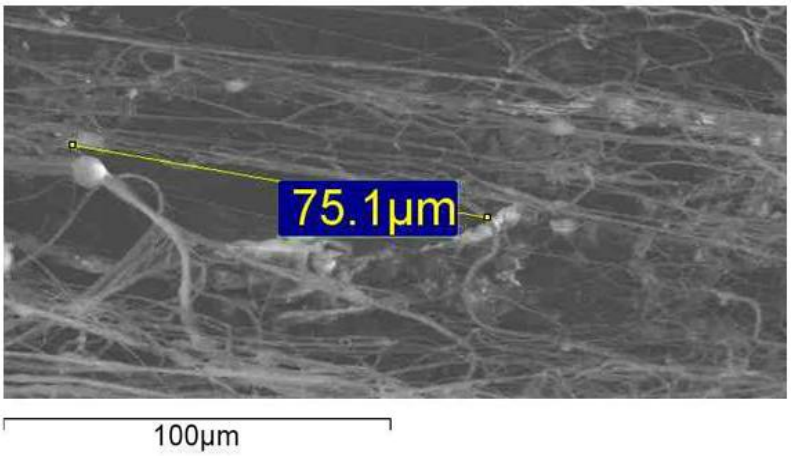

Fig 4.6 SEM of pore sizes for PEO/collagen/cα-MEM scaffolds at ratio 6:1:1. (A) Smallest pore size recorded. (B) Largest pore size recorded. Fibres electrospun using optimal parameters of flowrate 3µL/min, voltage ~7-9kV. 23 gauge single needle and PD 24mm.

A

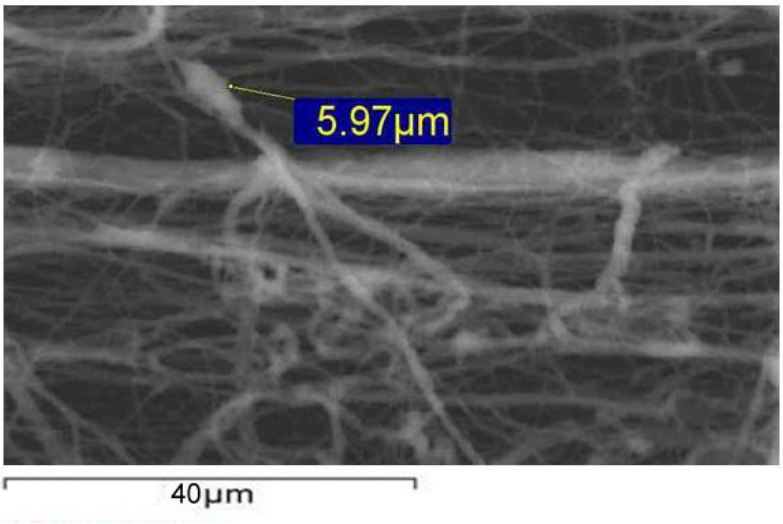

B

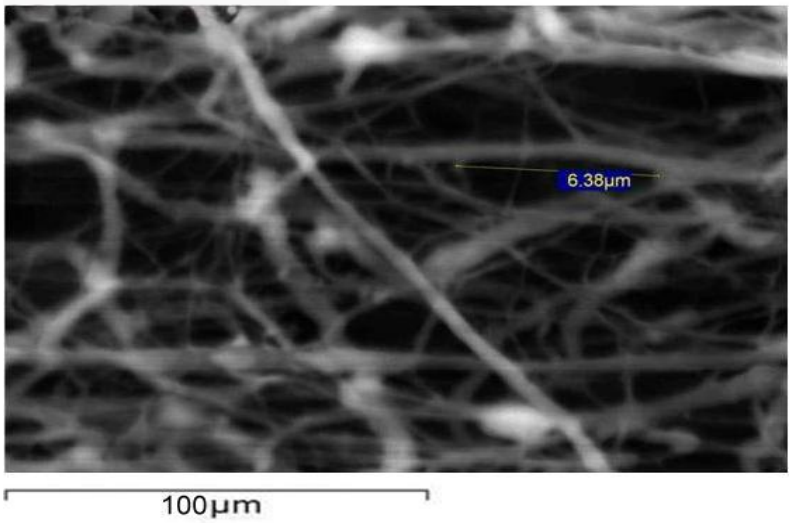

Fig 4.7 SEM of pore sizes for PEO/agarose/cα-MEM scaffolds at ratio 6:1:1. (A) Smallest pore size recorded. (B) Largest pore size recorded. Pore sizes appear consistent. Fibres electrospun using optimal parameters of flowrate 3µL/min, voltage ~7-9kV. 23 gauge single needle and PD 24mm.

4.7 Electrospun PEO/collagen/cα-MEM fibre diameters varied in thickness compared to uniform PEO/agarose/cα-MEM fibres

Electrospun fibres provide scaffolds with critical similarities to natural ECM. Establishing an ideal fibre size is vital when electrospinning fibres as they can provide excellent interconnectivity and control porosity of scaffolds (Pham *et al.*, 2006). Scaffold fibres can range from nano - micro scale. However nanofibres are preferred, as they have been cited on numerous occasions to closely mimic natural properties of the ECM (Rim *et al.*, 2013; Ladd *et al.*, 2011; Pham *et al.*, 2006).

Fibre diameters for both collagen and agarose type scaffolds were investigated. SEM analyses indicated electrospun fibre diameters for PEO/collagen/cα-MEM ranged from 795nm - 3.18μm (Fig 4.8). In addition SEM imagining also demonstrated fibre diameters for PEO/agarose/cα-MEM scaffolds measured between 1.57μm – 1.58μm (Fig. 4.9). Although fibre thickness remained uniform amongst agarose scaffolds, fibre diameters remained at micro level. Mean results consistent with several constructs fabricated using these polymer mixtures.

A

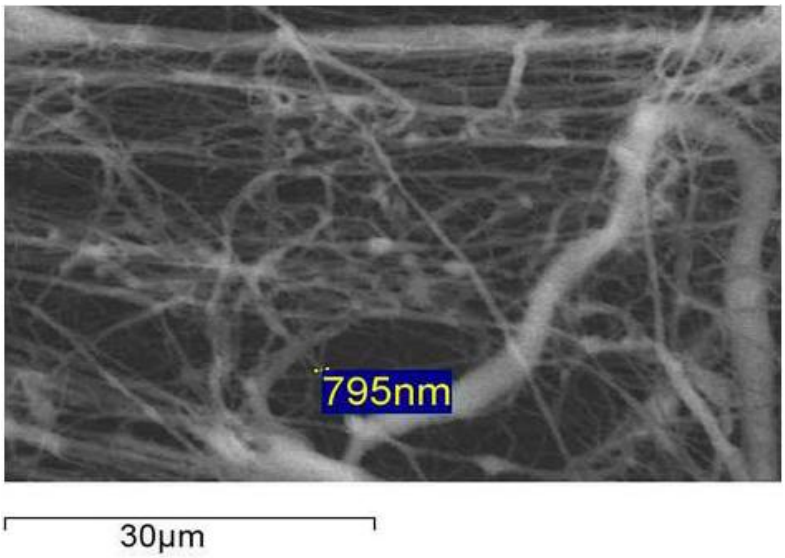

B

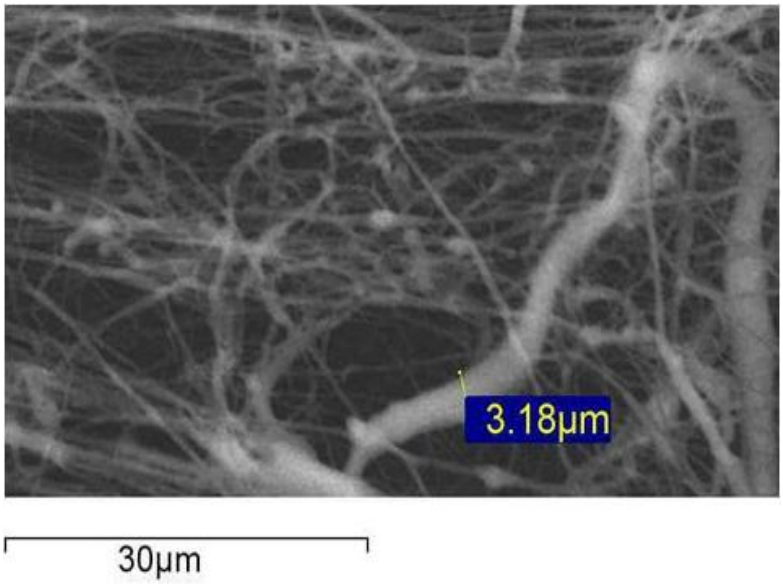

Fig 4.8 SEM of fibre diameters for PEO/collagen/cα-MEM scaffolds at ratio 6:1:1. (A) Thinnest fibre diameter recorded for these scaffolds. (B) Thickest fibre diameter evident for these scaffolds. Wide variation in fibre diameters was observed using SEM for electrospun scaffolds using optimal parameters of flowrate 3µL/min, voltage ~7-9kV. 23 gauge single needle and PD 24mm.

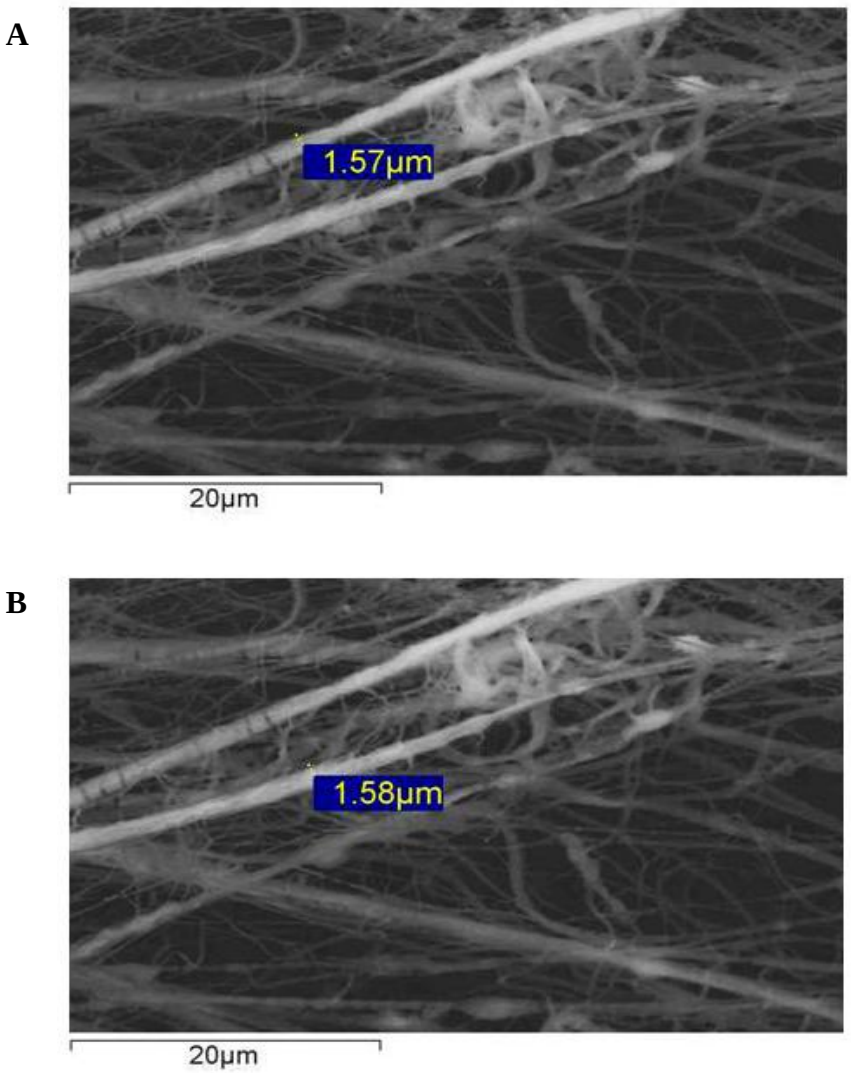

Fig 4.9 SEM of fibre sizes for PEO/agarose/cα-MEM scaffolds at ratio 6:1:1. (A) Thinnest fibre diameter recorded. (B) Thickest fibre diameter measured. Based on several fabricated constructs fibre size appear uniform in diameter, yet remain at the micro level. Fibres electrospun using optimal parameters of flowrate 3µL/min, voltage ~7-9kV. 23 gauge single needle and PD 24mm.

4.8 Discussion

Significant advances have been made in the development of biomaterials for TE applications, however there is still a pressing need for viable clinical alternatives to current the gold standard treatment of autografting and allografting. Electrospinning nanofibres have become extremely prominent in TE field over the last two decades. In addition to being a relative simple and cheap process, features such as scalability, adaptability, and capacity to form fibres on both the nano and micro scale, make it most favourable method for scaffold fabrication (Sill & von Recum, 2008).

A significant problem with the electrospinning process is the ability to employ a single system for scaffold fabrication. As it's relatively simple and cheap to build an electrospinning apparatus, almost every study describes using an in-house device when electrospinning fibres. However, current studies also reported enhancing their in-house electrospinning set-up by combining it with more complicated devices, to fabricate a more effective 3D construct. Therefore, the possibilities replicating these studies are virtually impossible. Li et al (2013) combined femtosecond lasers with electrospinning. Stankus *et al.*, (2007) developed a dual electrospraying/electrospinning apparatus where simultaneous electrospraying of cells and electrospinning of nanofibres occurred. Techniques such as microcontact printing and photolithography have also been employed in combination with electrospinning, to develop scaffolds with more advanced multiscale structures (Li and Xia, 2004, Liang *et al.* 2007). Although these complex systems have discovered new ways to address various issues associated with scaffolds including fibre and pore size, fundamentally, they negatively impact on the ability to replicate similar scaffolds between different labs.

As the aforementioned apparatuses design cannot simply be reproduced, it renders the groups optimal parameters established per apparatus obsolete. Furthermore, the time taken to establish the optimal parameters per instrument can be a lengthily process, prolonging the investigations into more significant experiments including the scaffold application in TE.

In addition to the electrospinning apparatus, the biomaterials selected are crucial to scaffold fabrication. Over 150 known polymers have been electrospun with the expectation to advance cellular transplantation in TERM. However, difficulties in developing scaffolds with adequate fibre thickness for cell adhesion, pore sizes for increased cell infiltration through scaffold, and appropriate GF and nutrients to induce cell differentiation, still remain. Polymers are usually selected based on their mechanical and physical properties for electrospinning purposes, their capacity to provide a cellular microenvironment that closely mimics the natural ECM, and their ability to degrade. Typically, synthetic polymers are selected based on FDA approval, implying these polymers are compatible with *in vivo* applications.

In an effort to challenge these issues, the primary focus in this study was to establish a universal system with optimal parameters for scaffold replication between labs. By simply modifying the ground electrode shape for the commercially available apparatus Spraybase®, this provided the components to establish reproducible optimal parameters to electrospin commonly used polymers such as PEO and collagen (Fig. 4.1). Fibres electrospun from these polymers provided a benchmark for voltage, PD, flowrate, needle gauge and even polymer concentration for the commercial system.

Furthermore, supplying a commercially available apparatus with optimal parameters can eliminate the immense timescale required, when optimising in-house apparatus. Therefore, this allows additional time to focus on the generation of new biomaterials, which can electrospin fibres closely mimicking the natural ECM.

In addition to process parameters (voltage, flowrates, PD etc.), this study's preliminary investigations demonstrated the importance of solution parameters to the electrospinning process. As described in chapter 1, the solution parameters include polymer concentration, solution conductivity and solution viscosity. Due to the high volume of successful studies wherein PEO and PEG electrospun fibres were utilised, our initial investigations involved using these soluble solvents to electrospin fibres. However, regardless of the ratio of polymer mixture for either solvent, the solution regularly lacked the ability to electrospin fibres, using the commercial device. Moreover, the ability to electrospin this polymer mixture with the apparatus proved inconsistent such that, every electrospinning experiment involving this polymer blend used different process parameters, frequently ending with failed attempts in producing fibres. A possible reason for this maybe due to issues with low viscous levels of the solution. In order to electrospin fibres with the commercial electrospray, the ratio of polymer mixture used often had a liquid appearance to the solution. This generally indicated the solution had low viscosity levels, whereas the collagen and agarose mixtures usually had a honey-type consistency to the solution. Therefore the ability to electrospin fibres when using the commercial apparatus and the PEO/PEG mixtures, were practically impossible. The addition of agarose to this mix increased the viscosity levels such that agarose concentrations of 50%w/v and 100%w/v in water electrospun fibres.

However, the fabricated PEO/PEG/agarose scaffolds remained extremely fragile and dissolved almost immediately post electrospinning at room temperature. Therefore new polymer mixtures incorporating PEO and/or collagen were designed, and their electrospinning capabilities were examined.

PEO and collagen are polymers commonly used in the electrospinning process. PEO has excellent high viscosity and strong elasticity properties, whereas collagen is a primary structural protein in the ECM in various connective tissues in animals. In addition to essential electrospinning properties, PEO has been used for various studies due to its ability to dissolve in water. Baker *et al.* (2008) and Phipps *et al.* (2012) overcame issues with small pore sizes by using PEO as a "sacrificial component" in their electrospun scaffolds. This involved co-electrospinning PEO fibres with the main scaffold component, dissolving the PEO from the scaffold by submerging it in water after fabrication, inevitably leaving behind larger pores within main scaffold.

Collagen has been reported in numerous studies as a key component in providing cell adhesion and/or inducing cell differentiation to electrospun scaffolds. Chan *et al.* (2009) demonstrated more than 45% hMSC adhered to electrospun pure collagen nanofibres after 30 min at room temperature. Prabhakaran *et al.* (2009) made the first report of MSC differentiation on 3D poly(L-lactic acid)-co-poly-(ε-caprolactone)/Collagen (PLCL/Col) nanofibrous scaffolds. Whereas Kazemnejad *et al.* (2009) fabricated a variety of 3D scaffolds and examined their ability to induce hBMSC to differentiate into functional hepatocytes.

Electrospun poly(ε-caprolactone), collagen and polyethersulfone (PCL/collagen/PES) nanofibres were found to be the most successful and the investigators speculated that the addition of collagen to PCL/PES nanofibres was the critical factor. These studies therefore prompted the polymer mixture of PEO with collagen. The introduction of cα-MEM culture medium to the mixture was suggested due to it being the culture medium for MSC, therefore providing nutrients to cells. PEO/collagen/cα-MEM scaffolds were successfully electrospun using the commercial electrospinning apparatus. The optimal established process and solution parameters provided a benchmark for future electrospinning using this apparatus with PEO and/or collagen. Furthermore, having previously established some success with the addition of agarose to PEO and PEG polymer blends, and the reported success of Bonino *et al.* (2011) using a combination of PEO and alginates, a further polymer mixture was developed combining PEO, agarose and cα-MEM. Surface texture, fibre morphology and pore and fibre sizes were investigated for PEO/collagen/cα-MEM and PEO/agarose/cα-MEM scaffolds.

Several studies describe the surface texture of the fibres as the critical component in maximising the adhesive properties of scaffolds. Both Li *et al.* (2013) and Gustafsson *et al.* (2012) reported similar findings when they investigated *in vitro* biocompatibility of their synthetic 3D PCL nanofibre scaffolds and electrospun polyethylene terephthalate (PET) and polyurethane (PU) scaffolds respectively. Their results found that coating the scaffolds with adhesion proteins yielded no increase in cell density or proliferation compared to non-coated scaffolds. This suggested it was scaffold surface texture that was vital to their cell/scaffold interactions.

The fabricated collagen scaffolds demonstrated a rough, perforated surface texture, with uneven fibre distribution throughout the scaffold (Fig. 4.2). In contrast, the agarose scaffolds demonstrated a smooth and refined surface texture, with no perforations present. The fibres for the agarose scaffolds also aligned in a random pattern developing a symmetrical layered mesh, indicating these may provide a surface area acceptable to cell adhesion (Fig. 4.4).

A possible reason for the contrast in the surface textures for the collagen and agarose scaffolds maybe due to viscosity levels for PEO/collagen/cα-MEM solution. Regardless of how little collagen was added to the blend, its presence caused the solution to remain quiet liquid. Therefore, PEO was increased to counteract the liquidity generating a more viscous blend of polymers. Although the polymer solution was viscous enough to electrospin fibres using the commercial electrospray, the mixture appeared more liquid than glutinous when compared to the agarose mixture. In addition, temperature has been shown to change the viscosity of the polymer jet (Pham *et al.*, 2006). It was recorded on several occasions how temperature dictated whether electrospinning of the collagen scaffolds transpired. Optimal temperatures for electrospinning these scaffold varied between 18-25°C, in comparison to the agarose scaffolds which could electrospin up to 32°C. It is possible temperature had a negative impact on the already low viscous collagen solution, generating a fragile fibre, with a rough and perforated surface texture.

SEM for collagen scaffolds demonstrated the presence of bead formation on its electrospun fibres using the commercial apparatus (Fig. 4.3). Deitzel *et al.* (2001) reported that by increasing the voltage when using PEO in water solution causes the Taylor cone to subside, which enhances beading of fibres. This is one possible reason as to why beading was observed on PEO/collagen/cα-MEM scaffolds. Although voltage fluctuated within experiments, it was generally in the direction from low to high, i.e. increasing from 6-9kV. Voltage remained between ~6-7kV for agarose-based studies, with SEM indicating no obvious beading on the fibres of these scaffolds (Fig. 4.5). In addition to increasing voltage, high humidity may have also impacted on the collagen fibres morphology. Pham *et al.*, (2006) described how excessive humidity may prevent solvent evaporation during the electrospinning process, resulting in bead formation on the fibres. RH for these experiments ranged between 30-48%. Although RH did not seem to affect the electrospinning of PEO/agarose/cα-MEM scaffolds, it may have contributed to bead formation within collagen scaffolds, in combination with increased voltages.

Optimally designed pore sizes provide structural space for cell migration and enable the exchange of nutrients between the scaffold and environment, while eliminating waste. Small pore sizes have proven problematic to these processes, and are recorded to range between ~10–15 μm (Leong *et al.*, 2010; Shabani *et al.*, 2012). Regarding the current study the electrospun collagen scaffolds fabricated pore sizes ranged from 10.1 - 75.1μm, whereas the agarose scaffolds electrospun pores measuring as little as 5.97 - 6.38μm (Fig. 4.6 and Fig. 4.7). Although PEO/collagen/cα-MEM polymer blends electrospun pores ranging from small to medium sizes, pores were constantly inconsistent in size for each fabricated collagen construct.

Whereas PEO/agarose/cα-MEM polymer mixture electrospun scaffolds with uniform pores, however, these were miniature in size, thus rendering them ineffective to any possible future cellular activity.

In an attempt to address the issues with pore size inconsistencies for collagen scaffolds and extremely small pore sizes for agarose scaffolds, both were placed in water with the intention to dissolve PEO, making it a "sacrificial component" as described by Baker *et al.* (2008) and Phipps *et al.* (2012). However, both scaffolds fully dissolved once submerged in water. This raised questions to both scaffolds strength and their ability for hosting cells while also culturing them in medium, for future experiments.

It has been well documented that polymer concentration greatly influences fibre formation. Dissolving sufficient amount of polymer in a solvent is critical to fibre structure, as polymer strands must overlap in order to physically link and form fibres (Sill & von Recum, 2008). Controlling fibre thickness is a prominent issue when electrospinning polymers. Gupta *et al.* (2005) and Chen *et al.* (2008) demonstrated that increased polymer concentration correlated with increased fibre thickness. For the electrospun collagen scaffolds SEM demonstrated that the fibre diameters measured between 759nm - 3.18μm, whereas agarose fibres electrospun between 1.57 - 1.58μm (Fig. 4.8 and Fig. 4.9). Controlling fibre thickness for collagen scaffolds proved difficult. Increasing the collagen polymer concentration resulted in a liquefied polymer mix, incapable of electrospinning fibres using the commercial device.

Whereas increased PEO polymer concentrations resulted in a high viscous solution which blocked the conducting needle tip, preventing the electrospinning process from occurring. Final ratio of PEO:collagen:cα-MEM, provided the correct polymer mixture to electrospin fibres using commercial apparatus. However, fibre diameters remained inconsistent for this mixture resulting in the electrospinning of both nanofibres and microfibers. Agarose-based polymer blends electrospun uniform fibres, with diameters on the micrometre scale. However, various studies reported that nanofibrous scaffolds had closer behaviours to natural ECM than microfibres. The nanofibres provided a more functional connective microenvironment for cell adhesion and differentiation, when compared to those on the microfibril scaffolds. Nonetheless, Li *et al.* (2013) demonstrated that microfibres can permit successful cellular and nutrient infiltration with fibre and pore sizes as little as of 0.6μm and 1.2μm respectively. However, in comparison to our agarose-based scaffolds, their specially designed laser/electrospun hybrid matts were extremely durable. Agarose scaffolds although strong enough to remain functional at room temperature, dissolved once cells were seeded onto them, and submerged in media.

As a result, it is proposed that these scaffolds may contribute to new system such that, both nanofibres and microfibers are incorporated within the same scaffold. Study by Ju *et al.* (2010) described how combining both nano and microfibers allowed for better integration of smooth muscle cells (SMC), and development of multiple SMC layers when examining the potential to create vascular grafts. Luminal epithelial cell (EC) monolayer was supported when PCL/collagen nanofibres were electrospun with fibres approximately 270 nm in diameter.

Surrounding this layer, PCL/collagen fibres with diameters of approximately 1μm, 2.4μm and 4.45μm in different groups were added in order to increase the pore size. Scaffolds were found to support EC on the luminal nanofiber layer and SMC growth on the outer microfiber layer. SMC infiltration significantly increased when 2.4 μm and 4.45 μm fibres were used, as these fibre sizes provide pore sizes large enough for cells to grow into. This is not a feature generally observed with pure nanofibers.

In summary the primary investigation for this study was to establish a universal apparatus with standardised, optimal parameters to electrospin fibres. Simple modifications to ground electrode from the commercial electrospray apparatus, provided the components required for electrospinning to occur. Specific process and solution parameters such as voltage, polymer concentration, solution viscosity, temperature and humidity directly influenced the electrospinning of both collagen and agarose type scaffolds, when using the commercial electrospinning apparatus. Although both constructs had similar electrospinning parameters applied, the final fabricated scaffold was in complete contrast to each other. Collagen scaffolds proved fragile with perforations throughout the construct. Its uneven, rough surface texture was fabricated from fibres of varying thickness, measuring from nano to micro metres. This adversely impacted on pore size electrospinning both small and medium sized pores for these scaffolds. In addition, fibre morphology showed obvious bead formation on the fibres.

In contrast, agarose scaffolds proved more robust with smooth, even surface textures. Fibre diameters and pore sizes appeared uniform and consistent within these scaffolds. However pore size measured below par for any possible cellular activity to take place on these constructs. However, agarose electrospun fibres may hold some promise in the fabrication of superior scaffolds. By incorporated the micron thick fibres with nanofibrous scaffolds may potentially create 3D constructs with large pore sizes, enabling cell and nutrient infiltration through scaffold, while eliminating waste.

Significant successes have been demonstrated in this study as we've accomplished establishing a commercial electrospinning apparatus, with reproducible, optimal parameters for polymer blends incorporating PEO, collagen and agarose and/or alginates. In addition, fabrications of PEO/agarose/cα-MEM electrospun scaffolds have the potential to aid in advancing TE applications. However, it's been elucidated throughout the polymer study that, these are primary investigations, and further investigations are required. In addition to scaffold durability, essential scaffold properties such as fibre tensile, porosity and permeability measurements still need to be investigated, for these scaffolds.

Chapter 5

Cellular and immunological analyses of bio-electrosprayed mBMSC and the development of the bio-electrospray process as a cell delivery method to target sites at low voltages

5.1 Introduction

Current gold standard treatments for replacing damaged tissue in TE involve the use of autografting and allografting. Various problems associated with these methods include lack of donor availability, risk of infection, rejection, disease transmission from donor to patient and GvHD (Younger and Chapman (1989). Similarly, serious concerns have arisen in connection to existing patient MSC cell therapy. To date, MSC are predominantly administered through I.V. injection, which allows cells to move through the blood stream to any site in the body, regardless of the intended target site. The efficiency of MSC targeting the injury site can be low. Furthermore, a well-documented phenomenon, MSC entrapment, can occur after MSC are administrated by I.V. injection whereby MSC remain in the lungs and liver of rodents (Eggenhofer *et al.*, 2012). This has also been reported in patient trials (English *et al.*, 2010; Nystedt *et al.*, 2013). As a result, careful patient monitoring is essential due to high risk of acute or chronic adverse side effects from entrapment of cells in the lungs or liver.

With the global market for TE estimated to grow to $89.7 billion by 2016 (bcresearch for TE), and cell therapy market valued to be worth close to $8.8 billion by 2016 (Syed and Evans, 2013), developing new substitute treatments in these fields is critical. Electrospinning polymers to fabricate artificial 3D scaffolds, has excelled in the last two decades as a progressive cell delivery method for TERM purposes.

While critically analysing our results (Chapter 4), in combination with reports from numerous other investigations, it became clear that similar difficulties associated with scaffold surface texture, fibre morphology, fibre and pore sizes are continuously occurring. The wide variation in electrospinning apparatuses and polymers used contribute to lack of a permanent solution in addressing these issues.

This study focuses on providing an alternative cell delivery method wherein cells are directly sprayed onto a targeted injury site. Employing the optimal parameters established in chapter 3 for the Spraybase® apparatus, we proposed using the BES process to electrospray mBMSC directly to injury sites. However, limited investigations into viability and functionality of the mBMSC post BES were carried out in Chapter 3. Therefore, this study analysed the expression of specific surface markers, multilineage differentiation, suppression of T- cell activation and pro-reparative capabilities, for both BES and pipette (control) mBMSC, following the jetting process.

Our previous studies have indicated this cell delivery method has potential as an alternative strategy for TERM and cell therapies. However, the apparatus set-up of connecting the single needle to a syringe, which is then fixed to a pump, is not clinically applicable. In addition, the ground electrode cannot be placed *in vivo* to attract the spray towards the injured region.

Therefore, the ability of potentially moving from translation into the clinic using this technology was introduced by AVECTAS. The company provided our group with their newest commercial device, a BES catheter named SprayCell™. SprayCell™ electrospray apparatus includes a specially designed catheter which incorporates the single needle configuration and ground electrode within the catheter. It fits all type of endoscopes allowing for the BES of cells to various body parts, through keyhole surgery.

In an effort to demonstrate the viability and function of BES MSC *in vivo* using this catheter, a 3D model using mBMSC and CG scaffolds was developed *in vitro*. As described in chapter 1, GAGs are linear polysaccharides which are found within the ECM and on cell surfaces. These are involved in cell-matrix interactions and wound healing which induce cells to migrate, infiltrate and differentiate on scaffolds. These behave similarly to tissue and crosslinked scaffolds involving GAGs have been successfully used in applications including cartilage and bone regeneration (Lee *et al.*, 2003; Farrell *et al.*, 2006). Primarily the aim of this study was to determine whether mBMSC attached, and differentiated on these scaffold following BES with the catheter. A secondary study was to demonstrate that BES chondrocytes also attached to the scaffolds, indicating a potential therapeutic for cartilage diseases, such as articular-cartilage lesions and osteoarthritis, where there is limited potential for wound healing. Using the innovative SprayCell™ device in combination with BES methodology, may subsequently enable targeted delivery of MSC and/or other cell types to an injury site *in vivo*, and potentially avoid the complications associated with MSC entrapment and the limitations associated with artificial scaffolds.

5.2 Bio-electrosprayed mBMSC retain associated surface markers

Three principle stipulations for MSC characterisation are adherence to plastic, specific cell surface marker expression and tri-lineage differentiation (Tropel *et al.*, 2004). BES mBMSC adherence to plastic has already been determined with cells adhering to tissue culture wells after 24 hrs (Fig. 3.5).

In order to confirm the phenotype of the mBMSC population used in these studies, surface marker expression was examined pre- and post- BES. Expression of thirteen characteristic MSC cell surface markers, as described by the ISCT, were examined using flow cytometry (Dominici *et al.*, 2006). Expression of CD105, CD44, Sca-1, CD106, CD73, CD90 with no MHC Class I expression and the absence of CD117, endothelial marker CD11b, the haematopoietic marker CD45, lymphocyte maker CD34, co-stimulatory marker and CD86 and MHC Class II confirmed the expected mBMSC phenotype pre- electrospray. Similar results were found for BES mBMSC demonstrating that this jetting process did not alter cell surface marker expression in these cells (Fig. 5.1) (Table 7).

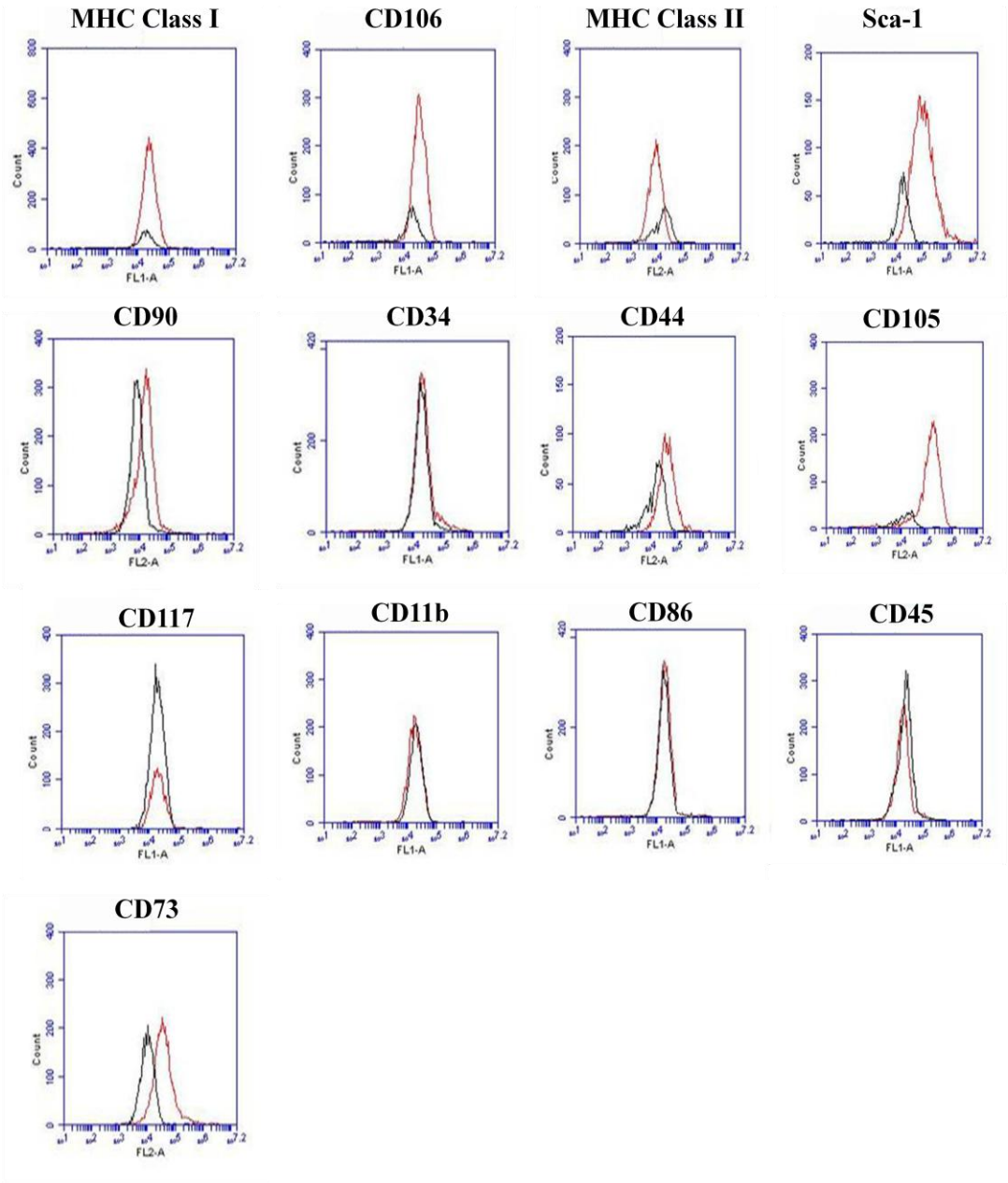

Fig. 5.1 Bio-electrosprayed mBMSC characterisation for cell surface markers. BES mBMSC at flowrate of 5µL/min, 30 gauge single needle, 22mm PD and voltages ~3-6kV were characterised by staining the cells for variety of cell surface markers (red line) against their corresponding isotypes (black line). The cells were analysed using flow cytometry with 10,000 events were recorded for each marker. mBMSC retained their characteristic profile of surface markers following BES.

Table 7: Summary for surface marker expression on mBMSC following BES

Surface Markers	Expression
CD 11b	-
CD 34	+
CD 44	+
CD 45	-
CD 73	+
CD 86	-
CD 90	+
CD 105	+
CD 106	+
CD 117	-
Sca-1	+
MHC Class l	-
MHC Class ll	-

5.3 mBMSC differentiated into their multilineages following the bio-electrospraying process

By definition, MSC must show multilineage differentiation capability, for example towards osteocyte, adipocyte and chondrocyte lineages (Pittenger *et al.*, 1999). Therefore the ability of mBMSC to differentiate towards osteoblast, adipocyte and chondrocyte lineages for both pipette, and BES cells was examined. Determining if the electrospray process adversely affected this capability is essential when promoting this as a potential delivery method for mBMSC.

For osteoblast, adipocyte and chondrocyte differentiation, mBMSC were cultured under specific differentiation conditions for 21 days. Cells were then analysed for expression of differentiation-specific features. Osteoblasts were stained with Alizarin Red S Stain to visualise calcium deposits, adipocytes were stained with Oil Red O Isopropanol to visualise fat deposits and RNA was extracted from chondrocytes for detection of expression of markers genes. The differentiation markers were observed in each of the three lineages for both pipette mBMSC and BES mBMSC (Fig. 5.2 A & B). Similar patterns of calcium and fat deposits were present in pipette mBMSC and BES mBMSC differentiated cells. Similarly, expression of aggrecan and collagen IIa was increased in both pipette mBMSC and BES mBMSC (Fig. 5.2 C). These results indicate that that the differentiation capability of mBMSC is not adversely affected by this bio-electrospray methodology.

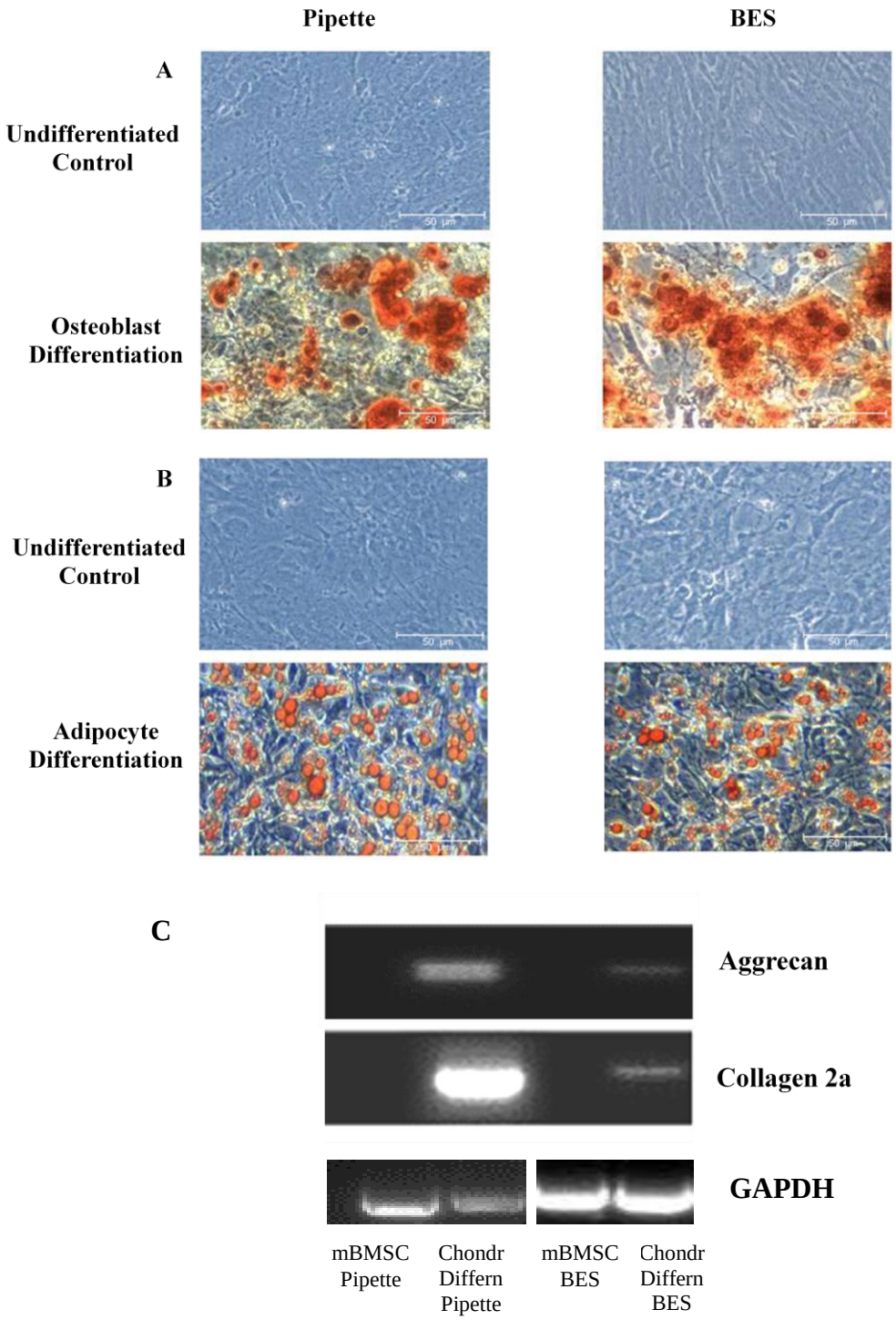

Fig. 5.2 Differentiation of mBMSC following BES. (A) and (B) show successful differentiation of pipette and BES mBMSC after 21 days towards osteoblast and adipocyte lineages as demonstrated by positive staining calcium deposits and fat deposits respectively (x10 magnification). (C) Expression of aggrecan and collagen IIa mRNA was detected by PCR in both pipette and BES mBMSC after 21 days differentiation towards a chondrocyte lineage. Flowrate of 5μL/min, 30 gauge single needle, 22mm PD and voltages ~3-6kVwere used.

5.4 Bio-electrosprayed mBMSC suppressed T-cell proliferation

Suppression of T-cell proliferation *in vitro* has become synonymous with MSC. This important function makes these cells attractive for therapeutic applications (Dwyer *et al.*, 1981; Di Nicola *et al.*, 2002; Glennie *et al.*, 2005; Ding *et al.*, 2009). BES mBMSC were examined for their capacity to suppress both autologous and allogeneic proliferation T-cells. MHC mis-matched splenocytes were cultured with both pipette and BES mBMSC, and analysed by CFSE uptake into replicating DNA after 72hr. In a second study, identical parameters where implemented with the inclusion of Concovalin A (ConA) at day 0. This is a mitogen known for inducing T-cell proliferation, and was used as a positive control. Although some proliferation was identified for both studies, significant immunosuppressive capacity for both pipette and BES mBMSC was demonstrated for alloantigen and mitogen driven proliferation (Fig. 5.3 A & B).

Results from these studies indicated proliferation of T-cells was significantly reduced in the presence of both pipette mBMSC and BES mBMSC, with 4 fold proliferation reduction rates respectively compared to controls (Fig. 5.4).

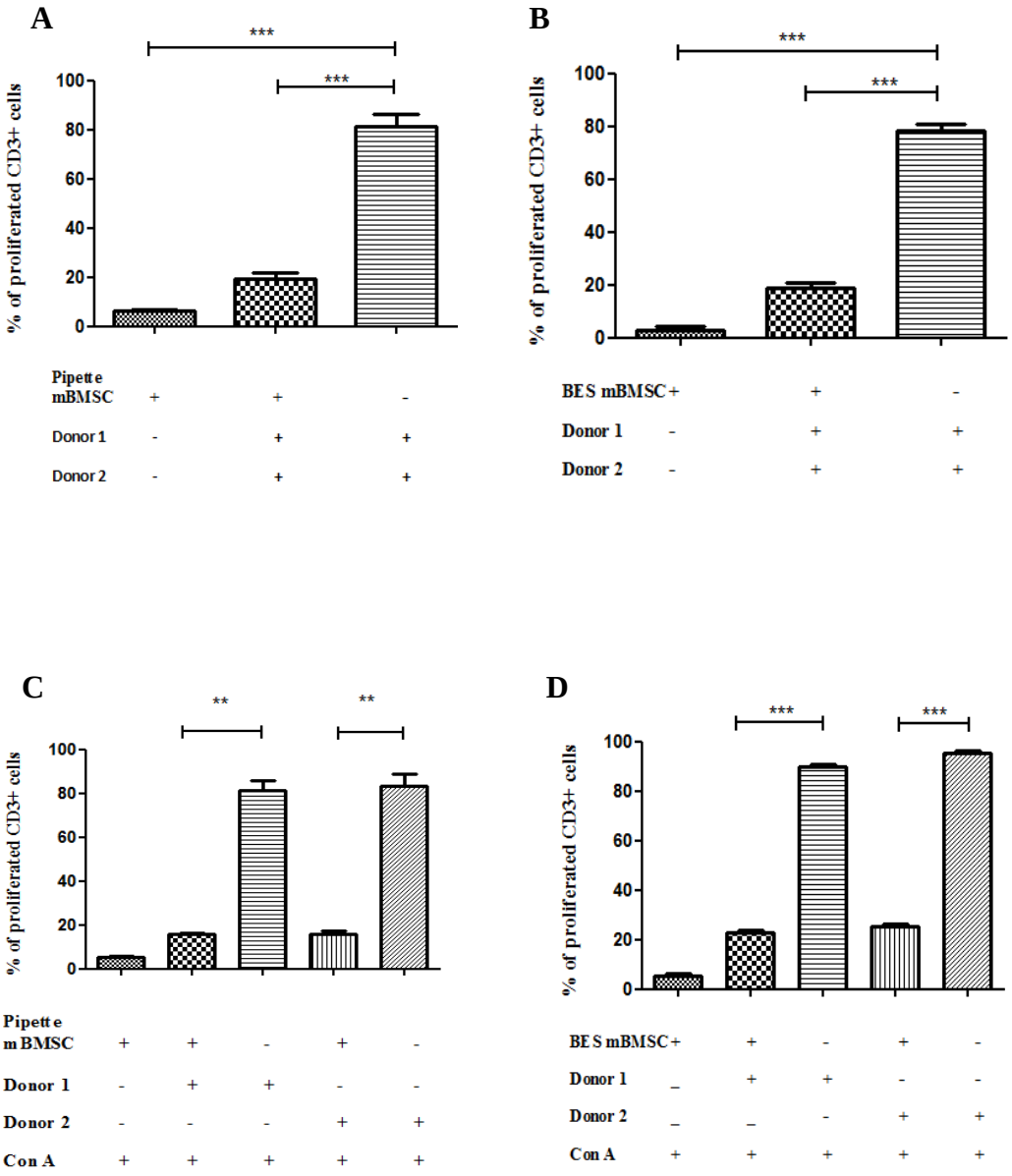

Fig. 5.3 BES mBMSC inhibit A) alloantigen and B) mitogen driven spleen cell proliferation. Pipette and BES mBMSC were co-cultured with splenocytes from BALB/c (donor 1) and C57BL/6 (donor 2) mice for 72h. Proliferation was measured by CFSE intake after 72hr and analysed by flow cytometry. Mitogen driven proliferation was examined using Con A (5ug/ml) added at day 0. Statistical significance determined by ANOVA analysis (p**<0.01), (p***<0.001). BES mBMSC preformed similar to pipette mBMSC in their ability to suppress T-cell proliferation.

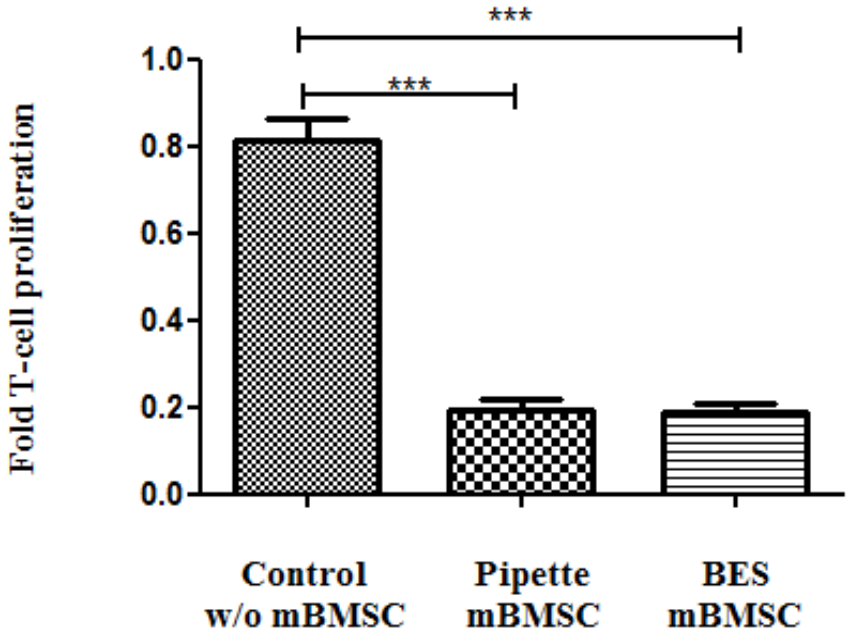

Fig. 5.4 Suppression of T-cell proliferation by mBMSC following BES. T-cell proliferation was reduced by 4 fold in the presence of pipette mBMSC and mBMSC subjected to BES respectively. This indicated the electrosprayed cells were behaving similarly to the non-BES cells. Parameters for the electrospray included flowrate of 5µL/min, 30 gauge single needle, 22mm PD and voltages ~3-6kV.

5.5 Bio-electrosprayed mBMSC induced wound closure for two separate cell types

Studies have shown that MSC migrate to injury sites and promote repair through the production of trophic factors, including growth factors, cytokines, and antioxidants (Chen *et al.*, 2008; Karp and Leng 2009). Therefore the jetting process was investigated to determine whether if it would adversely affect the pro-reparative properties of mBMSC. For this study two independent *in vitro* wound closure assays were set-up and wound closure was examined using the A549 and BEAS-2B lung epithelial cell lines. Similar results were demonstrated for two studies with both pipette and BES mBMSC induced significantly higher rates of wound closure compared to controls.

Analysis for A549 assay revealed wound sizes of 16 ±2.2% remained for the pipette mBMSC and 15 ±3.1% for the BES mBMSC compared to control wounds. There was no significant difference between the wounds remaining in wells treated with pipette or BES mBMSC (Fig. 5.5). Similar results were obtained when the BEAS-2B lung cell line was used as an alternative to A549 in the wound closure assay. Wound closure of 15 ±2.8% remained for pipette mBMSC, with 12 ±3.2% for BES mBMSC. Again, no significant differences were observed between pipette and BES mBMSC treated wells for wound closure (Fig. 5.6).

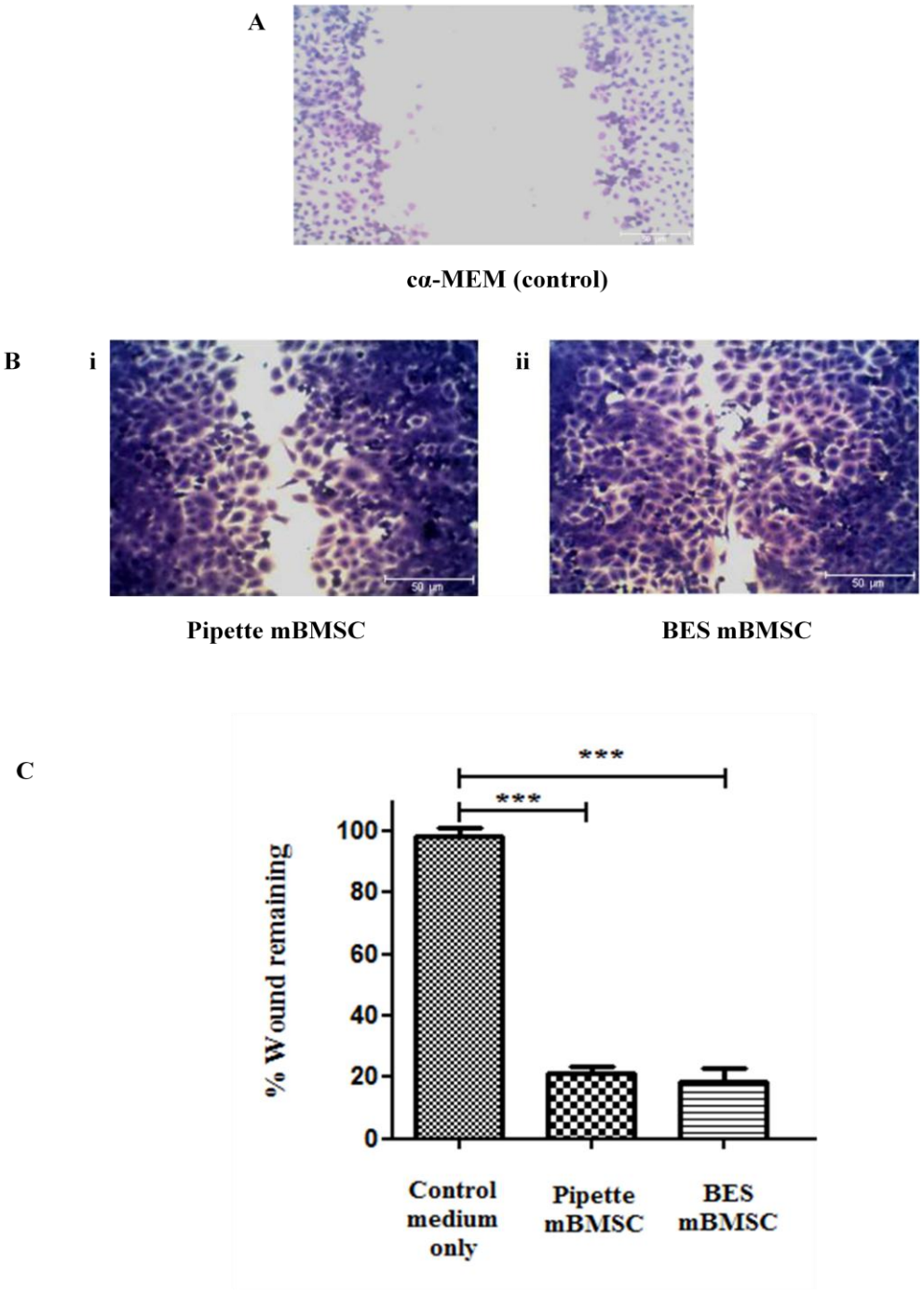

Fig. 5.5 Enhancement of wound closure by BES mBMSC. A wound was created and observed over 24 hr. (A) Crystal violet staining of A549 cells show little to no closure to controls. (B) Plates with transwells containing either (i) pipette or (ii) BES mBMSC illustrate wound closure. After 20 hr, wound was fully closed in wells containing BES mBMSC. (C) % A549 wound closure was significantly enhanced in the presence of both pipette and BES mBMSC. (n=3). Statistical significance determined by ANOVA analysis (p**<0.01), (p***<0.001).

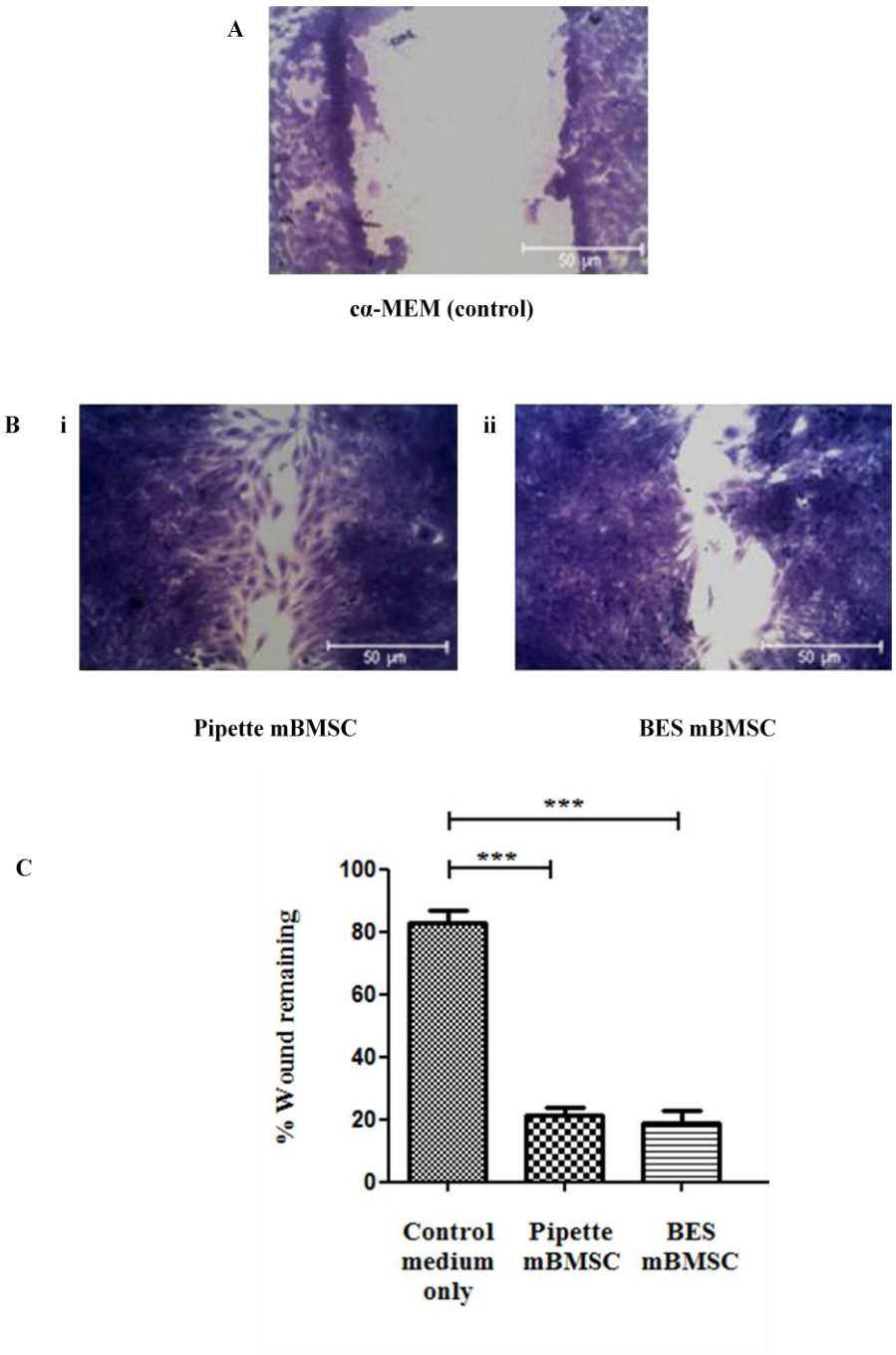

Fig. 5.6 Enhancement of wound closure by mBMSC. Second study demonstrating wound created and observed over 24 hr. (A) Crystal violet staining of BEAS-2B cells show little to no closure to controls. (B) Plates with transwells containing either (i) pipette or (ii) BES mBMSC illustrate wound closure. After 20 hr, wound was fully closed in wells containing pipette mBMSC. (C) % BEAS-2B wound closure was significantly enhanced in the presence of both pipette and BES mBMSC. (n=3). Statistical significance determined by ANOVA analysis (p**<0.01), (p***<0.001).

5.6 Bio-electrospray of various cell types using commercial electrospray

In addition to MSC, it may be appropriate in some situations to deliver differentiated cells types for *in vivo* therapeutic applications. As previously reported a number of cell types have been electrosprayed using in-house systems (Abeyewickreme *et al.*, 2009; Sahoo *et al.*, 2010; Bartolovic *et al.*, 2010; Ng *et al.*, 2011; Guan *et al.*, 2009; Ye *et al.*, 2014). Therefore electrospraying of different cell types was examined using Spraybase® at the optimised parameters with flowrate of 5µL/min, 30 gauge single needle, 22mm PD and voltages ~3-6kV.

Osteocytes and adipocytes obtained from differentiated mBMSC as described in section 2.8.2 and 2.8.3 respectively, were BES using the Spraybase® apparatus at low voltages (5kV). Parameters were identical to those used for mBMSC except that PD was changed from 22 mm to 25 mm to avoid spark generation due to the higher conductivity of these cell suspensions compared with mBMSC suspensions. Cells were subjected to BES, collected in 6 well plates, cultured for 24 hr and then stained with either alizarin red, for calcium deposits in osteocytes, or Oil red O, for fat deposits in adipocytes. Calcium and adipose deposits were observed in the respective cell types and there were no visible differences between these cells and pipette counterparts (Fig. 5.7). This indicates that differentiated cells, as well as MSC, can be delivered to substrates using Spraybase® without adverse effects on cell functionality.

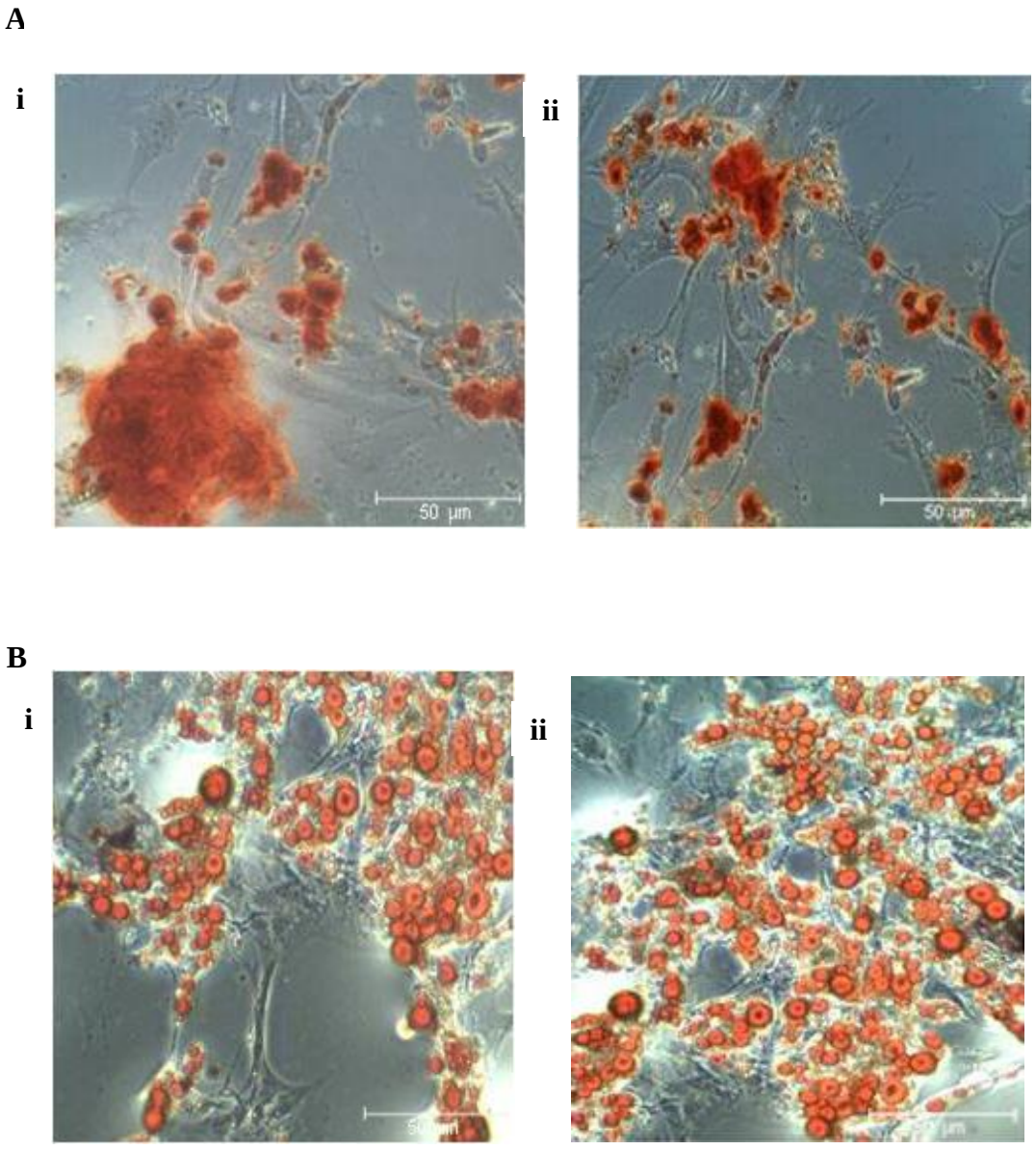

Fig. 5.7 BES Bone and Fat deposits. (A) (i) Pipette and (ii) BES calcium deposits. (B) (i) Pipette and (ii) BES adipose deposits. Both cells were BES using flowrate of 5µL/min, 30 gauge single needle, 22mm PD and voltages ~3-6kV and the results showed they adhered to 6-well plate after 24 hr. Staining with either alizarin red (for calcium deposits) or Oil red O (for adipose deposits) demonstrated that both the calcium and adipose deposits could be electrosprayed with no apparent damage to the aggregates themselves when compared to pipette control after 24hr.

5.7 Addition of catheter to electrospray apparatus developed more medically applicable device named SprayCell™

Addressing critical issues associated with MSC therapies and TERM involved developing an alternative strategy for MSC delivery to target sites. Therefore the addition of the specially designed catheter, SprayCell™, by AVECTAS, provided a more medically applicable BES system.

In addition to the basic electrospray set up, SprayCell™ system includes IEC standard approved power supply unit, laser and camera visualization system and most importantly the addition of the catheter. This catheter incorporates the single needle configuration and ground electrode within its specially designed outer tubing. This is then attached to syringe in place of the needle (Fig. 5.8). The catheter fits all types of endoscopes, making it possible to deliver cells directly to a target site, through keyhole surgery (Fig 5.9).

A

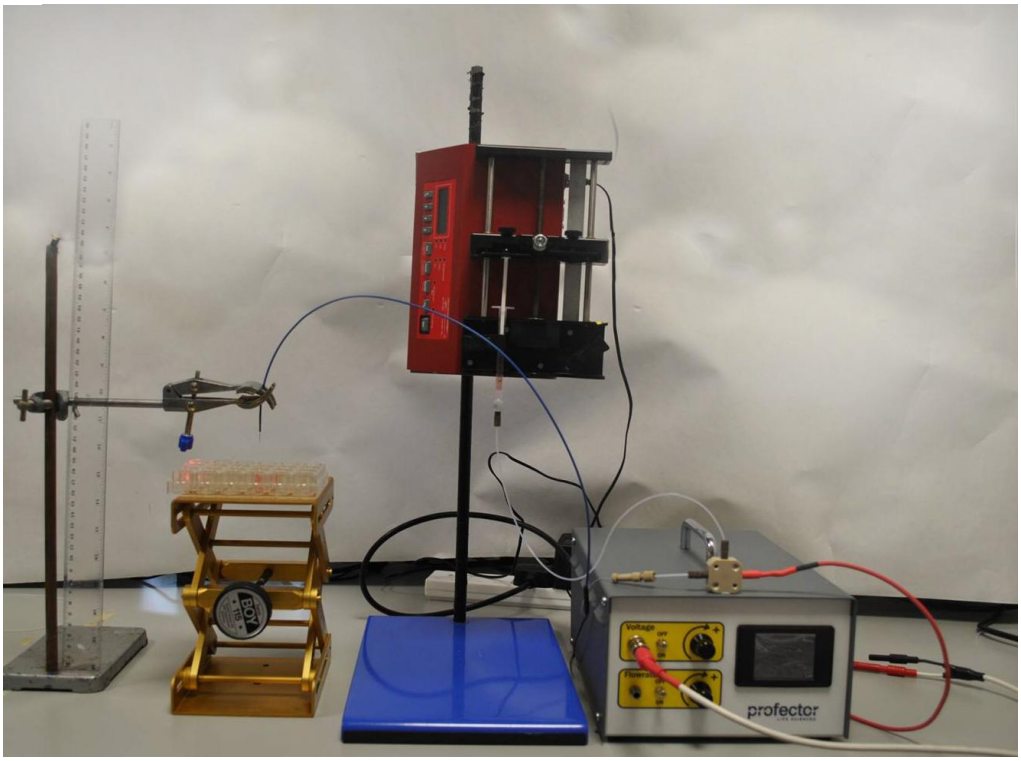

B

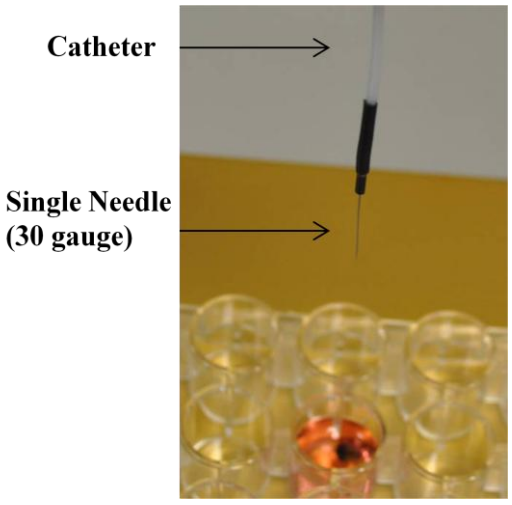

Fig. 5.8 SprayCell™ Configuration. Addition of specially designed catheter with incorporated single needle configuration and ground to electrospray apparatus supplied by AVECTAS. Set up retains IEC standard approved power supply unit, with laser and camera.

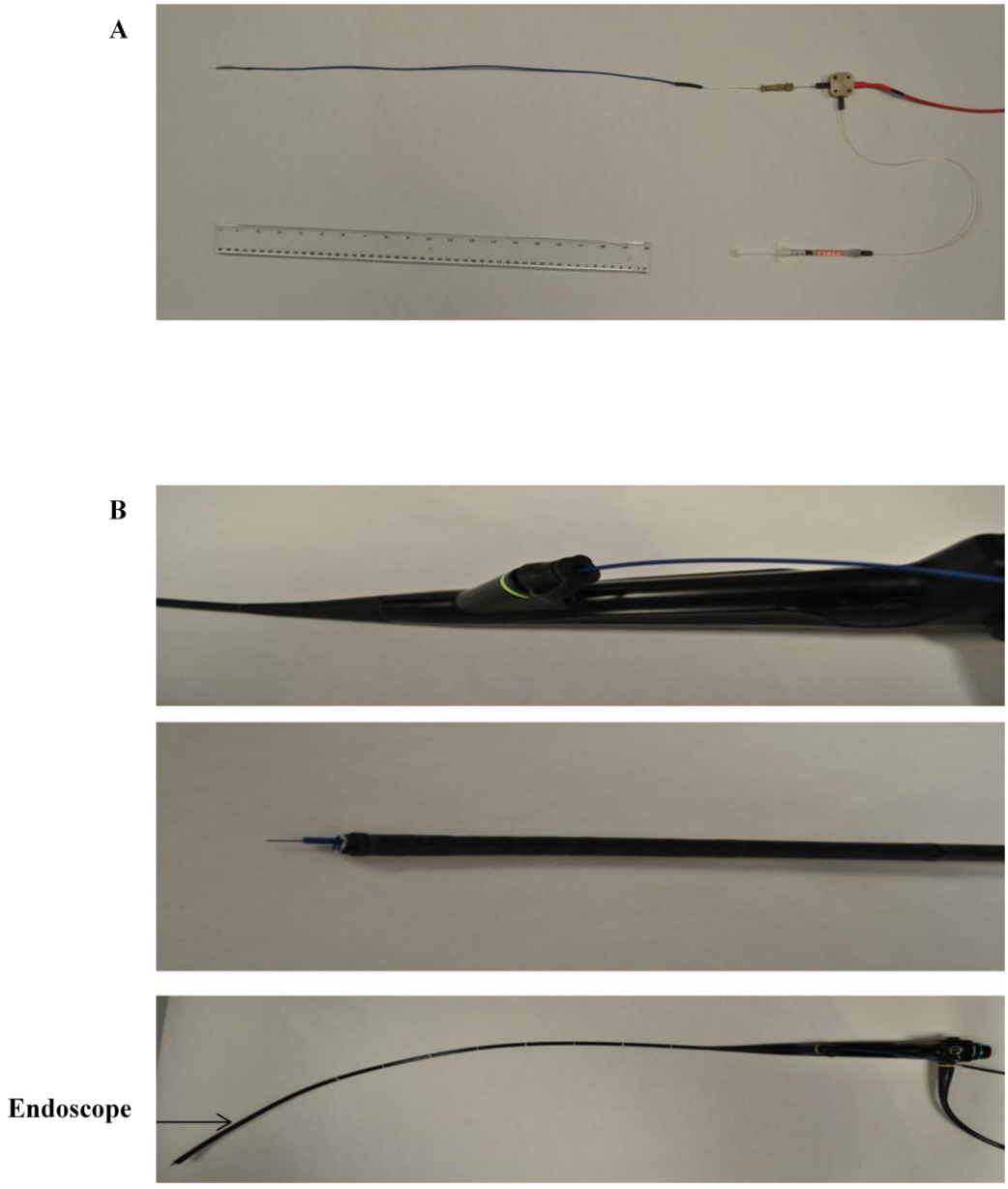

Fig. 5.9 Specially designed catheter for SprayCell™. (A) Illustrates length of catheter with syringe containing mBMSC in complete culture medium attached. (B) Depicts the catheter within an endoscope. For this demonstration a bronchoscope was used to indicate catheter length can be modified to fit all types of endoscopes, regardless of size, making it applicable for all types of keyhole surgeries.

5.8 Adherence of mBMSC onto 3D collagen-glycosaminoglycan scaffold post bio-electrospray using SprayCell™

To date our studies consisted of 2D experiments which are sufficient for investigations into mBMSC viability and function following electrospraying. However, to move towards a more medically applicable cell delivery strategy, it became essential to have more comprehensive results. Therefore mBMSC were BES onto the spongy type 3D CG-scaffolds using SprayCell™ and their adhesion capabilities were examined.

Using optimised parameters established for Spraybase®, mBMSC were BES at 1x 10^6 cells/mL using Spraycell™ onto CG-scaffolds. Voltage remained at 6kV irrespective of RH with flowrate 10μL/min to compensate for distance travelled by cells through catheter. mBMSC were then stained with DAPI and MitoTracker Red and analyses from immunofluorescence microscopy demonstrated that the cells had successfully adhered on the scaffolds after 24hr (Fig. 5.10).

mBMSC viability was also analysed using same 7-AAD exclusion assay as shown for BES cells using Spraybase®. It was found that 94 ± 2.08% mBMSC cells remained viable following electrospraying with SprayCell™ compared with 97 ± 1.21 for pipette cells. Interestingly, when compared to those BES using Spraybase®, viability using SprayCell™ had increased by approx 14% (Fig. 5.11).

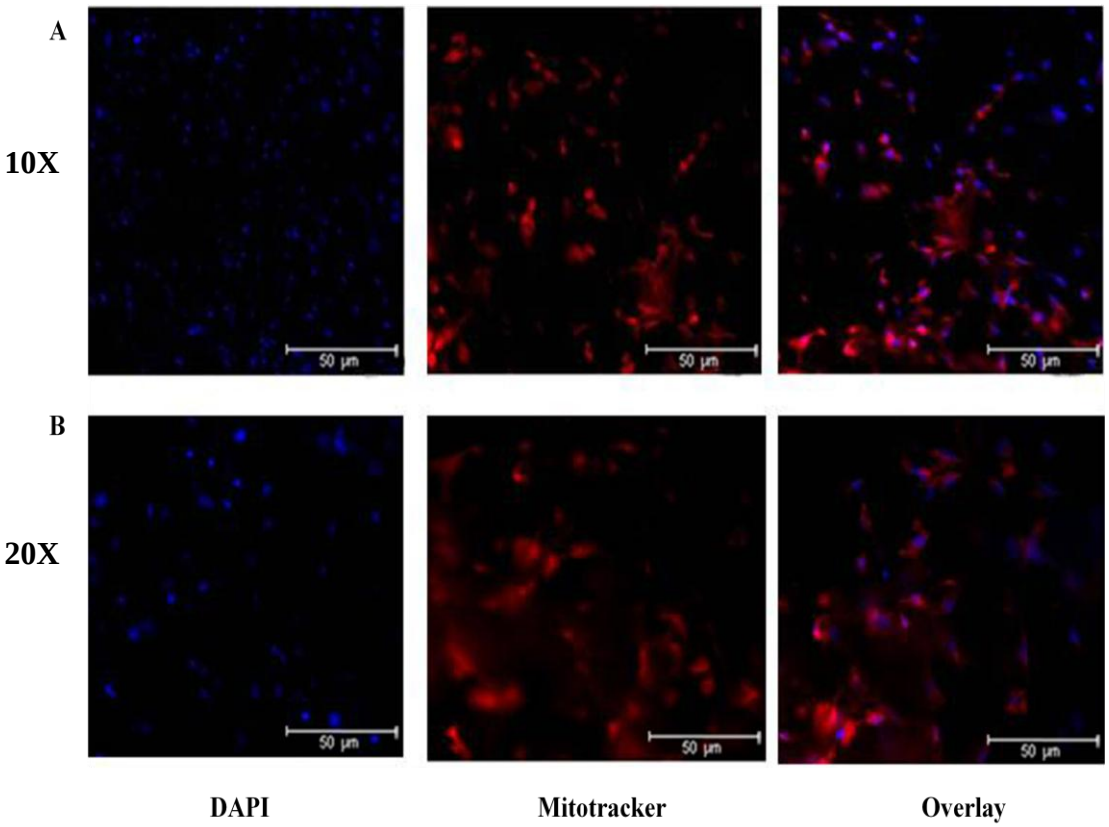

Fig. 5.10 Adhesion capabilities of BES mBMSC onto CG-scaffolds using SprayCell™. (A) and (B) DAPI and MitoTracker Red staining of mBMSC 24hr after electrospraying using SprayCell™ at x10 and x20 respectively. mBMSC were BES using SprayCell™ onto CG scaffolds at flowrate of 10µL/min, 30 gauge single needle, 22mm PD and voltage 6kV, and immunofluorescence determined cells adhered to the scaffolds after 24hrs.

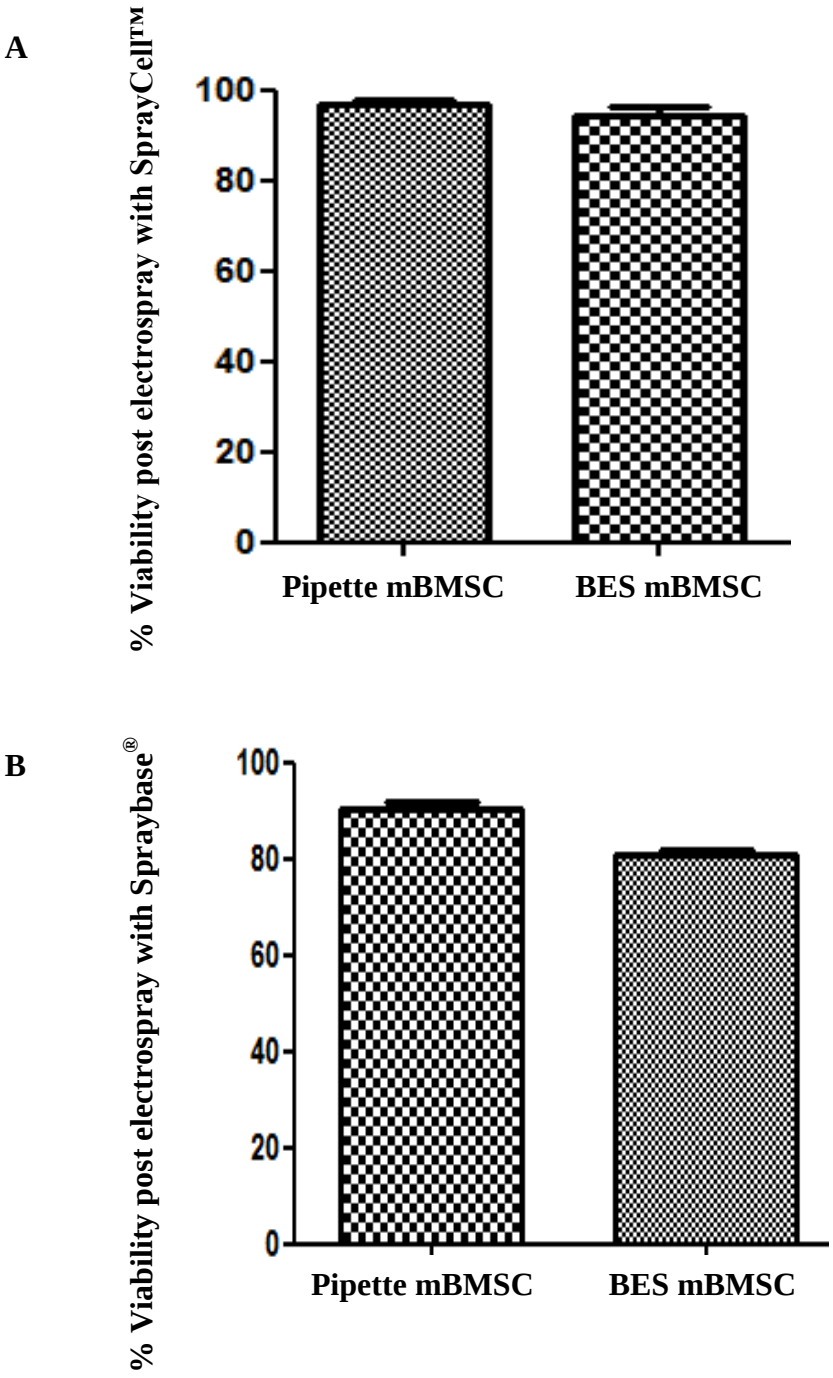

Figure 5.11 Viability of BES mBMSC for SprayCell™. (A)Viability of mBMSC was 94 ± 2.08% following BES with SprayCell™ compared with 97 ± 1.21% for pipette cells (n=3). (B) Viability of mBMSC was 80 ± 1.3% following BES with Spraybase® compared with 90 ± 1.5 for pipette cells (n=3). High yields of viable mBMSC are electrosprayed when using both systems. However, results also indicated increased viability (approx 14%) with catheter (SprayCell™) compared to apparatus without (Spraybase®). Statistical significance determined by ANOVA analysis (p**<0.01), (p***<0.001).

5.9 Bio-electrosprayed mBMSC shown to penetrate deeper into collagen-glycosaminoglycan scaffolds in comparison to pipette control

Organs and body structures are composed into multiple tissue types including connective, muscle, nervous and epithelial. Each of these varies in thickness from nano to micro metre scale. In order to demonstrate mBMSC BES with SprayCell™ can penetrate through composites, cell penetration through the scaffold was examined following electrospray. Confocal microscopy demonstrated the BES mBMSC penetrated deeper into the scaffold compared to cells delivered using a micropipette after 24hr (Fig. 5.12).

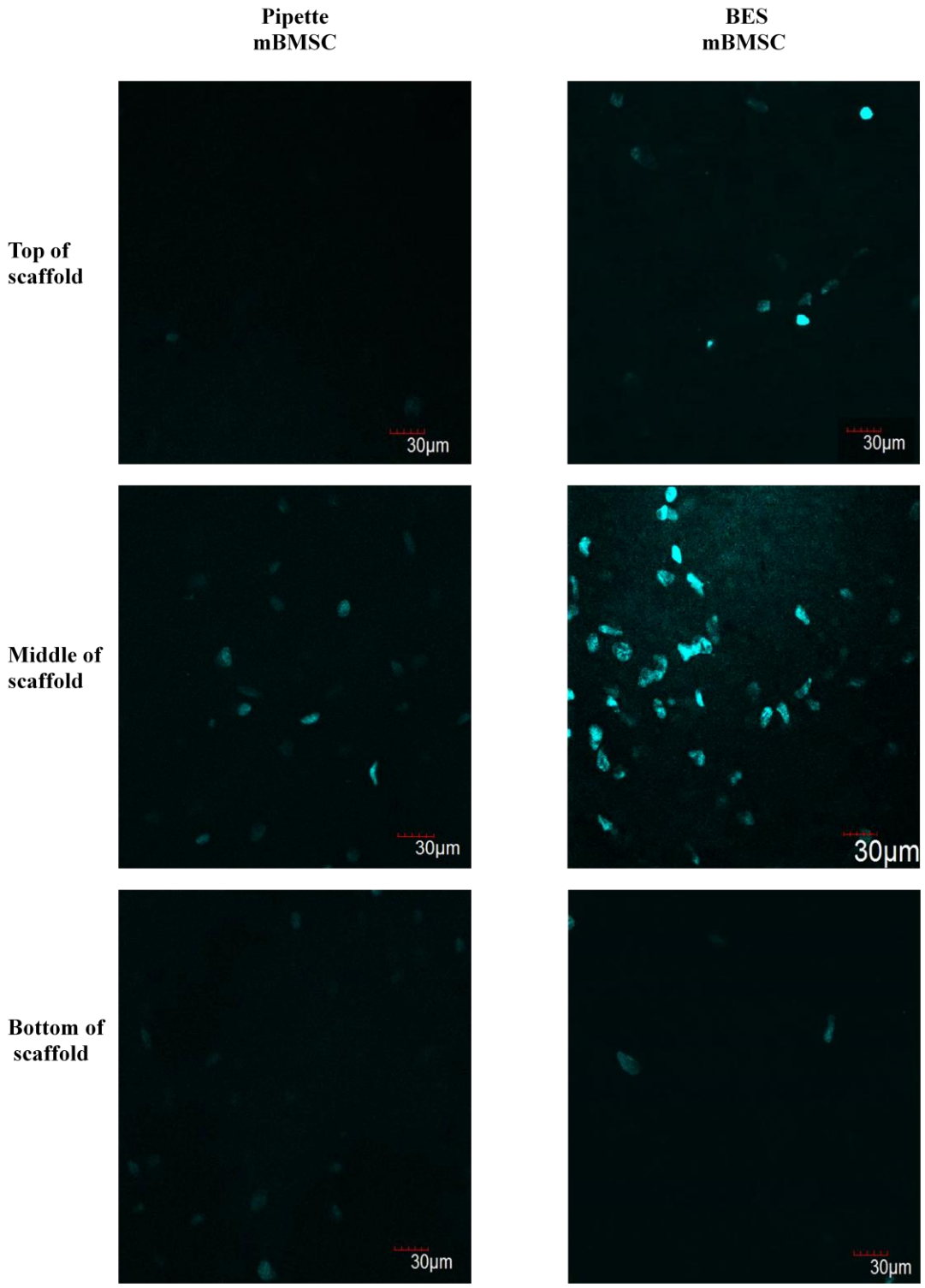

Fig. 5.12 Permeation of BES mBMSC through CG-scaffolds using SprayCell™. Confocal microscopy demonstrated that mBMSC delivered onto scaffolds with SprayCell™ at penetrated deeper through scaffold after 24 hr compared with cells delivered using a pipette (n-3).

5.10 mBMSC bio-electrosprayed using SprayCell™ apparatus differentiated into chondrocytes on collagen-glycosaminoglycan scaffolds.

Chondrocytes are the only cells present in cartilage, and their death by apoptosis contributes to cartilage loss in joint diseases, such as OA (Buckwalter and Mankin, 1997; Gilbert 1998; Messner and Gillquist). The ability of mBMSC to differentiate along a chondrocyte lineage following BES onto scaffolds was examined. mBMSC were BES onto CG-scaffolds and cultured in chondrocyte differentiation medium for 21 days. Scaffolds were then stained with toluidine blue O such that cartilaginous extracellular matrix stained purple (metachromasia) while undifferentiated or fibrous tissue stained blue (scaffold). Successful differentiated of electrosprayed mBMSC into chondrocytes was demonstrated with purple cells evident and scattered around the scaffold (Fig. 5.13 B). Control involved culturing pipette mBMSC within a 15mL polypropylene tube in chondrocyte differentiation medium for 21 days. Result demonstrated singular differentiated chondrocyte pellet which was placed onto scaffold. Staining with toluidine blue O demonstrated clear metachromasia in pellet (purple), on the blue stained scaffold (Fig. 5.13 A). BES differentiated pellets appeared similar to pipette control on scaffold.

Chondrocyte differentiation was further verified for BES mBMSC when RNA was extracted from the scaffolds and expression of chondrocyte marker genes aggrecan and collage IIa was demonstrated using RT-PCR (Fig. 5.13 C).

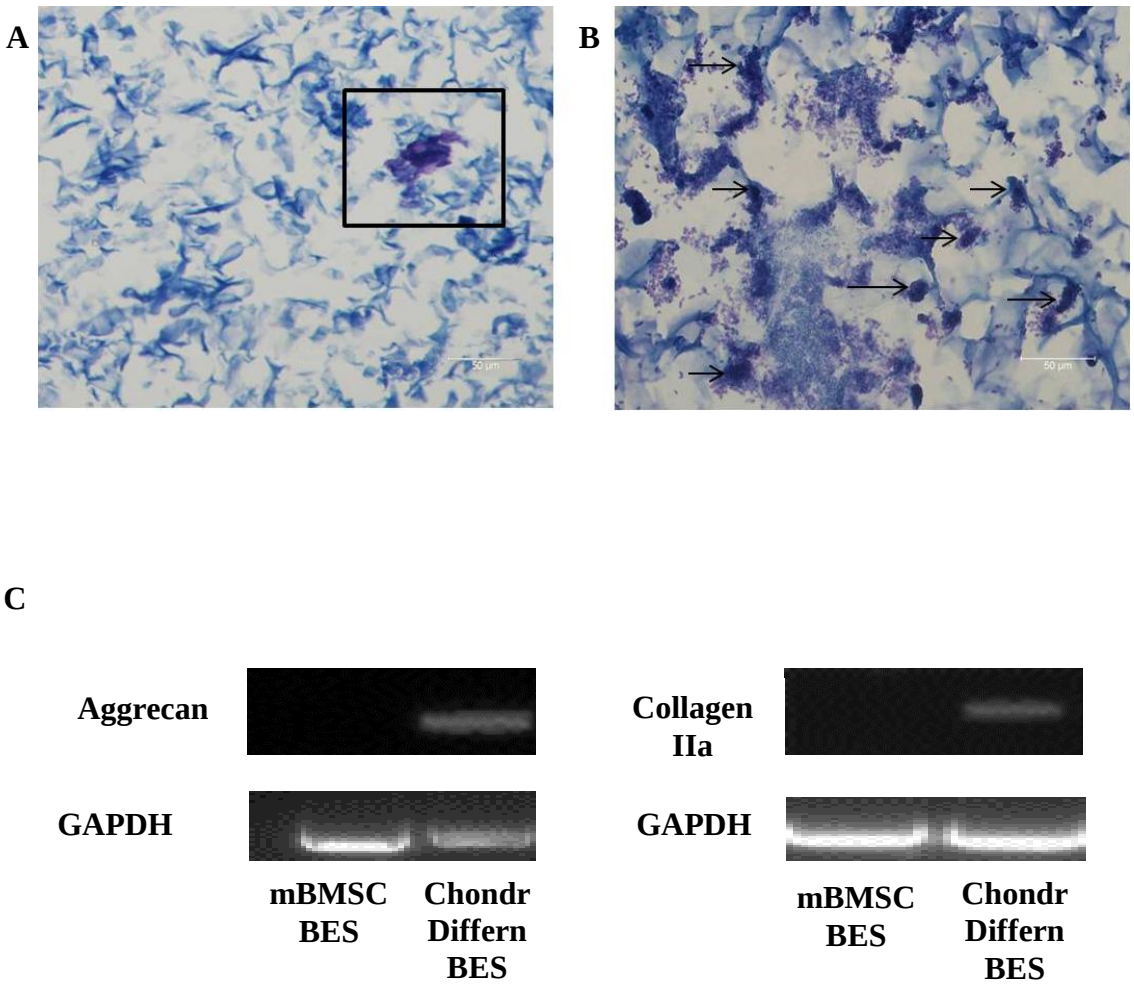

Fig. 5.13 Differentiation of mBMSC towards a chondrocyte lineage following BES onto CG-scaffolds. (A) mBMSC cultured in 15mL polypropylene tube in chondrocyte differentiation medium for 21 days was placed onto scaffold. (B) mBMSC were BES onto CG-scaffolds using SprayCell™ and cultured in chondrocyte differentiation medium for 21 days. Chondrocytes were detected by staining scaffolds with toluidine blue O. Purple stain indicates cartilaginous extracellular matrix of chondrocytes while undifferentiated cells and scaffold stained blue (x10 magnification). (C) Expression of aggrecan and collagen IIa mRNA was detected by RT-PCR for BES mBMSC after 21 days differentiation towards a chondrocyte lineage on scaffolds.

5.11 SprayCell™ capable of bio-electrospraying chondrocytes directly to specific target site

We have demonstrated that bone and fat cells can electrospray using Spraybase® (Fig. 5.7) at low voltages (5kV). We therefore examined whether SprayCell™ could replicate these results using differentiated cartridge cells. Chondrocytes obtained from differentiated mBMSC as described above were BES onto CG-scaffolds using SprayCell™ at low voltages (6kV). A specific site located on the scaffold was targeted with the spray. After 24 hr, the scaffold was stained with toluidine blue O. Chondrocyte aggregates were observed at the specific target site on the scaffold (Fig. 5.14). This indicates that differentiated cells, as well as MSC, can be delivered to substrates using BES method without adverse effects on cell functionality. Furthermore, in contrast to pipette delivery, it is possible to target cells to a specific location on a scaffold using the SprayCell™ electrospray catheter regardless of area size.

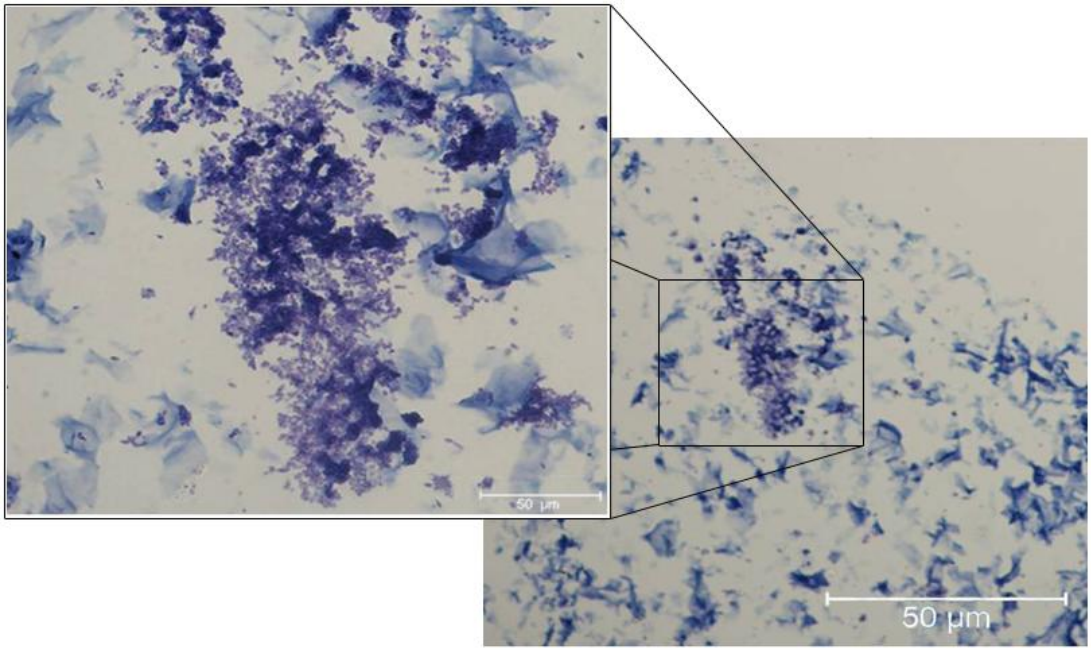

Fig. 5.14 BES of differentiated chondrocytes onto CG-scaffolds using SprayCell™. mBMSC were differentiated towards a chondrocyte lineage and then delivered onto CG-scaffolds using SprayCell™. Photomicrographs demonstrate aggregates of chondrocyte at 24 hr post-BES onto CG-scaffolds at (A) x10 magnification and (B) x40 magnification.

5.12 Discussion

Serious problems with donor availability, infection, rejection, and GvHD are associated with current gold standard methodologies for TERM. In addition, MSC cell therapies experience problems associated with I.V. injections which may prevent cells reaching an intended target site, while also presenting a dangerous phenomenon named MSC entrapment. As a result alternative substitutes are being developed for these therapeutic applications. Significantly, fabrication of functional scaffolds using the electrospinning process is currently dominating the TE field. This is due to the processes easy fabrication of nanofibres from polymers which can provide an artificial platform for cellular implantation, which mimics the natural ECM *in vivo*. However, difficulties with scaffold surface texture, fibre morphology and pore and fibre sizes still remain due to large variations in electrospinning apparatuses, and polymers used for this process. Therefore, the aim of this study evolved towards the development of an alternative strategy for cell delivery, wherein the cells are electrosprayed directly towards a targeted injury region, potentially eliminating problems associated with scaffolds and I.V. injections for *in vivo* applications.

Successful electrospraying of mBMSC using Spraybase® at low voltages (~3-6kV) have been demonstrated using optimal and reproducible parameters (Chapter 3). Cell viability, morphology and adherence to plastic were investigated in which the cells displayed similar behaviours to their pipette control counterparts (Fig. 3.5 and Fig. 3.8). However, as with previous studies, a full phenotypic analysis of MSC post BES had not been described (Sahoo *et al.*, 2010 and Ye *et al.*, 2014). Therefore, a key part of this study was the analysis of the effects low voltage electrospraying had on mBMSC function.

MSC are characterised after they are isolated from a tissue and cultured *ex vivo*. This is to prove the isolated cells are non- hematopoietic MSC. Tropel *et al.,* (2004) described adherence to plastic, surface marker expression and multilineage differentiation as three fundamental characteristics associated with MSC. In the present study, specific assays demonstrating surface marker expression and multilineage differentiation were conducted for both isolated MSC from mouse bone marrow, and BES mBMSC. By using identical characterisation assays for both isolated and BES mBMSC, this indicated if the low-voltage electrospray process adversely affected the BES cells, when compared to their non-BES counter parts. It was confirmed that expression of thirteen markers described by ISCT were either present or absent as appropriate for the BES cells (Fig. 5.1). Similar results were observed when the electrosprayed mBMSC differentiated into osteocytes, adipocytes and chondrocytes after 21days (Fig. 5.2). These results support the concept that low-voltage BES had no perturbing adverse effects to mBMSC.

Another significant feature for MSC is the modulation of lymphocytes through inhibition mechanisms occurring via various pathways involving cell contact and soluble factors (Di Nicola *et al.*, 2002, Krampera *et al.*, 2003). One method MSC are believed to modulate T cells is through direct suppression of proliferation, as it has been reported that T cells cultured with MSC did not progress past G1 phase of the cell cycle (Glennie *et al.,* 2005). The inability of this trait to function can lead to major consequences in clinical trials where MSC have been used to treat patients. For example, increased T cell proliferation in patients with GvHD can enhance an immune response resulting in graft rejection.

Similarly, by suppressing T cell activation in patients with autoimmune diseases can potentially stop an immune response and the immune system attacking itself. However, if this function is compromised, T cell proliferation can activate an immune response which can be detrimental to the patient. Therefore, it was imperative to investigate the immunosuppressive effects of mBMSC following electrospraying. Analyses from two studies examining suppression of alloantigen and mitogen driven T-cell proliferation, indicated low-voltage BES did not compromise this vital characteristic of mBMSC. Although a small amount of proliferation occurred for both studies, T-cell proliferation was significantly reduced by 4 fold in the presence of pipette mBMSC and mBMSC subjected to BES respectively (Fig. 5.3 and Fig.5.4).

MSC have been reported to induce repair through cell education and trophic manipulation of the micro-environment (Phinney and Prockop, 2007, Caplan and Dennis, 2006). Given the heterogeneity of *in vitro* cultured MSC, the concepts of regeneration and trophic repair may not be mutually exclusive, (Phinney and Prockop, 2007, English *et al.*, 2013). This suggests that if MSC are heterogeneous mixed populations, the regeneration effects may be performed by different sub-populations. However, in order to determine if low-voltage affected mBMSC pro-reparative properties, *in vitro* assays were used. BES mBMSC were evaluated *in vitro* when two separate cell lines were monitored for wound closure, over 24hrs. Results implied that trophic factors from either pipette or electrosprayed mBMSC induced wound closure for each cell line, as medium only control containing growth factors and no cells resulted in little to no wound closure (Fig. 5.5 and Fig. 5.6).

This indicates that BES mBMSC pro-reparative capabilities are not adversely affected by low-voltage electrospraying using Spraybase®, suggesting similar results may occur for *in vivo* regeneration and/or trophic repair.

A full phenotypic analysis of mBMSC following low-voltage electrospraying using Spraybase®, provided critical data in suggesting this jetting process has potential as an alternative cell delivery method, for TERM and cell therapy applications. It was confirmed that BES mBMSC maintained vital cellular and immunological characteristics similar to pipette controls, indicating the low-voltage electrospraying did not affect these abilities. Spraybase® is a benchtop instrument and its configuration is more suitable for laboratory experiments. Therefore, in promoting BES as a cell delivery method it was necessary to have an apparatus that was more medically applicable.

Procuring the electrospray device, SprayCell™, provided the instrument required for medical environments. SprayCell™ specially designed catheter is the systems most unique and essential component. To date, no other electrospray apparatus has been constructed with such a feature. The catheter incorporates both the single needle and ground electrode within the catheter tubing, and can be modified to fit any type endoscope for keyhole surgery. Thus, this generated a jetting device which is compatible with *in vivo* applications (Fig 5.8 and Fig. 5.9). Interestingly, unlike the Spraybase® apparatus where voltage fluctuated between ~3-6kV due to RH of the lab, voltage for SprayCell™ remained at 6kV throughout all experiments. This is a crucial improvement for the use of this method in medical environments, as theatres are generally monitored at constant temperatures and RH.

Therefore, it is suggested that the settings of these environments will not impact on the low-voltage applied for MSC administration, ensuring this method is safe for both the user and patient.

Furthermore, although it was necessary to adjust the flowrate to accommodate endoscope length, it was shown that the addition of the catheter provided higher cell viability compared to Spraybase® apparatus (Fig 5.11). One suggestion for this is possibly due to the tubing protecting the cells from the force of the spray, causing less shearing, which ultimately leads to cell death.

In order to assess the potential behaviours of BES MSC *in vivo* a comprehensive 3D study using CG scaffolds and SprayCell™ electrospray was carried out. The results from these investigations demonstrated BES mBMSC adhered to the scaffold, but more significantly, penetrated deeper into the scaffold compared to their pipette counterparts (Fig. 5.10 and Fig. 5.12). As tissues vary in thickness this may prove to be an essential attribute for the electrospraying method for *in vivo* applications. Furthermore, it was demonstrated that BES mBMSC differentiated into chondrocytes on scaffolds indicating the cells maintained their functions (Fig. 5.13). The last decade has seen a major focus towards developing novel therapeutic strategies for cartilage defects. Current medical treatments lack in techniques to regenerate articular-cartilage, and existing therapeutic treatments only alleviate pain instead of controlling disease progression.

BES MSC directly to injured cartilage areas using SprayCell™ device, through keyhole surgery, may hold some potential towards new articular-cartilage regeneration therapeutics. As mBMSC have been shown to adhere and differentiate into chondrocytes on CG-scaffolds, it suggests similar results may be attained for *in vivo* purposes.

Furthermore, this study also proposes to BES chondrocytes to injured regions with the potential to enhance previously developed cartilage regeneration therapies such as the ACI method. Autologous chondrocyte implantation is considered new and effective therapy aimed at re-establishing the articular tissue. This was shown in a study by Frisbie *et al.* (2008) when they evaluated ACI transplantation via a collagen membrane in equine articular defects. However, in addition to immune rejection, a major obstacle for autologous transplantation is the lack of large numbers of chondrocytes available. Issues with maintaining chondrocyte viability during *in vitro* expansion has also proven problematic (Ashraf *et al.*, 2015). Our final study demonstrated successful electrospraying of chondrocytes to a specific area at low voltages of 6kV. Cells adhered to scaffolds after 24 hr at a specific targeted site (Fig. 5.14). This demonstrates potential for advancing ACI such that BES autologous chondrocytes using SprayCell™ directly to injured sites may possibly eliminate problems with scaffold transplantation and immune rejection. It may also aid problems associated with cell numbers and viability.

Chondrocytes have been reported to respond slowly to trauma such as articular-cartilage lesions, demonstrating limited proliferative capacity and a reduced potential for the de-novo synthesis of an extracellular matrix *in vivo* (Shapiro *et al.*, 1993; Hunziker 2002).

Our hypothesis is to BES *in vitro* cultured autologous chondrocytes to a defected cartilage area, wherein the cells adhere and potentially divides into daughter cells *in vivo*. These daughter cells will originate as chondroblasts which can potentially secrete new ECM while maturing into new chondrocytes at the source of the defect. Moreover we also suggest the possibility wherein the new electrosprayed chondrocytes may stimulate signally pathways of its surrounding microenvironment, potentially inducing an immune response to close the lesion wound, before it escalates to the onset of OA.

In addition, this study demonstrates the accuracy of controlled spray from the catheter. Lack of toluidine blue O staining on scaffold except at designated chondrocyte sites, suggests chondrocytes electrosprayed solely to intended area of scaffold. This supports our hypothesis in employing SprayCell™ to directly BES MSC/chondrocytes to injured regions, as an innovative delivery strategy for cell/regenerative therapies.

In summary, MCS hold great promise as therapeutic entities and as such are receiving significant levels of attention. However, the challenges encountered with current delivery methods illustrate that new and innovative methods for MSC administration are required. BES holds potential as a delivery method for MSC, and other cell types, as it could enable direct delivery of known number of cells to a target area *in vivo*. This is a critical step towards the translation of electrospray technologies for delivery of cells for therapeutic purposes *in vivo*.

Conclusions and Future Directions

6. Conclusions

Employing jetting methodologies to deliver live cells is as still a relatively new concept. This study evaluated a commercial electrospray instrument which permitted the establishment of standardised optimal parameters to BES cells, generating a system for reproducing data between experiments and potential medical environments. In addition, it was proven that a stable Taylor cone of cells in suspension can be achieved using a single needle configuration at low voltages, a result not yet reported. High yields of viable cells can BES using either the bench-top, or the medically designed electrospray apparatuses, at low voltages. Essential cellular and immunological characteristics of mBMSC were demonstrated to behave similar to those of non-BES counterparts, indicating that the low voltages did not adversely affect the cells. This was shown for 2D and 3D experiments. Finally, electrosprayed cells were shown to deliver directly to a target site either in culture wells or on scaffolds, while distributing in equal volumes. These studies have demonstrated that BES possesses the potential to be a delivery method for MSC, and other cell types, as it could facilitate direct delivery of known number of cells to a target area *in vivo*. This is a significant result in moving the electrospray process forward, taking the BES of cells from “bench to beside” for therapeutic purposes *in vivo*.

The commercial electrospray was also shown to electrospin fibres at the nano and mirco scale, for newly designed polymer blends, at reproducible optimal parameters. The fabrication of two contrasting 3D constructs involving collagen and agarose, demonstrated how various parameters affect scaffold surface texture, fibre morphology and fibre and pores sizes, characteristics essential for functional 3D scaffolds for TERM.

7. Future Directions

This work involved using MSC for applications involved in TERM and cell therapy purposes. All experiments were performed using BMSC derived from mice. Future experiments should use either autologous expanded human MSC, or the genetically reprogrammed adult stromal cells, iPSC. Performing the same characteristic assays on BES hMSC or BES iPSC, can potentially give more accurate results of the effects low-voltages electrospraying may have on the cells *in vivo*. BES autologous harvested cells may also reduce issues with heterogeneity of *in vitro* cultured MSC, such that the concepts of regeneration and trophic repair may not be mutually exclusive.

In addition, the optimisation of a commercial electrospray for the BES of cells at low voltages demonstrated vital cellular and immunological characteristics behaved similar to their non-BES counterparts. All assays, except for chondrocyte differentiation, were performed using 2D culture systems. Therefore, conducting the osteogenic and adipogenic differentiation assays on MSC electrosprayed onto 3D scaffolds will give more accurate results to the differential potential of MSC *in vivo,* when BES at low voltages.

The aforementioned are preliminary studies for future work, and will be followed by investigations into the most critical future direction for the BES of MSC as a cell delivery strategy. These will include examining if BES MSC can adhere, proliferate, differentiate and induce wound healing at an injured region *in vivo*, using the medically designed electrospray apparatus with catheter. The purpose of this catheter is to fit all types of endoscopes.

Therefore, it is necessary to carry out keyhole surgeries using animal models, where in MSC are BES at low voltages to injuries at various sites of the animal body, relevant to MSC therapies. This would allow complex experimental data to be evaluated for the effects low-voltage BES has on MSC viability and function capabilities, specifically differentiation and pro-reparative properties necessary for TERM applications. In addition, it is essential to investigate the immunosuppressive properties of BES MSC *in vivo*. Using animal models for GvHD disease can give excellent experimental data for the immunosuppressive capabilities of BES MSC, which is essential for cell therapy purposes.

Following examination of the affects low-voltage BES has on MSC *in vivo*, investigations into electrospraying autologous expanded chondrocytes to articular-cartilage lesions will be crucial, to promote new possibilities for cartilage regeneration therapy. BES autologous chondrocytes through arthroscopy using the electrospraying catheter to cartilage lesions *in vivo,* will demonstrate if cells can adhere to the injured site without the aid of scaffolds. In addition, it will allow assessment of the ability of chondrocytes to induce new chondroblasts, which ultimately produces new chondrocytes and cartilage ECM, post BES, resulting in either a more enhanced ACI therapy or the generation of a new regenerative cartilage therapy.

Future directions for agarose electrospun fibres may hold some promise in the fabrication of superior scaffolds. Incorporating the micron thick fibres with nanofibrous scaffolds may potentially create 3D constructs with large pore sizes, to enable cell and nutrient infiltration through scaffold, while eliminating waste, possibly assisting in advancing TE applications. It is necessary to examine critical scaffold properties such as fibre tensile, porosity and permeability measurements for these scaffolds. In addition, investigations into cellular activity upon and through these scaffolds are also essential for future applications.

8. Bibliography

- Abeyewickreme, A., Kwok, A.., McEwan, J.R. and Jayasinghe, S.N. 2009. Bio-electrospraying embryonic stem cells: interrogating cellular viability and pluripotency. *Integr. Biol. (Camb).*, 3, 260.

- Adán, N., Guzmán-Morales, J., Ledesma-Colunga, M.G., Perales-Canales, S.I., Quintanar-Stéphano, A., López-Barrera, F., Méndez, I., Moreno-Carranza, B., Triebel, J., Binart, J., Martínez de la Escalera, G., Thebault, S. and Clapp, C. 2013. Prolactin promotes cartilage survival and attenuates inflammation in inflammatory arthritis. *J Clin Invest.*, 123(9): 3902-3913.

- Agarwal, S., Wendorff, J.H. and Greiner, A. 2008. Use of electrospinning technique for biomedical applications. *Polymer*, 49, 5603.

- Aigner, T. and Soder, S. 2008.Typing, grading and staging of osteoarthritis: histopathological assessment of joint degeneration. *Z Rheumatol.*, 67. 32-36, 38-40.

- Altman, R.D., Kates, J., Chun, L.E., Dean, D.D., Eyre, D. 1992. Preliminary observations of chondral abrasion in a canine model. *Ann Rheum Dis.*, 51:1056-62.

- Asanbaeva, A., Masuda, K., Thonar, E.J., Klisch, S.M., Sah, R.L. 2008. Cartilage growth and remodeling: Modulation of balance between proteoglycan and collagen network *in vitro* with β-aminopropionitrile. *Osteoarthritis and Cartilage,* 16(1): 1-11.

- Ashraf, S., Cha, B.H., Kim, J.S., Ahn, J., Han, I, Park, H. and Lee, S.H. 2015. Regulation of senescence associated signaling mechanisms in chondrocytes for cartilage tissue regeneration. *Osteoarthritis and Cartilage*, (Epub ahead of print).

- Baker, B.M. *et al.* 2008. The potential to improve cell infiltration in composite fiber-aligned electrospun scaffolds by the selective removal of sacrificial fibers. *Biomaterials*, 29(15), pp.2348-2358.

- Baran, G., Kiani, M. and Samuel, S. 2014. Tissue Engineering: Growing Replacement Human Tissue in the Lab, in Healthcare and Biomedical Technology in the 21st Century2014. *Springer New York.*, p. 343-382.

- Bartolovic, K., Mongkoldhumrongkul, N., Waddington, S.N., Jayasinghe, S.N. and Howe, S.J. 2010. The differentiation and engraftment potential of mouse hematopoietic stem cells is maintained after bio-electrospray. *Analyst.* 135(1), 157.

- Baumgarten, P.K. 1971. Electrostatic spinning of acrylic microfibers. *J of Colloid and Interface Science*., 36:71–9.

- Bhatia, D., Bejarano, T., Novo, M. 2013. Current interventions in the management of knee osteoarthritis. *J Pharm Bioallied Sci,* 5:30-8.

- Bonino, C.A., Krebs, M.D., Saquing, C.D., Jeong, S.I., Shearer, K.L., Alsberg, E., Khan, S.A. 2011. Electrospinning alginate-based nanofibers: From blends to crosslinked low molecular weight alginate-only systems. *Carbohydrate Polymers.,* 85(1): 111-119.

- Braddock, M., *et al.* 2001. Born again bone: tissue engineering for bone repair. *News Physiol Sci,* 16: 208-13.

- Brittberg, M., Lindahl, A., Nilsson, A., Ohlsson, C., Isaksson, O., Peterson, L. 1994. Treatment of deep cartilage defects in the knee with autologous chondrocyte transplantation. *N Engl J Med.,* 331:889-95.

- Bromley, M. and Woolley, D.E. 1984. Histopathology of the rheumatoid lesion. Identification of cell types at sites of cartilage erosion. *Arthritis Rheum*, 27:857-63

- Browne, J.E. and Branch, T.P. 2000. Surgical alternatives for treatment of articular cartilage lesions. *J Am Acad Orthop Surg.,* 8: 180-9.

- Buckwalter, J.A. and Brown, T.D. 2004. Joint injury, repair, and remodeling: roles in post-traumatic osteoarthritis. *Clin Orthop Relat Res.,*7-16.

- Buckwalter, J.A. and Mankin, H.J. 1997. Articular cartilage. 2: degeneration and osteoarthrosis, repair, regeneration, and transplantation. *J Bone Joint Surg Am.*, 79: 612-32.

- Candela, M.E., Yasuhara, R., Iwamoto, M., Enomoto-Iwamoto, M. 2014. Resident mesenchymal progenitors of articular cartilage. *Matrix Biol,* 39:44-9.

- Caplan, A.I. and Dennis, J.E. 2006. Mesenchymal stem cells as trophic mediators. *J Cell Biochem.,* 98: 1076-84.

- Cassatella, M. A., Mosna, F., Micheletti, A., Lisi, V., Tamassia, N., Cont, C., Calzetti, F., Pelletier, M., Pizzolo, G. and Krampera, M. 2011. Toll-Like Receptor-3-Activated Human Mesenchymal Stromal Cells Significantly Prolong the Survival and Function of Neutrophils. *Stem Cells,* 29**,** 1001-1011.

- Castromalaspina, H., Gay, R. E., Resnick, G., Kapoor, N., Meyers, P., Chiarieri, D., McKenzie, S., Broxmeyer, H. E. and Moore, M. A. S. 1980. Characterization of Human-Bone Marrow Fibroblast Colony-Forming Cells (Cfu-F) and Their Progeny. *Blood,* 56**,** 289-301.

- Center for Disease Control and Prevention. Leading causes of death. [cited 01/08/2014]; Available from: http://www.cdc.gov/nchs/fastats/lcod.htm.

- Chaganti, R.K. and Lane N.E. 2011. Risk factors for incident osteoarthritis of the hip and knee. *Curr Rev Musculoskelet Med.*, 4: 99-104.

- Chamberlain, L.J., *et al.*1998. Collagen-GAG substrate enhances the quality of nerve regeneration through collagen tubes up to level of autograft. *Exp Neurol.,* 154(2): 315-29.

- Chan, C.K, Liao, S., Li, B., Lareu, R.R., Larrick, J.W., Ramakrishna, S. and Raghunath, M. 2009. Early adhesive behavior of bone-marrow-derived mesenchymal stem cells on collagen electrospun fibers. *Biomed Mater.,* 4(3):035006.

- Chen, H., Sun, J., Hoemann, C.D., Lascau-Coman, V., Ouyang, W., McKee, M.D., *et al.* 2009. Drilling and microfracture lead to different bone structure and necrosis during bone-marrow stimulation for cartilage repair. *J Orthop Res.,* 27:1432-8.

- Chen, F., Li, X., Mo, X., He, C., Wang, H., Ikada, Y. 2008 Electrospun chitosan-P(LLA-CL) nanofibers for biomimetic extracellular matrix. *J Biomater Sci Polym Ed.,*19(5):677–91.

- Chen, L., Tredget, E.E., Wu, P.Y. and Wu, Y. 2008. Paracrine factors of mesenchymal stem cells recruit macrophages and endothelial lineage cells and enhance wound healing. *PLoS One,* 3(4), e1886.

- Chen, M., Patra, P.K, Warner, S.B. and Bhowmick, S. 2007. Role of fiber diameter in adhesion and proliferation of NIH 3T3 fibroblast on electrospun polycaprolactone scaffolds. *Tissue Eng.* 13(3):579-87.

- Chen, W., Han, Y., Chen, Y., Xie, J.T. 1998. Field-induced electroconformational damages in cell membrane proteins: A new mechanism involved in electrical injury. Bioelectrochem *Bioenerg.,* 47(2):237–245.

- Choi, J.S. *et al.,* 2008. The influence of electrospun aligned poly(ε-caprolactone)/collagen nanofiber meshes on the formation of self-aligned skeletal muscle myotubes. *Biomaterials*, 29(1) 9: 2899-2906.

- Clarke, J.D.W., and Suwan N Jayasinghe, S.N. 2008. Bio-electrosprayed multicellular zebrafish embryos are viable and develop normally. (2008). *Biomedical Materials*, 3(1).

- Cloupeau, M. and Prunet-Foch, B. 1994. Electrohydrodyanmic spraying functioning modes: a critical review. *J. AerosolSci.,* 25: 1021–1036.

- Dazzi, F., Ramasamy, R., Glennie, S., Jones, S. P. and Roberts, I. 2006. The role of mesenchymal stem cells in haemopoiesis. *Blood Rev,* 20**,** 161-71.

- DeBruin, K.A. and Krassowska, W. 1999. Modeling electroporation in a single cell. I. Effects of field strength and rest potential. *Biophys J.,* 77(3), 1213.

- DeGarmo, P.E. Black, J.T., Kohser, R. 2011. *Online book,* ISBN-13: 978-0470924679

- Dehne, T., Karlsson, C., Ringe, J., Sittinger, M., Lindahl, A. 2009. Chondrogenic differentiation potential of osteoarthritic chondrocytes and their possible use in matrix-associated autologous chondrocyte transplantation. *Arthritis Res Ther.,* 11:R133.

- Deitzel, J.M. *et al.,* 2001. The effect of processing variables on the morphology of electrospun nanofibers and textiles. *Polymer*, 42, pp.261-272.

- Deitzel, J.M., Kleinmeyer, J., Hirvonen, J.K., Beck, T.N.C. 2001.Controlled deposition of electrospun poly(ethylene oxide) fibers. *Polymer,* 42:8163–70.

- Dell'accio, F. and Vincent, T.L. 2010. Joint surface defects: clinical course and cellular response in spontaneous and experimental lesions. *Eur Cell Mater*, 20:210-7.

- Ding, Y.C., Xu, D.M., Feng, G., Bushell, A., Muschel, R.J. and Wood, K.J. 2009. Mesenchymal stem cells prevent the rejection of fully allogenic islet grafts by the immunosuppressive activity of matrix metalloproteinase-2 and -9. *Diabetes* 58: 1797.

- Di Nicola, M., Carlo-Stella, C., Magni, M., Milanesi, M., Longoni, P.D., Matteucci, P., Grisanti, S. and Gianni, A.M. 2002. Human bone marrow stromal cells suppress T-lymphocyte proliferation induced by cellular or nonspecific mitogenic stimuli. *Blood* 99: 3838.

- Dole, M., Mack, L.L., Hines, R.L., Mobley, R.C., Ferguson, L.D. and Alice, M.B. 1968 Molecular beams of macroions. *J. Chem. Phys.,* 49: 2240–2249.

- Dominici, M., Le Blanc, K., Mueller, I., Slaper-Cortenbach, I., Marini, F.C., Krause, D.S., Deans, R.J., Keating, A., Prockop Dj. and Horwitz, E.M. 2006. Minimal criteria for defining multipotent mesenchymal stromal cells. The International Society for Cellular Therapy position statement. *Cytotherapy*, 8: 315.

- Doshi, J. and Reneker, D.H., 1995. Journal of Electrostatics. *Journal of Electrostatics*, 35(2-3), pp.151-160.

- Driesang, I.M. and Hunziker, E.B. 2000. Delamination rates of tissue flaps used in articular cartilage repair. *J Orthop Res.,* 18: 909-11.

- Dwyer, J.M. and Johnson, C. 1981. The use of concanavalin A to study the immunoregulation of human T cells. *Clin Exp Immunol*., 46: 237.

- Eagles, P.A, Qureshi, A.N, Jayasinghe, S.N. 2006. Electrohydrodynamic jetting of mouse neuronal cells. *Biochem J.*, 394(Pt 2):375–378.

- Eggenhofer, E., Benseler, V., Kroemer, A. *et al.* 2012. Mesenchymal stem cells are short-lived and do not migrate beyond the lungs after intravenous infusion. *Front Immunol.*, 3.

- English, K., Mahon, B.P. and Wood, K.J. 2013. Mesenchymal Stromal Cells; Role in Tissue Repair, Drug Discovery and Immune Modulation. *Curr Drug Deliv*., 11(5):561-71.

- English, K., French, A. and Wood, K.J. 2010. Mesenchymal Stromal Cells: Facilitators of Successful Transplantation? *Cell Stem Cell*, 10, 1016.

- English, K., Barry, F.P., Field-Corbett, C.P., Mahon, B.P. 2007. IFN-gamma and TNFalpha differentially regulate immunomodulation by murine mesenchymal stem cells. *Immunol Lett.*, 110, 91.

- Farrell, E., *et al.* 2006. A collagen-glycosaminoglycan scaffold supports adult rat mesenchymal stem cell differentiation along osteogenic and chondrogenic routes. *Tissue Eng.*, 12(3): 459-68.

- Fenn, J.B. 2003.Electrospray wings for molecular elephants (Nobel Lecture), *Angew. Chem., Int. Ed.*,42: 3871–3894.

- Fenn, J.B., Mann, M., Meng, C.K., Wong, S.F. and Whitehouse, C.M. 1998.Electrospray ionization for mass spectrometry of large biomolecules. *Science,* 246: 64–71.

- Fong, H. and Reneker, D.H. 2001. Electrospinning and formation of nanofibers. *Structure formation in polymeric fibers,* 225–46.

- Formhals A. US patent, 2,349,950, 1944.
- Formhals A. US patent, 2,323,025, 1943.
- Formhals A. US patent, 2,187,306, 1940.
- Formhals A. US patent 2,160,962, 1939.
- Formhals A. US patent 1,975,504, 1934.
- Friedenstein, A. J., Piatetzky, S., II and Petrakova, K. V. 1966. Osteogenesis in transplants of bone marrow cells. *J Embryol Exp Morphol,* 16**,** 381-90.
- Frisbie, D.D., Bowman, S.M., Colhoun, H.A., DiCarlo, E.F., Kawcak, C.E., McIlwraith, C.W. 2008. Evaluation of autologous chondrocyte transplantation via a collagen membrane in equine articular defects: results at 12 and 18 months. *Osteoarthritis Cartilage*,16: 667-79.
- Gass G.V., Chernomordik, L.V. 1990. Reversible large-scale deformations in the membranes of electrically-treated cells: Electroinduced bleb formation. *Biochim Biophys Acta.,* 1023(1):1–11.
- Ghasemi-Mobarakeh, L. *et al.*, 2008. Electrospun poly(ε-caprolactone)/gelatin nanofibrous scaffolds for nerve tissue engineering. *Biomaterials*, 29(34): 4532-4539
- Giannini, S., Buda, R., Grigolo, B., Vannini, F., De Franceschi, L., Facchini, A. 2005. The detached osteochondral fragment as a source of cells for autologous chondrocyte implantation (ACI) in the ankle joint. *Osteoarthritis Cartilage.*, 13:601-7.
- Giannoudis, P.V., *et al.* 2011.What should be the characteristics of the ideal bone graft substitute? *Injury,* 42(2):1-2.

- Gilbert J.E. 1998. Current treatment options for the restoration of articular cartilage. *Am J Knee Surg*., 11:42-6.

- Gilbert, W. 1991. *De Magnete*. Dover Publications. ISBN 978-0-486-26761-6. Republication of the 1893 unabridged and unaltered translation by Paul Fleury Mottelay.

- Glennie, S., Soeir, I., Dyson, P.J., Lam, E.W. and Dazzi, F. 2005. Bone marrow mesenchymal stem cells induce division arrest anergy of activated T cells. *Blood* 105: 2821.

- Grande, D.A., Pitman, M.I., Peterson, L., Menche, D., Klein, M. 1989. The repair of experimentally produced defects in rabbit articular cartilage by autologous chondrocyte transplantation. *J Orthop Res*., 7:208-18.

- Granero-Molto F., Weis, J.A., Miga, M.I, Landis, B. Myers, T.J., O'Rear, L., Longobardi, L., Jansen, E.D., Mortlock, D.P., and Spagnoli, A. 2009. Regenerative effects of transplanted mesenchymal stem cells in fracture healing. *Stem Cells*, 27:1887–1898.

- Gratz, K.R., Wong, B.L., Bae, W.C., Sah, R.L.2008. The effects of focal articular defects on intra-tissue strains in the surrounding and opposing cartilage. *Biorheology*, 45:193-207.

- Grenier, S, Bhargava, M.M., Torzilli, P.A. 2013. An in vitro model for the pathological degradation of articular cartilage in osteoarthritis. *J Biomech*, 47:645-52.

- Greiner, A. & Wendorff, J.H., 2007. Electrospinning: a fascinating method for the preparation of ultrathin fibers. *Angewandte Chemie*, 46(30), pp.5670-5703.

- Grinnemo, K. H., Mansson, A., Dellgren, G., Klingberg, D., Wardell, E., Drvota, V., Tammik, C., Holgersson, J., Ringden, O., Sylven, C. and Le Blanc, K. 2004. Xenoreactivity and engraftment of human mesenchymal stem cells transplanted into infarcted rat myocardium. *J Thorac Cardiovasc Surg*, 127**,** 1293-300.

- Gruenloh, W., Kambal, A., Sondergaard, C., McGee, J., Nacey, C., Kalomoiris, S., Pepper, K., Olson, S., Fierro, F. and Nolta, J. A. 2011. Characterization and in vivo testing of mesenchymal stem cells derived from human embryonic stem cells. *Tissue Eng Part A*, 17**,** 1517-25.

- Guan, J., Wang, F., Li, Z., Chen, J., Guo, X., Liao, J. and Moldovan, N.I. 2011. The stimulation of the cardiac differentiation of mesenchymal stem cells in tissue constructs that mimic myocardium structure and biomechanics. *Biomaterials*, 32(24), 5568.

- Guilhem, F., Thibault, B., Minh, B.H., Dulce, P.G., José, C. and Patricia, A. 2012. Glycosaminoglycans mimetics potentiate the clonogenicity, proliferation, migration and differentiation properties of rat mesenchymal stem cells. *Stem Cell Research*, 8: 180–192.

- Gustafsson, Y., Haag, J., Jungebluth, P., Lundin, V., Lim, M.L., Baiguera, S., Ajalloueian, F., Del Gaudio C., Bianco A., Moll G., Sjöqvist S., Lemon G., Teixeira A.I. and Macchiarini P. 2012. Viability and proliferation of rat MSCs on adhesion protein-modified PET and PU scaffolds. *Biomaterials*, 33(32):8094–103.

- Gupta, P. *et al.* 2005. Electrospinning of linear homopolymers of poly(methyl methacrylate):exploring relationships between fiber formation, viscosity, molecular weight and concentration in a good solvent. *Polymer*, 46: 4799-4810.

- Haviv, B., Bronak, S., Thein, R. 2013. The complexity of pain around the knee in patients with osteoarthritis. *Isr Med Assoc J* 15: 178-81.

- Hayati, A. and Tadros, T.F. 1986.Mechanism of stable jet formation in electrohydrodynamic atomization. *Nature.,* 319: 41–43.

- Hjelle, K., Solheim, E., Strand, T., Muri, R., Brittberg, M. 2002. Articular cartilage defects in 1,000 knee arthroscopies. *Arthroscopy.,* 18:730-4.

- Hoemann, C.D., Sun, J., McKee, M.D., Chevrier, A., Rossomacha, E., Rivard, G.E., *et al.* 2007.Chitosan-glycerol phosphate/blood implants elicit hyaline cartilage repair integrated with porous subchondral bone in microdrilled rabbit defects. *Osteoarthritis Cartilage,* 15:78-89.

- Ho, S.Y., Mittal, G.S. 1996. Electroporation of cell membranes: A review. Crit Rev *Biotechnol.,* 16(4):349–362.

- Horwitz, E. M., LE Blanc, K., Dominici, M., Mueller, I., Slaper-Cortenbach, I., Marini, F. C., Deans, R. J., Krause, D. S., Keating, A. and International Society for Cellular, T. 2005. Clarification of the nomenclature for MSC: The International Society for Cellular Therapy position statement. *Cytotherapy*, 7**,** 393-5.

- Huang, Z.M., Zhang, Y.Z., Kotaki, M. and Ramakrishna, S. 2003. A review on polymer nanofibers by electrospinning and their applications in nanocomposites. *Composites Science and Technology*, 63(15), 2223.

- Hunziker, E.B. and Stahli, A. 2008. Surgical suturing of articular cartilage induces osteoarthritis-like changes. *Osteoarthritis Cartilage,* 16:1067-73.

- Hunziker, E.B. 2002. Articular cartilage repair: basic science and clinical progress. A review of the current status and prospects. *Osteoarthritis Cartilage,* 10: 432-63.

- Hunziker, E.B., Quinn, T.M., Hauselmann, H.J. 2002. Quantitative structural organization of normal adult human articular cartilage. *Osteoarthritis Cartilage*, 10:564-72.

- Hunziker, E.B. and Rosenberg, L.C. 1996. Repair of partial-thickness defects in articular cartilage: cell recruitment from the synovial membrane. *J Bone Joint Surg Am*., 78:721-33.

- Hunziker, E.B. 1992. Articular cartilage structure in humans and experimental animals. *Articular Cartilage and Osteoarthritis. New York: Raven Press*, 183-99.

- Hutmacher, D.W. 2000. Scaffolds in tissue engineering bone and cartilage. *Biomaterials,* 21(24): 2529-43.

- Insall, J. 1974. The Pridie debridement operation for osteoarthritis of the knee. *Clin Orthop Relat Res*., 61-7.

- Insall, J.N.1967. Intra-articular surgery for degenerative arthritis of the knee. A report of the work of the late K. H. Pridie. *J Bone Joint Surg Br*., 49:211-28.

- Irvine, S., Sullivan, A.C., McEwan, J.R., and Jayasinghe, S.N. 2008. A unique physical-chemistry approach for fabricating cell friendly surfaces. *Biotechnol. J.*,3: 124–128.

- Jackson, D.W., Lalor, P.A., Aberman, H.M., Simon, T.M. 2001. Spontaneous repair of full-thickness defects of articular cartilage in a goat model. A preliminary study. *J Bone Joint Surg Am*., 83: 53-64.

- Jayasinghe, S. N. 2007. Bio-electrospraying living cells: a rapidly emerging jetting protocol having direct implications to the regenerative and therapeutic medicinal areas of research, *Biotechnol. J.,* 2: 934–937.

- Jayasingh S.N., AN Qureshi and PAM Eagles. (2006). Electrohydrodynamic jet processing: an advanced electric-field-driven jetting phenomenon for processing living cells. Small *2*:216–219.

- Jayasinghe S.N., PAM Eagles and AN Qureshi. (2006) Electric field driven jetting: an emerging approach for processing living cells. Biotechnol. J 1:86–94.

- Jayasinghe, S.N., Edirisinghe, M.J, Wilde, T. De. 2003. A novel process for simultaneous printing of multiple tracks from concentrated suspensions, *Mater. Res. Innovat*., 7, 63-64.

- Jaworek, A. and Krupa, A. 1999. Classification of the modes of EHD spraying. *J.Aerosol Sci.,* 30: 873–893.

- Jeong, S.I., Kim, S.Y., Cho, S.K., Chong, M.S., Kim, K.S., Kim, H., *et al.* 2007. Tissue-engineered vascular grafts composed of marine collagen and PLGA fibers using pulsatile perfusion bioreactors. *Biomaterials,*28(6):1115–22.

- Ji, W., Sun, Y., Yang, F., van den Beucken, J.J.J.P., Fan, M. W., Chen, Z. and Jansen, J.A. 2011. Bioactive electrospun scaffolds delivering growth factors and genes for tissue engineering applications. *Pharm. Res.*, 28, 1259.
- Jones G. 2013. Osteoarthritis: where are we for pain and therapy in 2013? *Aust Fam Physician*, 42:766-9.

- Jones, C.W., Willers, C., Keogh, A., Smolinski, D., Fick, D., Yates, P.J., *et al.* 2008. Matrix-induced autologous chondrocyte implantation in sheep: objective assessments including confocal arthroscopy. *J Orthop Res.,* 26:292-303.

- Ju, Y.M. *et al.* 2010. Bilayered scaffold for engineering cellularized blood vessels.*Biomaterials*, 31(15), pp.4313-4321.

- Karageorgiou, V. and Kaplan, D. 2005.Porosity of 3D biomaterial scaffolds and osteogenesis. *Biomaterials*, 26:5474-91.

- Karp, J.M. and Leng, Teo G.S. 2009. Mesenchymal stem cell homing: the devil is in the details. *Cell Stem Cell*, 4: 206.

- Katsara, O., Mahaira, L. G., Iliopoulou, E. G., Moustaki, A., Antsaklis, A., Loutradis, D., Stefanidis, K., Baxevanis, C. N., Papamichail, M. and Perez, S. A. 2011. Effects of Donor Age, Gender, and In Vitro Cellular Aging on the Phenotypic, Functional, and Molecular Characteristics of Mouse Bone Marrow-Derived Mesenchymal Stem Cells. *Stem Cells and Development,* 20**,** 1550-1562.

- Kazemnejad S., Allameh A., Soleimani, M., Gharehbaghian, A., Mohammadi, Y., Amirizadeh, N., and Jazayery, M. 2009. Biochemical and molecular characterization of hepatocyte-like cells derived from human bone marrow mesenchymal stem cells on a novel three-dimensional biocompatible nanofibrous scaffold. *J Gastroenterol Hepatol.*, 24(2):278-87.

- Kebriaei, P., Isola, L., Bahceci, E., Holland, K., Rowley, S., McGuirk, J., Devetten, M., Jansen, J., Herzig, R., Schuster, M., Monroy, R. and Uberti, J. 2009. Adult human mesenchymal stem cells added to corticosteroid therapy for the treatment of acute graft-versus-host disease. *Biol Blood Marrow Transplant,* 15**,** 804-11.

- Kim, H.K., Moran, M.E., Salter, R.B. 1991. The potential for regeneration of articular cartilage in defects created by chondral shaving and subchondral abrasion. An experimental investigation in rabbits. *J Bone Joint Surg Am.*,73:1301-15.

- Knutsen, G., Drogset, J.O., Engebretsen ,L., Grontvedt, T., Isaksen, V., Ludvigsen, T.C., *et al.* 2007. A randomized trial comparing autologous chondrocyte implantation with microfracture. Findings at five years. *J Bone Joint Surg Am.,* 89:2105-12.

- Krampera, M., Glennie, S., Dyson, J., Scott, D., Laylor, R., Simpson, E. and Dazzi, F. 2003. Bone marrow mesenchymal stem cells inhibit the response of naive and memory antigen-specific T cells to their cognate peptide. *Blood,* 101: 3722-9.

- Kumbar, S.G. *et al.* 2008. Electrospun poly(lactic acid-*co*-glycolic acid) scaffolds for skin tissue engineering. *Biomaterials*, 29(30), pp.4100-4107.

- Ladd, M.R., Hill, T.K., Yoo, J.J. and Lee, S.J. 2011. Electrospun Nanofibers in Tissue Engineering. *Nanofibers - Production, Properties and Functional Applications*. Dr. Tong Lin, eds. ISBN: 978-953-307-420-7, InTech, DOI: 10.5772/24095. Available from: http://www.intechopen.com/books/nanofibers-production-properties-and-functional-applications/electrospun-nanofibers-in-tissue-engineering.

- Lama, V.N., Smith, L., Badri, L., Flint, A., Andrei, A.C., Murray, S., *et al*. 2007. Evidence for tissue–resident mesenchymal stem cells in human adult lung from studies of transplanted allografts. *J Clin Invest.,* 117: 989–96.

- Langer, R. and Vacanti, J.P. 1993. Tissue engineering. *Science,* **260**(5110): 920-6.

- Lee, J.H., Rim, N.G., Jung, H.S. and Shin, H. 2010. Control of osteogenic differentiation and mineralization of human mesenchymal stem cells on composite nanofibers containing poly[lactic-co-(glycolic acid)] and hydroxyapatite. *Macromol Biosci.,* 10(2):173-82.

- Lee, R. H., Pulin, A. A., Seo, M. J., Kota, D. J., Ylostalo, J., Larson, B. L., Semprun-Prieto, L., Delafontaine, P. and Prockop, D. J. 2009. Intravenous hMSCs Improve Myocardial Infarction in Mice because Cells 223 Embolized in Lung Are Activated to Secrete the Anti-inflammatory Protein TSG-6. *Cell Stem Cell,* 5**,** 54-63.

- Lee, S.H. and Shin, H. 2007. Matrices and scaffolds for delivery of bioactive molecules in bone and cartilage tissue engineering. *Adv Drug Deliv Rev.,* 59(4-5), 339.

- Lee, R. H., Seo, M. J., Reger, R. L., Spees, J. L., Pulin, A. A., Olson, S. D. and Prockop, D. J. 2006. Multipotent stromal cells from human marrow home to and promote repair of pancreatic islets and renal glomeruli in diabetic NOD/scid mice. *Proceedings of the National Academy of Sciences of the United States of America,* 103**,** 17438-17443.

- Lee, C.R., Grodzinsky, A.J., Spector, M. 2003. Modulation of the contractile and biosynthetic activity of chondrocytes seeded in collagen-glycosaminoglycan matrices. *Tissue Eng.,* 9(1): 27-36.

- Lee, C.R., Grodzinsky, A.J., Hsu, H.P., Martin, S.D., Spector, M. 2000. Effects of harvest and selected cartilage repair procedures on the physical and biochemical properties of articular cartilage in the canine knee. *J Orthop Res*., 18:790-9.

- Lefkoe, T.P., Trafton, P.G., Ehrlich, M.G., Walsh, W.R., Dennehy, D.T., Barrach, H.J., *et al.* 1993. An experimental model of femoral condylar defect leading to osteoarthrosis. *J Orthop Trauma,* 7: 458-67.

- Leong, M.F., Chan,W.Y., Chian, K.S., Rasheed, M.Z., Anderson, J.M. 2010. Fabrication and *in vitro* and *in vivo* cell infiltration study of a bilayered cryogenic electrospun poly (D, L-lactide) scaffold. *J Biomed Mater Res. A,* 94:1141–9.

- Li, H., Wong, Y.S., Wen, F., Ng, K.W., Ng, G.K., Venkatraman, S.S., Boey, F.Y. and Tan, L.P. 2013. Human mesenchymal stem-cell behaviour on direct laser micropatterned electrospun scaffolds with hierarchical structures. *Macromol Biosci.*, 13(3):299-310.

- Li, Y. P., Paczensny, S., Lauret, E., Poirault, S., Bordigoni, P., Mekhloufi, F., Hequet, O., Bertrand, Y., Ou-Yang, J. P., Stoltz, J. F., Miossec, P. and Eljaafari, A. 2008. Human mesenchymal stem cells license adult CD34+ hemopoietic progenitor cells to differentiate into regulatory dendritic cells through activation of the Notch pathway. *J Immunol,* 180**,** 1598-608.

- Li, D. and Xia, Y.N. 2004. Electrospinning of nanofibers: reinventing the wheel? *Adv. Mater.,* 16: 1151–1170.

- Lian, Q. Z., Zhang, Y. L., Zhang, J. Q., Zhang, H. K., Wu, X. G., Zhang, Y., LAM, F. F. Y., Kang, S., Xia, J. C., Lai, W. H., Au, K. W., Chow, Y. Y., Siu, C. W., Lee, C. N. & Tse, H. F. 2010. Functional Mesenchymal Stem Cells Derived From Human Induced Pluripotent Stem Cells Attenuate Limb Ischemia in Mice. *Circulation,* 121**,** 1113-U91.

- Liang, D., Hsiao, B.S. and Chu, B. 2007. Functional electrospun nanofibrous scaffolds for biomedical applications. *Adv. Drug Deliv. Rev.*, 59:1392–1412.

- Liechty, K.W., MacKenzie, T.C., Shaaban, A.F., Radu, A., Moseley, A.M., Deans, R., *et al.* 2000. Human mesenchymal stem cells engraft and demonstrate site-specific differentiation after in utero transplantation in sheep. *Nat Med.,* 6: 1282–6.

- Madry, H., Luyten, F.P., Facchini, A. 2011. Biological aspects of early osteoarthritis. *Knee Surg Sports Traumatol Arthrosc*, 20: 407-22.

- McKernan, R., McNeish, J., Smith, D. 2010. Pharma's developing interest in stem cells. *Cell Stem Cell* 6, 517.

- Megelski, S. et al. 2002. Micro- and nanostructured surface morphology on electrospun polymer fibers. *Macromolecules*, 35(22), pp.8456-8466.

- Messner, K and Maletius, W. 1996. The long-term prognosis for severe damage to weight-bearing cartilage in the knee. A 14-year clinical and radiographic follow-up in 28 young athletes. *Acta Orthop Scand.*, 67 (2): 165-8.

- Messner, K., Gillquist, J. 1996. Cartilage repair. A critical review. *Acta Orthop Scand.*, 67: 523-9.

- Metsaranta, M., Kujala, U.M., Pelliniemi, L., Osterman, H., Aho, H., Vuorio, E. 1996. Evidence for insufficient chondrocytic differentiation during repair of full-thickness defects of articular cartilage. *Matrix Biol.*,15: 39-47.

- Mills, C. R. 2009. Osiris Therapeutics Reports Interim Data for COPD Stem Cell Study.

- Molyneux, P. 1983. Water-Soluble Synthetic Polymers: Properties and Behavior. *CRC Press*, 1.

- Mongkoldhumrongkul, N., Swain, S.C., Jayasinghe, S.N. and Stürzenbaum, S. 2010. Bio-electrospraying the nematode *Caenorhabditis elegans*: studying whole genome transcriptional responses and key life cycle parameters. *Journal of the Royal Society, Interface*, 7: 595-601.

- Mongkoldhumrongkul N., Flanagan, J.M, Jayasinghe, S.N. 2009. Direct jetting approaches for handling stem cells. *Biomed Mater.,* 4(1):15018.

- Muller, B. and Kohn D. 1999. Indication for and performance of articular cartilage drilling using the Pridie method. *Orthopade*, 28:4-10.

- Murphy, C.M., Haugh, M.G., O'Brien, F.J. 2010. The effect of mean pore size on cell attachment, proliferation and migration in collagen-glycosaminoglycan scaffolds for bone tissue engineering. *Biomaterials,* 31(3): 461-6.

- Murray, K.K., Boyd, R.K., Eberlin, M.N., Langley, G.J., Li, L., Naito, Y. 2013. IUPAC Recommendations. *Pure Appl. Chem.,* 85: 1515-1609.

- Ng, K.E., Joly, P., Jayasinghe, S.N., Vernay,B., Knight, R., Barry, S.P., McComick, J., Latchman, D., Stephanou A. 2011. Bio-electrospraying primary cardiac cells: in vitro tissue creation and functional study. *Biotechnol J.,* 6(1):86-95.

- Nystedt, J., Anderson, H., Tikkanen J. *et al.* 2013. Cell surface structures influence lung clearance rate of systemically infused mesenchymal stromal cells. *Stem Cells,* 31: 317.

- O'Brien, F.J. 2011. Biomaterials & scaffolds for tissue engineering. *Materials Today*, 14(3): 88-95.

- O'Brien, F.J. *et al.* 2005. The effect of pore size on cell adhesion in collagen-GAG scaffolds. *Biomaterials,* 26(4):433-441.

- O'Brien, F.J., Harley, B.A., Yannas, I.V., Gibson, L. 2004. Influence of freezing rate on pore structure in freeze-dried collagen-GAG scaffolds. *Biomaterials*; 25:1077-86.

- Odenwalder P., Irvine S., McEwan J.R., Jayasing S. N. Bio-electrosprays: a novel electrified jetting methodology for the safe handling and deployment of primary living organisms. Biotechnology Journal 2:5, 655, 2007.

- Omatsu, Y., Sugiyama, T., Kohara, H., Kondoh, G., Fujii, N., Kohno, K. and Nagasawa, T. 2010. The Essential Functions of Adipo-osteogenic Progenitors as the Hematopoietic Stem and Progenitor Cell Niche. *Immunity,* 33**,** 387-399.

- Pearle, A.D., Warren, R.F., Rodeo, S.A. (2005). Basic Science of Articular Cartilage and Osteoarthritis. *Clinics in Sports Medicine,* 24(1): 1–12.

- Peister, A., Mellad, J.A., Larson, B.L., Hall, B.M., Gibson, L.F., Prockop, D.J. 2004. Adult stem cells from bone marrow (MSCs) isolated from different strains of inbred mice vary in surface epitopes, rates of proliferation, and differentiation potential. *Blood,* 103, 1662.

- Pham, Q.P., Sharma, U., Mikos, A.G. 2006. Electrospun poly(epsilon-caprolactone) microfiber and multilayer nanofiber/microfiber scaffolds: characterization of scaffolds and measurement of cellular infiltration. *Biomacromolecules*, 7: 2796-805.

- Pham, Q.P., Sharma, U., and Mikos, A.G. 2006. Electrospinning of polymeric nanofibers for tissue engineering applications: a review. *Tissue Engineering*, 12(5), pp.1197-1211.

- Phinney, D.G. and Prockop, D.J. 2007.Concise review: mesenchymal stem/multipotent stromal cells: the state of transdifferentiation and modes of tissue repair--current views. *Stem Cells*, 25: 2896-902.

- Phipps, M.C., Clem, W.C., Grunda, J.M., Clines, G.A. and Bellis, S.L. 2012. Increasing the pore sizes of bone-mimetic electrospun scaffolds comprised of polycaprolactone, collagen I and hydroxyapatite to enhance cell infiltration. *Biomaterials,* 33(2):524-34.

- Pirlo R. K., Dean, D. M.D., Knapp, D.R. and Gao, B.Z. 2006. Cell deposition system based on laser guidance. *Biotechnol. J.,* 1: 1007–1013.

- Pittenger, M.F., Mackay, A.M., Beck, S.C., Jaiswal, R.K., Douglas, R., Mosca, J.D., Moorman, M.A., Simonetti, D.W., Craig, S. and Marshak, D.R. 1999. Multilineage potential of adult human mesenchymal stem cells. *Science,* 284(5411), 143.

- Plock, J.A., Schnider, J.T., Schweizer, R. *et al.* 2013. Are cultured mesenchymal stromal cells an option for immunomodulation in transplantation? *Front Immunol,* 4.

- Prabhakaran, M.P., Venugopal, J.R. and Ramakrishna, S. 2009. Mesenchymal stem cell differentiation to neuronal cells on electrospun nanofibrous substrates for nerve tissue engineering. *Biomaterials,* 30(28):4996-5003.

- Quah, B.J.C. and Parish, C. 2012. New and improved methods for measuring lymphocyte proliferation in vitro and in vivo using CFSE-like fluorescent dyes. *Journal of Immunological Methods* 3791.

- Quinn, T.M., Hauselmann, H.J., Shintani, N., Hunziker, E.B. 2013. Cell and matrix morphology in articular cartilage from adult human knee and ankle joints suggests depth-associated adaptations to biomechanical and anatomical roles. *Osteoarthritis Cartilage,* 24:1904e12.

- Rayleigh, L. F. 1878. On the instability of jets. *Proc. London Math. Soc.*, 10: 4–13.

- Reneker, D. H., & Chun, I., 1996. Nanometre diameter fibres of polymer, produced by electrospinning. *Nanotechnology,* 7, pp.216-223.

- Research, B. 2012 [cited 03/02/2014]; Available from: http://www.bccresearch.com/market-research/healthcare/tissue-engineeringregeneration-technologies-markets-hlc101a.html.

- Rim, N.G., Shin, C.S. and Shin, H. 2013. Current approaches to electrospun nanofibers for tissue engineering. *Biomed Mater.,* 8(1), 014102.

- Sahoo, S., Cheng Lee, W.C., Hong Goh, J.C. and Toh, S.L. 2010. Bio-Electrospraying: A Potentially Safe Technique for Delivering Progenitor Cells. *Biotechnol Bioeng*., 106(4), 690.

- Sanjana, N.E and Fuller, S. 2004. A fast flexible ink-jet printing method for patterning dissociated neurons in culture. *J. Neurosci.* Methods, 136: 151–163.

- Saris, D.B., Vanlauwe, J., Victor, J., Haspl, M., Bohnsack, M., Fortems, Y., *et al.* 2008. Characterized chondrocyte implantation results in better structural repair when treating symptomatic cartilage defects of the knee in a randomized controlled trial versus microfracture. *Am J Sports Med.,* 36:235-46

- Schmitt, L.C., Quatman, C.E., Paterno, M.V., Best, T.M., Flanigan, D.C. 2014. Functional outcomes after surgical management of articular cartilage lesions in the knee: a systematic literature review to guide post-operative rehabilitation. *J Orthop Sports Phys Ther.*, 1-53.

- Schu, S., Nosov, M., O'Flynn, L. *et al.* 2012. Immunogenicity of allogeneic mesenchymal stem cells. *J Cell Mol Med,* 16, 2094.

- Shabani, I., Haddadi-Asl, V., Seyedjafari, E., Soleimani, M. 2012.Cellular infiltration on nanofibrous scaffolds using a modified electrospinning technique. *Biochem Biophys Res Commun.*, 423(1) 50-54.

- Shapiro, F., Koide, S., Glimcher, .MJ. 1993. Cell origin and differentiation in the repair of full-thickness defects of articular cartilage. *J Bone Joint Surg Am.,*75: 532-53.

- Shin, S.H., Purevdorj, O., Castano, O., Planell, J.A. and Kim, H.W. 2012. A short review: Recent advances in electrospinning for bone tissue regeneration. *J Tissue Eng.,* 3(1).

- Sill, T.J. & von Recum, H. 2008. Electrospinning: applications in drug delivery and tissue engineering. *Biomaterials*, 29(13), pp.1989-2006.

- Simon, T.M. and Aberman, H.M. 2009. Cartilage regeneration and repair testing in a surrogate large animal model. *Tissue Eng Part B Rev.,*16:65-79.

- Stankus, J.J., Soletti L., Fujimoto, K., Hong, Y., Vorp, D.A. and Wagner, W.R. 2007. Fabrication of cell microintegrated blood vessel constructs through electrohydrodynamic atomization. *Biomaterials,* 28(17): 2738–2746.

- Sullivan, A.C., Scott, K. and Jayasinghe, S.N. 2007. Nanofabrication by electrohydrodynamic jetting of a tailor-made living siloxane sol. *Macromol. Chem. Phys.,* 208: 2032–2038.
- Syed, B. A. and Evans, J. B. 2013. From the Analyst's Couch Stem Cell Therapy Market. *Nature Reviews Drug Discovery,* 12**,** 185-186.

- Takahashi, K., Tanabe, K., Ohnuki, M., Narita, M., Ichisaka, T., Tomoda, K. and Yamanaka, S. 2007. Induction of pluripotent stem cells from adult human fibroblasts by defined factors. *Cell*, 131**,** 861-872.

- Tamayol, A., Akbari, M., Annabi, N., Paul, A., Khademhosseini, A. and Juncker D. 2013. Fiber-based tissue engineering: Progress, challenges, and opportunities. *Biotechnol Adv.,* 31(5), 669.

- Tang, K. and Gomez, A. 1996. Monodisperse electrosprays of low electric conductivity liquids in the cone-jet mode. *J. Colloid Interface Sci.,* 184: 500–511.

- Taylor, G. I. 1964. Disintegration of water drops in an electric field. *Proc. R.Soc. London, Ser. A,* 280: 383–397.

- Theron, A., Zussman, E. and Yarin, A., 2001. Electrostatic field-assisted alignment of electrospun nanofibres. *Nanotechnology,* 12, pp.384-390.

- Tierney, C.M., *et al.* 2009. The effects of collagen concentration and crosslink density on the biological, structural and mechanical properties of collagen-GAG scaffolds for bone tissue engineering. *J Mech Behav Biomed Mater,* 2(2):202-9.

- Tropel, P. Noel, D., Platet, N., Legrand, P., Benabid, A.L. and Berger, F. 2004. Isolation and characterisation of mesenchymal stem cells from adult mouse bone marrow. *Exp Cell Res,* 295: 395-406.

- Van Osch, G. J.V.M., Brittberg, M., Dennis, J.E., Bastiaansen-Jenniskens, Y.M., Erben, R.G., Konttinen, Y.T., Luyten, F.P. 2009. Cartilage repair: past and future – lessons for regenerative medicine. *Journal of Cellular and Molecular Medicine,* 13(5): 792-810.

- Wang F., Li, Z., Tamama, K., Sen, C.K. and Guan, J. 2009. Fabrication and Characterization of Prosurvival Growth Factor Releasing, Anisotropic Scaffolds for Enhanced Mesenchymal Stem Cell Survival/Growth and Orientation. *Biomacromolecules,* 10:2609–2618.

- Wu, Y.N., Law, J.B.K., He, A.Y., Low, H.Y., Hui, J.H.P., Lim, C.T., Yang, Z., Lee, E.H. 2014. Substrate topography determines the fate of chondrogensis from human mesenchymal stem cells resulting in specific cartilage phenotype formation. *Nanomedicine: Nanotechnology, Biology and Medicine,* 10(7): 1507-1516.

- Xu, C., 2004. Aligned biodegradable nanofibrous structure: a potential scaffold for blood vessel engineering. *Biomaterials,* 25(5), pp.877-886.

- Yang, S. et al., 2001. The design of scaffolds for use in tissue engineering. Part I. Traditional factors. *Tissue Engineering*, 7(6), pp.679-689.

- Yannas, I.V. 2001. Tissue and Organ Regeneration in Adults. *New York: Springer*, ISBN: 978-0-387-95214-7

- Yannas, I.V. *et al.* 1989. Synthesis and characterization of a model extracellular matrix that induces partial regeneration of adult mammalian skin. *Proc Natl Acad Sci U S A*, 86(3):933-7.

- Yannas, I.V. and Burke, J.F. 1980. Design of an artificial skin. I. Basic design principles. *J Biomed Mater Res.*, 14(1): 65-81.

- Yannas, I.V., *et al*. 1975. Correlation of in vivo collagen degradation rate with in vitro measurements. *J Biomed Mater Res.*, 9(6): 623-8.

- Ye, C., He, Z., Lin, Y., Zhang, Y., Tang, J., Sun, B., Ma, M., Liu, J., Yang, L., Ren, H. and Zhao, B. 2014. Bio-electrospraying is a safe technology for delivering human adipose-derived stem cells. *Biotechnology Letters*, 1-8.

- Younger, E.M. and M.W. Chapman. 1989. Morbidity at bone graft donor sites. *J Orthop Trauma*, 3(3): 192-5.

- Zappia, E., Casazza, S., Pedemonte, E., Benvenuto F., Bonanni, I., Gerdoni, E., Giunti, D., Ceravolo, A., Cazzanti, F., Frassoni, F., Mancardi, G. and Uccelli, A. 2005. Mesenchymal stem cells ameliorate experimental autoimmune encephalomyelitis inducing T-cell anergy. *Blood*, 106**,** 1755-61.

- Zeleny J. 1914. The electrical discharge from liquid points and a hydrostatic method of measuring the electric intensity at their surface. *Phys. Rev.*, 3: 69–91.

- Zheng, H., Martin, J.A., Duwayri, Y., Falcon, G., Buckwalter, J.A. 2007. Impact of aging on rat bone marrow-derived stem cell chondrogenesis. *J Gerontol A Biol Sci Med Sci.*, 62: 136-48.

Appendix

A Jet mode - 3 x 10^6 mBMSC/mL BES with central ligament of cells at ~3-6kV

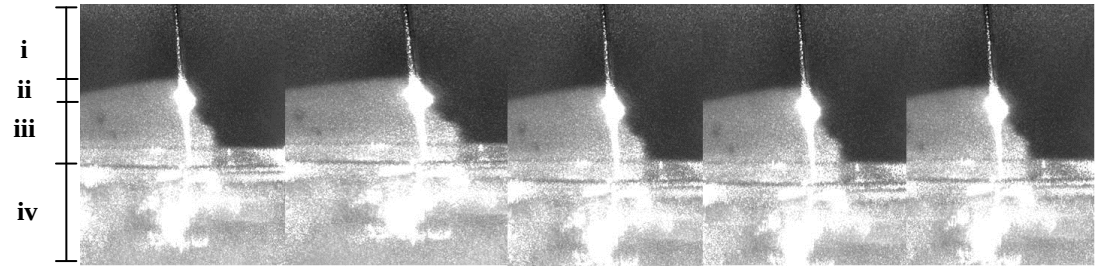

B Jet mode - 3 x 10^6 mBMSC/mL BES with central ligament of cells at ~3-6kV

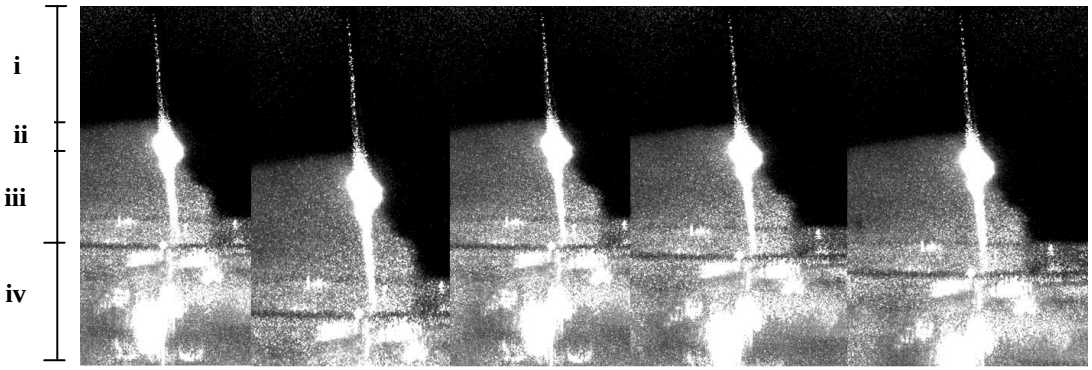

Fig. A1 Replicas of Jet Spray modes achieved with electrospray set-up. 3 x 10^6 mBMSC/mL suspended in cα-MEM culture medium were BES at 3-6kV (depending on RH), flowrate of 5µL/min, PD of 22 mm (A) Jet mode with central ligament of cells visible recorded on the 5th September 2013. (B) Jet mode with central ligament of cells visible recorded on 12th December 2013. All photographs were taken 1 frame/second for 5 frames.

Key: (i) Needle **(ii)** Taylor cone **(iii)** jet mode with central ligament of cells **(iv)** 24 - well plate

A Plume spray – 1 x 10^6 mBMSC/mL BES at ~3-6kV

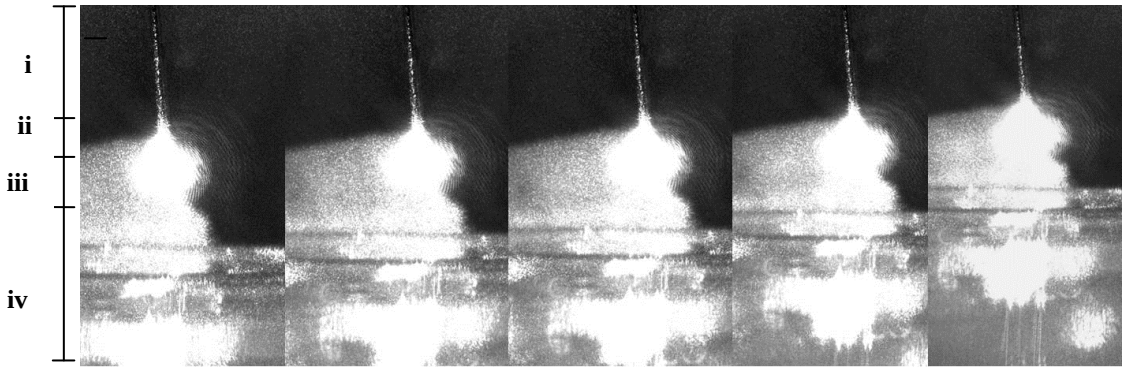

B Plume spray – 1 x 10^6 mBMSC/mL BES at ~3-6kV

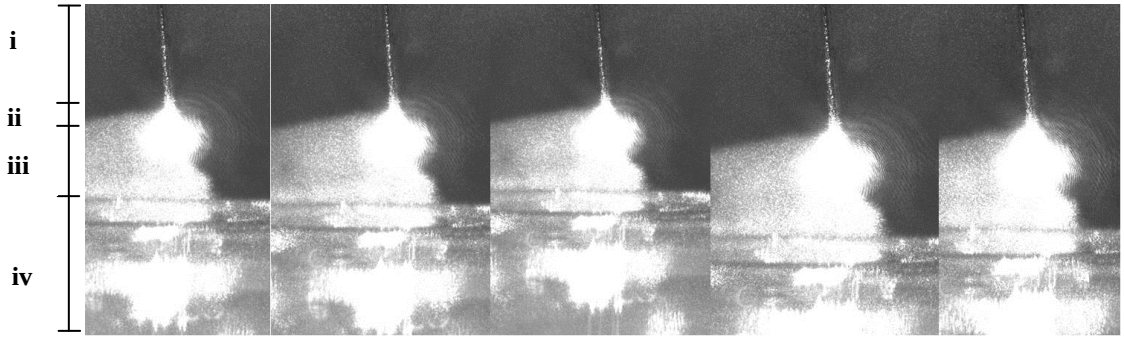

Fig. A2 Replicas of Plume Spray achieved with electrospray set-up. 1 x 10^6 mBMSC/mL suspended in cα-MEM culture medium were BES at 3-6kV (depending on RH), flowrate of 5µL/min, PD of 22 mm (A) Plume spray visible recorded on the 11th September 2013. (B) Plume spray visible recorded on 18th December 2013. All photographs were taken 1 frame/second for 5 frames.

Key: (i) Needle **(ii)** Taylor cone **(iii)** plume spray of cells **(iv)** 24 - well plate

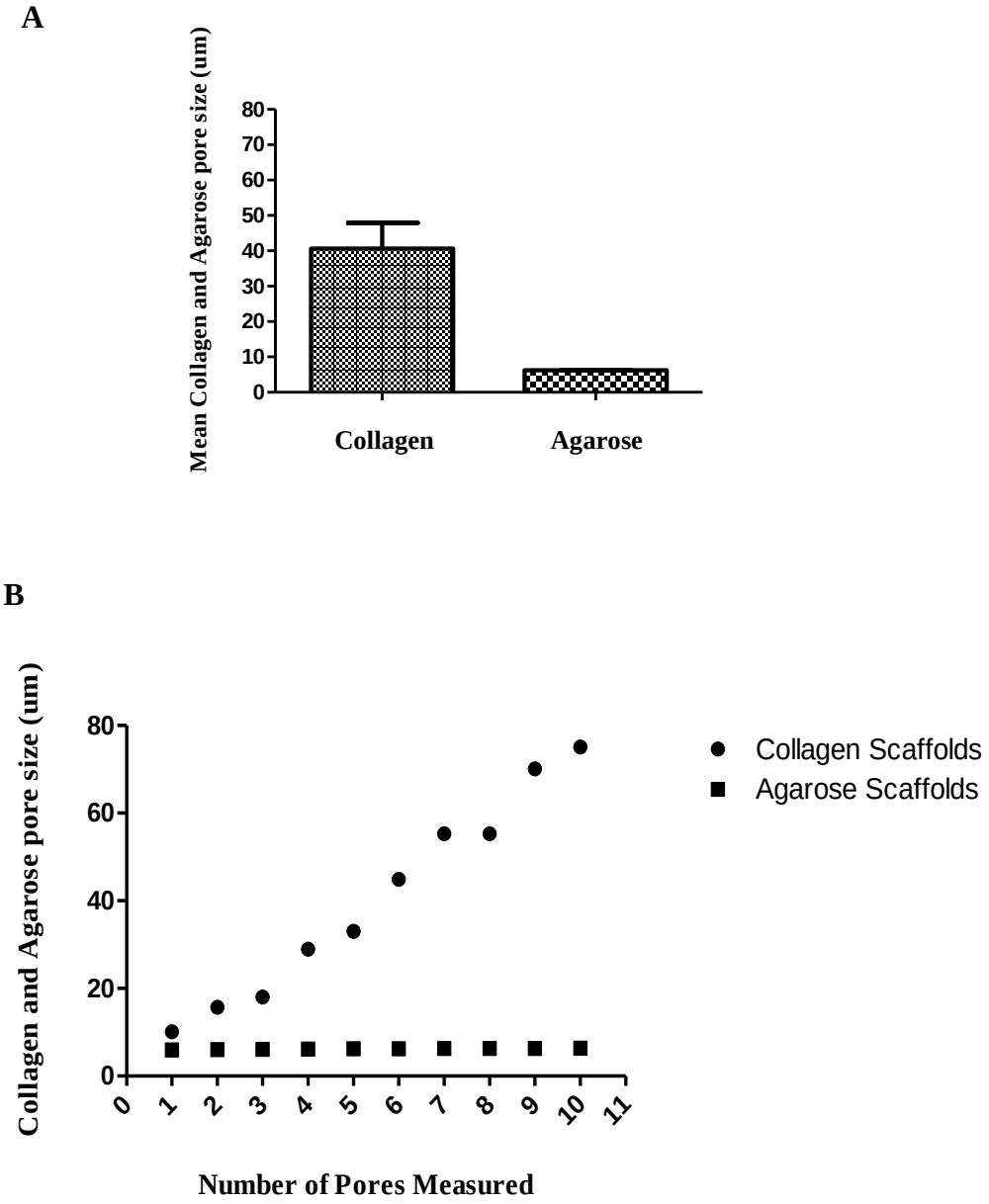

Fig. A3 Graphical representation for the measurements of pore sizes for collagen and agarose scaffolds. 10 random pore sizes were selected and measured using SEM for both constructs. (A) Demonstrates the mean pore size for collagen and agarose scaffolds. The mean pore size for collagen scaffolds was shown to be 41.96μm, while agarose scaffolds were recorded at 6.2μm. (B) Demonstrates inconsistent pore measurements for the collagen scaffolds, with the smallest pore size measured at 10.1 μm and the largest recorded at 75.1μm. In contrast the pore size for the agarose scaffolds, although small, indicated they were uniform. The smallest pore size for the agarose scaffolds was recorded at 5.97μm and the largest at 6.38μm.

A

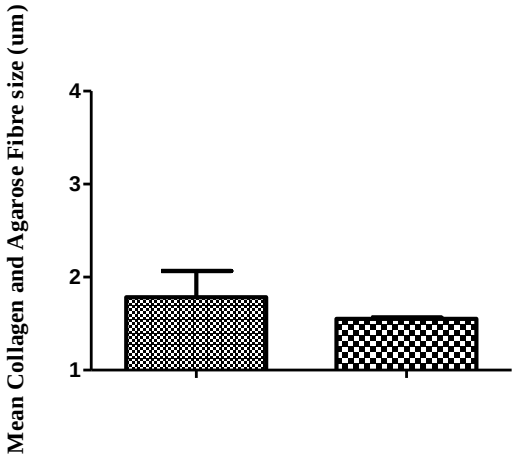

B

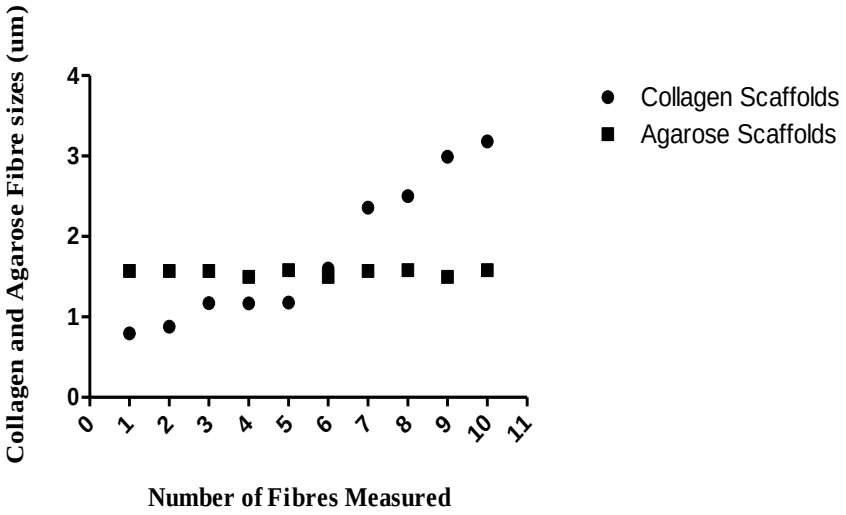

Fig. A4 Graphical representation for the measurements of fibre thickness for collagen and agarose scaffolds. 10 random fibres were selected and measured using SEM for both constructs. (A) Demonstrates the mean fibre thickness for collagen and agarose scaffolds. The mean fibre thickness for collagen scaffolds was shown to be 1.79µm, while agarose scaffolds were recorded at 1.56µm. (B) Demonstrates the inconsistencies in fibre thickness for the collagen scaffolds, with the thinnest fibre measured at 795nm and the thickness recorded at 3.18µm. In contrast the fibre thickness for the agarose scaffolds indicated they were uniform in diameter, although they remained at the µm scale. The thinnest fibre for the agarose scaffolds was recorded at 1.57µm and the thickest at 1.58µm.